Title
Regulation of neuronal polarity in C. elegans by TOE-2 and Wnt signaling

Author
Gurling, Mark Andrew

Publication Date
2012

Peer reviewed|Thesis/dissertation

Regulation of neuronal polarity in *C. elegans* by TOE-2 and Wnt signaling

by

Mark Andrew Gurling

A dissertation submitted in partial satisfaction of the
requirements for the degree of
Doctor of Philosophy

in

Molecular and Cell Biology

in the

GRADUATE DIVISION
of the
UNIVERSITY OF CALIFORNIA, BERKELEY

Committee in charge:
Professor Gian Garriga, Chair
Professor Sharon Amacher
Professor Louise Glass
Professor Iswar Hariharan

Fall 2012

Regulation of neuronal polarity in *C. elegans* by TOE-2 and Wnt signaling

by
Mark Andrew Gurling

Abstract

Regulation of neuronal polarity in *C. elegans* by TOE-2 and Wnt signaling

by

Mark Andrew Gurling
Doctor of Philosophy in Molecular and Cell Biology

University of California, Berkeley

Professor Gian Garriga, Chair

Cellular polarization is an important aspect of neural development. During the development of the *C. elegans* nervous system, many divisions are asymmetric and give rise to neurons and cells that die. While we understand how cells die in *C. elegans*, we know much less about how cells are instructed to adopt the apoptotic fate. To address this issue, I studied the Q.p neuroblast, which divides to produce a larger anterior cell and a smaller posterior cell that dies. The surviving Q.p daughter divides again to form the neurons A/PVM and SDQ. A forward-genetic screen for mutants with extra A/PVMs in order to identify genes that regulate the apoptotic fate was conducted previously in the lab. A mutant, *gm389*, was isolated. In *gm389*, I identified a mutation in the gene *toe-2*, which encodes a target of the worm ERK ortholog, MPK-1. I found that TOE-2 not only regulates the apoptotic fate of the posterior Q.p daughter, but it also plays a role in the asymmetric division of Q, the mother of Q.p. I found that TOE-2 functions autonomously in the Q lineage where it regulates several asymmetric cell divisions (ACDs). I also show that, during Q lineage cell divisions, TOE-2 localizes to centrosomes, to the posterior cortex and at the site where the cleavage furrow will form.

Cellular polarization is also required for the function of mature neurons. The function of a neuron is facilitated by its distinct morphology. Electrical signals are propagated along neuronal processes that extend from the cell body to form connections with muscle cells, sensory structures or other neurons. In vitro studies of developing neurons have shown that a neuronal process forms at random from one of many smaller processes protruding from the developing cell. Many intracellular molecules necessary for this process have been identified. However, many neurons display invariant polarity in vivo, suggesting specific regulation of the polarization process by external signals. Wnts and Frizzled receptors have been shown to direct polarization of mechanosensory neurons along the *C. elegans* anterior/posterior (AP) axis. It was shown that ectopic expression of MIG-1 in PLM reverses PLM polarity. I show that ectopic expression of the cysteine-rich domain of MIG-1 in PLM is not sufficient to cause a polarity reversal. I also show that the activity of MIG-1 in PLM is dependent upon the Wnt EGL-20.

To Mother Bear and Squid

Table of Contents

ACKNOWLEDGEMENTS

I would like to thank my advisor Gian Garriga, foremost, for his patience; mine was not the straightest path to degree, but Gian was a great support through all of the ruts and detours. His (infinite?) knowledge of nematode anatomy, development and genetics made him an invaluable resource and an excellent teacher. Apart from his mentorship, Gian was a true friend. He always had a good story to tell or a useful bit of wisdom to impart. One is sure in the knowledge that Gian wants what is best for him. I would also like to thank the members of my committee—Sharon, Iswar and Louise—for their advice, patience and encouragement.

I would like to thank the current members of the lab for making it a pleasant place to be. Jason, whom I've always looked up to for his hard work, willingness to help and tremendous lawn bowling skills. Jérôme, whom I could always count on to tell me the truth, in spite of what I wanted to hear. Richard, with whom I proved that Utahns and Canadians have much more in common than one might have thought. Falina, who made more than her share of birthday cakes and brought us all together in the spirit of crossword puzzles. I would also like to thank past members of the lab for their help and support: Peter, for sound advice and morning Mandarin lessons; Aakanksha, the big sister I never had; Ashley, the little sister I never had; Catarina, my most favorite Swede of all time; Maylee, for making me watch every SNL skit worth seeing during the 2008 election; Shaun, who always knew the best hiking spots; Amita, who gave me the courage to move to the other side of the lab; Pam, who taught me that it's okay if the scintillation counter readings are off the charts, it's probably just static; Karla, who screened and screened and screened; Julie, from whom I should have bought a painting, because it will be worth millions some day; and Eva, whom I want to be like: funny, kind and tough as nails.

I would like to thank Barbara Meyer and Abby Dernburg for use of their equipment and reagents. I would also like to thank the members of their labs, in particular Te-Wen Lo for sharing her expert knowledge and skills in relation to TALENs; Ericca Stamper, Hoang Pham and Ed Ralston for help with whole-genome sequencing; and Ofer Rog for help with confocal microscopy. I also thank my fellow classmates, especially Derek and Jess, for encouragement, good jokes, bad jokes and lunches; and Dan Richter for his invaluable help with annotation of whole-genome sequencing data and for his calming presence.

I want to thank the Graduate Affairs Office staff—Eric Buhlis, Christina Bianchi, Tanya Grimes and Berta Parra—for answering all of my questions and for doing countless other things in my behalf that I probably never even knew needed doing. I would also like to thank my professors at Westminster College who taught and encouraged me, wrote last minute recommendation letters, and made various aspects of biology memorable: Larry Anderson, Brian Avery and Judy Rogers.

I want to thank Mom and Dad for always expecting something of me; Charlie, for late-night video games and for being the jolliest of uncles; Beth, the little sister I'm glad I have and the sweetest aunt in the world.

And last but never least, my family: Ashley my loving wife, friend, supporter, heckler, organizer, encourager … . Your tolerance and support are unsurpassed. And Adeline, my favorite little friend, in whose presence life always seems to make sense.

CHAPTER 1

AN INTRODUCTION TO ASYMMETRIC CELL DIVISION

Developmental Biology

Herbert Spencer, the great English philosopher, saw everything—from the developing commerce of civilizations to the musings of the human mind—through an evolutionary lens. He is best known for his creation of a conceptual model for universal evolution: a homogeneous entity, be it a city-state or an idea, shifts and rattles itself into a new heterogeneous state of greater complexity (Spencer, 1898a).

However, it was Charles Darwin who applied this evolutionary lens specifically to one of the great problems of biology: how did the diversity of life on earth come to be? The mechanism he described, as illuminating now as it was then, was "descent with modification" (Darwin, 1859). The explanatory power of this concept roots, in a single-celled ancestor, a dense tree carrying unimaginably many and diverse creatures on each bough. This story of the derivation of all life from an ancient single-celled organism, which at a cursory glance seems an unlikely progenitor, has all the beauty of the great myths, but unlike the myths it happens also to be true.

As Spencer noted (1864, 1898b), this grand story of evolution is retold in the development of every organism; from a single cell comes the diverse apparatus and sinew of the fish, the fly, the worm ... . And, though smaller in scope, the question of how this dramatic transformation might occur is as daunting as, if not more daunting than, the question Darwin faced. This is the great question of developmental biology.

Asymmetric Cell Division

For a single cell to give rise to various tissues and organs the progeny of that cell must become distinct from one another. This is achieved through asymmetric cell division (ACD). Horvitz and Herskowitz (1992) define ACD as a cell division that produces two daughters with distinct fates. These fates are often defined by function or morphology, or both. The daughters of these divisions can be intrinsically different (i.e. from their inception, the cells are distinct from one another). This is achieved as fate determinants segregate asymmetrically along an axis of the cell. The mitotic spindle must also align along the same axis. This coordination between spindle orientation and localization of determinants results in unequal inheritance of the determinants, producing a difference in the fates of the daughter cells. This was observed as early as the turn of the century. Conklin (1905) described an abrupt segregation of "yellow protoplasm" to the vegetal pole of the one-cell *Styela (Cynthia) partita* embryo just after fertilization. This pigmented cytoplasm segregates through many subsequent divisions and always ends up in the tadpole muscle cells. While Conklin saw only a correlation between the muscle cell fate and the localization of the yellow cytoplasm, from work in *Drosophila* and *C. elegans* we now know of many specific fate-determining molecules. The mechanisms by which they promote ACD have also been elucidated, and some of these mechanisms have been shown to be conserved in mouse and chick ACDs. These molecules play roles in multiple organisms and developmental contexts and will be discussed in more detail later.

Sister cells formed by ACD may also be, at first, identical; only through experience do they become different. For example, the grasshopper (*Schistocerca americana*) midline precursor 3

(MP3) progeny are, at first, identical and later adopt distinct fates. The midline precursors (MP) are arranged along the antero-posterior axis of the grasshopper embryo on the dorsal surface of its neuroepithelium. Each MP divides only once to form two daughters that will become neurons. MP3, upon division, gives rise to the H cell—so named for the appearance of its axonal branching—and the H cell sib (apparently so named for its unremarkable morphology relative to that of its sister). Kuwada and Goodman (1985) ablated MP3 sisters and observed that the remaining cell almost always adopted the H cell sib fate. However, if one of the sisters were ablated slightly later in development (but before either sister had any morphology suggestive of either fate) the surviving sister adopted either fate with equal frequency. These results suggest that the MP3 daughters are born identical to one another. Only later do they acquire alternate fates. This may be due to signaling between the sisters or to positional differences that allow one to receive a signal that the other does not. Regardless, it is clear from this example that a division may produce two cells that are at first similar, but ultimately different.

The current understanding of how ACD is achieved comes mainly from studies conducted in *C. elegans* and *Drosophila melanogaster*. The following section is a discussion of the autonomous factors and signaling pathways known to be involved in ACD during the development of these two organisms. The section will focus on the first division of the *C. elegans* embryo and neuroblast (NB) and sensory organ precursor (SOP) lineages in the development of the *Drosophila melanogaster* nervous system.

The Molecular Themes of ACD

Much of the molecular machinery that establishes cellular polarity and promotes ACD is conserved between species and among various cell lineages. The Par complex, along with Galpha and the TPR-GoLoco protein Pins/GPR-1/2, plays a prominent role in establishing and maintaining cell polarity. This polarity allows the segregation of fate determinants within the cell and their unequal distribution between daughter cells following division (Gönczy, 2008; Knoblich, 2010). This asymmetric division also requires proper placement of the mitotic spindle, which is often asymmetric along the axis of division (Siller and Doe, 2009; Morin and Bellaïche, 2011). These themes will be first described generally, and then in more detail within a given developmental context.

The Par Complex

The Par complex consists of PAR-3/Bazooka and PAR-6 (PDZ-domain-containing proteins) and atypical protein kinase C (PKC-3/aPKC) (Kemphues et al., 1988; Tabuse et al., 1998; Hung and Kemphues, 1999; Wodarz et al., 2000). In Par complex mutants, the localization of fate determinants in the *C. elegans* zygote and in *Drosophila* neuroblasts and SOPs is compromised, making it clear that this complex is necessary for establishing and maintaining polarity prior to asymmetric division (Schober et al., 1999; Wodarz et al., 1999; Cuenca et al., 2003). The Par complex is also necessary for proper mitotic spindle orientation (Gönczy, 2008; Knoblich, 2010; Morin and Bellaïche, 2011). The Par complex is central to ACD in multiple developmental contexts; however, the way in which it functions and the additional molecules with which it cooperates to promote ACD in these contexts can be quite different.

Gα and Pins

Another pair of proteins that seems to play a recurring role in various ACDs is made up of the TPR-GoLoco protein GPR-1/2/Pins and the α subunit of a heterotrimeric G protein (Gotta and Ahringer, 2001; Colombo et al., 2003; Gotta et al., 2003; Srinivasan et al., 2003; Bowman et al., 2006; Izumi et al., 2006; Siller et al., 2006). Interaction between the proteins occurs via the GoLoco motif of GPR-1/2 (Takesono et al., 1999; Schaefer et al., 2001; Willard et al., 2004). In the *C. elegans* zygote, this complex is distributed throughout the cortex and is required for generating force on the mitotic spindle (Gotta and Ahringer, 2001; Colombo et al., 2003; Gotta et al., 2003; Srinivasan et al., 2003). In *Drosophila* NBs and SOPs, however, $G_{\alpha i}$ and GPR-1/2/Pins, in partnership with the Par complex, are also necessary for segregation of fate determinants (Bowman et al., 2006; Lee et al., 2006b). In NBs, $G_{\alpha i}$ and GPR-1/2/Pins localize with Par proteins at the cortex (Schober et al., 1999; Parmentier et al., 2000; Schaefer et al., 2000, 2001; Wodarz et al., 2000; Yu et al., 2000) (Figure 1A), whereas in SOPs these groups of proteins localize to complementary regions of the cell cortex (Bellaïche et al., 2001b; Schaefer et al., 2001) (Figure 1B and C).

Fate determinants: PIE-1 and PAL-1; Pros and Brat; and Numb

Once the polarity of a cell has been established, this information is communicated to proteins that localize asymmetrically, and, upon division of the cell, segregate unequally into the daughter cells. This causes the daughters to adopt different fates.

Two *C. elegans* fate determinants, PIE-1 and PAL-1, are segregated asymmetrically in the embryo and provide examples of different mechanisms by which segregation can occur (Hunter and Kenyon, 1996; Mello et al., 1996; Reese et al., 2000; DeRenzo et al., 2003). The first example is the inheritance of PIE-1 by the cells of the *C. elegans* embryo that are to become the germ line. The initial division of the embryo produces a large anterior cell (AB) and a smaller posterior cell (P1), which will give rise to the germ line and other cell types (Sulston et al., 1983). PIE-1 is a transcriptional repressor that prevents the expression of genes that would direct a cell toward a somatic fate (Batchelder et al., 1999; Zhang et al., 2003; Ghosh and Seydoux, 2008). Initially, PIE-1 protein is uniformly cytoplasmic in the one-cell embryo. Later, PIE-1 accumulates at one end of the embryo as changes to the protein cause it to diffuse more slowly in the posterior of the cell than in the anterior (Daniels et al., 2009). Ultimately, PIE-1 becomes concentrated in P1 and its descendants that form the germ line because it is preferentially degraded in cells destined for somatic fates (DeRenzo et al., 2003).

The second example is PAL-1, a homeodomain protein required for specification of muscle, hypodermis and neurons in the developing worm (Waring and Kenyon, 1991; Hunter and Kenyon, 1996; Hunter et al., 1999; Edgar et al., 2001). Initially (in oocytes and in the one-cell embryo), only *pal-1* mRNA (as opposed to PAL-1 protein) is present. Prior to the end of the second division, translation of *pal-1* mRNA is inhibited. This inhibition continues in the anterior cell AB and its descendants, leading later to localization of PAL-1 protein only in cells derived from the posterior daughter P1 (Hunter and Kenyon, 1996).

Prospero (Pros), a homeodomain transcription factor, and Brain tumor (Brat), a member of the NHL family of proteins—proteins involved in RNA metabolism—are fate determinants necessary for development of neurons derived from the divisions of *Drosophila* NBs (Doe et al.,

1991; Spana and Doe, 1995; Sonoda and Wharton, 2001; Betschinger et al., 2006; Lee et al., 2006b). Embryonic NBs delaminate from the ventral neuroectoderm and then divide asymmetrically with respect to size and fate. The larger of the NB daughters retains the NB fate and the smaller, called the ganglion mother cell (GMC), divides once more, giving rise to post-mitotic neurons and glia (Betschinger and Knoblich, 2004; Gönczy, 2008; Knoblich, 2010; Morin and Bellaïche, 2011) (type I, Figure 2A). Pros and Brat are inherited by the GMC and are necessary for realization of its fate (Doe et al., 1991; Hirata et al., 1995; Spana and Doe, 1995; Betschinger et al., 2006; Lee et al., 2006b) (Figure 1A). In type II larval neuroblast divisions, the NB gives rise to an intermediate neural precursor (INP), which goes through a maturation process and then gives rise to multiple GMCs. The INP does not inherit Pros from the NB; however, when the INP matures, it begins to express Pros, which is segregated to the GMC when the INP divides (reviewed in Homem and Knoblich, 2012) (Figure 2B). In *pros* or *pros* and *brat* mutants, GMCs over express cell-cycle markers (Li and Vaessin, 2000) or, in the case of larval NBs, INPs behave like NBs and continue to divide (Betschinger et al., 2006). Unlike the segregation of either of the *C. elegans* proteins described above, segregation of Pros and Brat does not seem to be dependent upon asymmetric protein degradation or translational inhibition. Rather, they segregate with other proteins that are localized to the basal cortex of the NB (Shen et al., 1998; Betschinger et al., 2006; Lee et al., 2006b) (Figure 1A).

Numb is a phospho-tyrosine-binding protein that is involved in the divisions of both NBs and SOPs in *Drosophila* (Uemura et al., 1989). However, Numb does not appear to function as a fate determinant in embryonic NB divisions as loss of Numb function does not seem to alter the fate of NB progeny; however, type II NBs divide to form more NBs at the expense of neurons in *numb* mutants (Lee et al., 2006a; Wang et al., 2006). Unequal Numb inheritance is important though for the daughters of the SOP, pIIa (the posterior daughter) and pIIb (the anterior daughter). Pins and $G_{\alpha i}$ localize to the anterior side of the SOP, and Numb localizes with them. Thus, Numb is inherited only by the pIIb daughter (Rhyu et al., 1994; Bellaïche et al., 2001b; Schaefer et al., 2001) (Figure 1B and C). This causes pIIb and pIIa to take on different fates by a mechanism that will be described later.

Positioning of the mitotic spindle: Mud and Dynein

Asymmetric segregation of fate determinants is absolutely necessary for ACD to produce two different daughter cells; however, the position of the mitotic spindle is equally important as improper spindle orientation could lead to equal inheritance of an asymmetrically localized fate determinant. LIN-5/Mud are coiled-coil proteins that interact with TPR-GoLoco proteins and the Dynein complex (Merdes et al., 1996; Bowman et al., 2006; Izumi et al., 2006; Siller et al., 2006; Wang et al., 2011). These associations form a link between cortically localized G_{α} and Pins proteins, and microtubules. Normally, Dynein walks toward the minus-end of microtubules (Schroer et al., 1989). In this case Dynein is tethered to the cortex, and it may be that it pulls microtubules toward itself, thereby generating force on the mitotic spindle allowing for both its rotational and translational placement. Though Mud is important for spindle orientation during *Drosophila* NB divisions, NBs still segregate fate determinants properly most of the time in *mud* mutants (Cabernard and Doe, 2009). Mud seems to play a much more important part in positioning the spindle of the one-cell *C. elegans* embryo. The first embryonic division is normally asymmetric with respect to size; however, in *lin-5* (*mud*) mutants, the cell divides symmetrically. (Nguyen-Ngoc et al., 2007) (Figure 3).

ACDs in *C. elegans* and *Drosophila*

In order for ACD to occur cells must be able to assess their inner polarity, segregate determinants to distinct parts of the cell, and then align their plane of division such that the asymmetrically localized determinants segregate to separate daughter cells. This is achieved through the coordination of the molecules described above. Though general themes exist in ACD, the following section will describe in more detail how the molecular components of ACD are employed in different developmental contexts.

The one-cell C. elegans embryo

The initial polarity of the *C. elegans* zygote is established by segregation of the Par complex and additional Pars, PAR-1 (a S/T kinase) and PAR-2 (a Ring-finger protein) (Kemphues et al., 1988; Etemad-Moghadam et al., 1995; Rose and Kemphues, 1998b). Prior to fertilization, PAR-3/PAR-6/PKC-3 are localized throughout the cortex (Cuenca et al., 2003). However, by the end of prophase they are restricted to the anterior half of the embryo (Cuenca et al., 2003). PAR-1 and PAR-2 are found at the posterior cortex, complementary to the localization of the PAR-3/PAR-6/PKC-3 complex (Cuenca et al., 2003) (Figure 3). This initial polarity is important for the asymmetric localization of fate determinants and polarity-mediating proteins in the zygote (Schubert et al., 2000; Cuenca et al., 2003).

The CCCH-Zn finger protein MEX-5, a polarity mediator, localizes to the anterior side of the embryo while the fate determinant PIE-1 remains in the posterior half (Mello et al., 1996; Schubert et al., 2000). This localization is probably achieved by regulation of the rates at which these proteins diffuse through the cytoplasm (Daniels et al., 2010). In the model, MEX-5 diffuses slowly in the anterior and more quickly in the posterior of the embryo leading to its accumulation in the anterior cytoplasm (Daniels et al., 2010). This difference in diffusion is, presumably, achieved through phosphorylation of MEX-5 by PAR-1 (Tenlen et al., 2008). Phosphorylated MEX-5 is the fast-diffusing form and this form will be most prevalent in the posterior embryo where PAR-1 is localized at the cortex (Tenlen et al., 2008; Daniels et al., 2010) (Figure 3). Recently it has been shown that there is also a cytoplasmic gradient of PAR-1 and that this gradient is sufficient to produce fast-diffusing MEX-5 (Griffin et al., 2011).

PIE-1 displays diffusion dynamics that are complementary to those of MEX-5 (Daniels et al., 2009). Though it is unknown how PIE-1 exists in rapid- and slow-diffusing forms, it is thought that the slower diffusion of PIE-1 in the posterior is due to its association with P-granules—RNA-rich cytoplasmic granules that segregate to cells that will form the germ line (Daniels et al., 2009). Later in embryonic development, MEX-5 activates Zinc finger-interacting factor 1 (ZIF-1), which links PIE-1 to a ubiquitin-ligase complex containing the cullin CUL-2 and the E2-conjugating enzyme UBC-5 (DeRenzo et al., 2003). This linkage leads to the degradation of PIE-1 specifically in the anterior somatic cells of the embryo.

MEX-3, like MEX-5, is active only in the anterior half of the embryo (Draper et al., 1996; Schubert et al., 2000). MEX-3 is a KH domain-containing RNA-binding protein whose asymmetric segregation in the first division of the zygote is dependent upon the initial polarity established by the Pars (Draper et al., 1996). PAR-1 prevents MEX-3 activity in the posterior end of the one-cell embryo (Draper et al., 1996). Anteriorly-active MEX-3 represses translation of

pal-1 RNA in the anterior half of the embryo (Huang et al., 2002), and this explains how PAL-1 protein becomes restricted to those posterior cells of the embryo that later form muscles, hypodermis and neurons.

The cells to which the MEX proteins and PIE-1 will eventually segregate are asymmetric in size (MEX-3 and MEX-5 end up in the larger anterior daughter AB; PIE-1 in the smaller posterior daughter P1). This size asymmetry is achieved by asymmetric placement of the mitotic spindle. G_{α}, GPR-1/2, LIN-5 and, to a lesser extent, Dynein (DHC-1) are required at the cortex to generate force on the spindle to place it asymmetrically in time for anaphase (Miller and Rand, 2000; Gotta and Ahringer, 2001; Colombo et al., 2003; Gotta et al., 2003; Srinivasan et al., 2003; Afshar et al., 2004). As we will see later, these proteins are localized asymmetrically in *Drosophila* NBs and SOPs (Jan and Jan, 2001; Chia and Yang, 2002; Betschinger and Knoblich, 2004) (Figure 1), and this asymmetry is important for establishing and maintaining cellular polarity. In the *C. elegans* zygote, however, G_{α}, GPR-1/2 and LIN-5 are found throughout the cortex on the anterior and posterior sides (Miller and Rand, 2000; Gotta and Ahringer, 2001; Colombo et al., 2003; Gotta et al., 2003; Srinivasan et al., 2003; Afshar et al., 2004) (Figure 3). This raises the question of how these proteins are able to asymmetrically pull the mitotic spindle into place. At least part of the answer is found in the DEP domain-containing protein, LET-99 (Tsou et al., 2003). In the zygote, LET-99 localizes in a lateral-posterior band and excludes GPR-1/2 from this region (Tsou et al., 2002, 2003). Concomitantly, GPR-1/2 are concentrated in the posterior pole of the embryo (Tsou et al., 2003). This causes the posterior pulling forces to be relatively greater than the anterior pulling forces, causing the spindle to shift toward the posterior. This disequilibrium of pulling forces leads, ultimately, to a division in which the posterior daughter claims less of the cytoplasm than its anterior sister (Figure 3).

We will now discuss the divisions of *Drosophila* NBs and SOPs, which generate parts of the central and peripheral nervous system, respectively (Jan and Jan, 2001; Chia and Yang, 2002; Betschinger and Knoblich, 2004). Though many of the molecules necessary for ACD in the one-cell *C. elegans* embryo are used again in the NBs and SOPs, one major difference is the use of G_{α} and GPR-1/2/Pins. In the *C. elegans* zygote they are uniformly distributed, and play a major role in spindle placement, while in *Drosophila* they, in concert with the Par complex, play a much larger role in establishing cellular polarity that leads to the proper segregation of fate determinants.

Drosophila embryonic NB divisions

Embryonic NBs are responsible for generating neurons that make up the central nervous system of fly larvae. These cells delaminate from the ventral neuroectoderm, an epithelial sheet. The NB divides along an apical-basal axis, giving rise to a large cell that retains NB character and a smaller ganglion mother cell (GMC) that divides to form post-mitotic neurons or glia (Jan and Jan, 2001; Chia and Yang, 2002; Betschinger and Knoblich, 2004) (Figure 2). The apical-basal polarity of the NB requires asymmetric localization of Par components, and $G_{\alpha i}$ and Pins. All of these proteins localize to the apical side of the NB. The polarity of the Par components is inherited from the epithelium, while the $G_{\alpha i}$ and Pins complex associates with the Par complex via a linking protein called Inscuteable. Inscuteable binds both Pins and Bazooka (Schaefer et al., 2000, 2001; Yu et al., 2000) (Figure 1).

These apical components are important for the basal localization of fate determinants Pros and Brat (Ikeshima-Kataoka et al., 1997; Shen et al., 1997; Matsuzaki et al., 1998; Lee et al., 2006b; Atwood and Prehoda, 2009). As discussed earlier, Pros and Brat must segregate to the GMC as they are required for the expression of GMC fate and proper differentiation of GMC's neuronal daughters (Doe et al., 1991; Spana and Doe, 1995; Sonoda and Wharton, 2001; Betschinger et al., 2006; Lee et al., 2006b) (Figure 1A). The basal localization of these fate determinants is achieved through the basal localization of yet other polarity-mediating proteins, the most prominent of which is Miranda (Ikeshima-Kataoka et al., 1997; Shen et al., 1997; Matsuzaki et al., 1998; Lee et al., 2006b; Atwood and Prehoda, 2009) (Figure 1A). Both Pros and Brat bind Miranda (Betschinger et al., 2006); therefore, in the absence of Miranda protein, Pros and Brat localize throughout the cytoplasm (Fuerstenberg et al., 1998; Lee et al., 2006b). In mutants for any of the apical complex members or *inscuteable*, basal Miranda localization is perturbed (Schober et al., 1999; Wodarz et al., 1999). This mislocalization occurs at metaphase, yet basal Miranda localization is often restored before telophase (Peng et al., 2000). This implies another pathway that localizes fate determinants after metaphase. Indeed, there is a microtubule-dependent localization of Miranda and fate determinants Brat and Pros. This pathway involves a Pins-binding protein, Discs large (DLG) and a kinesin, KHC73. KHC73 can bind DLG and move it to the plus-ends of microtubules. DLG binds Pins and brings it along for the ride (Siegrist and Doe, 2005). This provides another way for Pins—and associated proteins—to be localized to the cortex independent of the Par proteins.

There are two aspects of spindle positioning that are important for asymmetric NB division. First, the spindle must be rotated to align along the apical-basal axis. This seems to hinge mostly on Pins in the two pathways discussed above. In one pathway, Pins, by its association with $G_{\alpha i}$ and with the Par complex, localizes at the apical cortex. There Pins also interacts with Mud, which forms a connection between the cortex and the Dynein complex (Bowman et al., 2006; Izumi et al., 2006; Siller et al., 2006) (Figure 1A). This likely generates force on the spindle that is necessary to rotate it into place along the apical-basal axis. Consistent with this idea, *mud* mutant NBs sometimes divide orthogonally to the polarity of the epithelium (Cabernard and Doe, 2009). The second Pins pathway, which requires DLG and KHCD73, still allows for "telophase rescue" when NBs divide outside of the apical-basal axis. As a result, Prospero and Brat still segregate to the GMC most of the time (Siegrist and Doe, 2005).

The second aspect of spindle placement relates to the generation of size asymmetry by placing the spindle asymmetrically along the axis of division. Whereas the *C. elegans* zygote achieves this through an unequal tug-of-war between anterior and posterior cortical regions, *Drosophila* NBs use an altogether different mechanism. Visualization of the microtubules in the dividing NB has shown that the apical aster is much larger than the basal. This means that given equal forces generated at each pole, the spindle would settle nearer the basal end of the cell (Figure 1A). This is also, at least in part, dependent upon Pins and its association with microtubules via Mud (Cabernard and Doe, 2009). In *mud* mutants, the spindle can be symmetrically localized along the division axis, though not often, generating daughter cells of equal size to which fate determinants are not properly localized (Cabernard and Doe, 2009). Though aberrant spindle placement in *mud* mutants can result in improper placement of the cleavage furrow, Cabernard, Prehoda and Doe have more recently shown that furrow placement can occur in neuroblasts completely independent of the mitotic spindle (2010).

Drosophila SOP divisions

The SOP gives rise to four distinct cell types that form an organ of the peripheral nervous system that senses mechanical stimulation. Before its first division, the SOP resides within a polarized epithelial sheet (Knoblich, 2008). This polarization provides antero-posterior information, and the first division in the lineage (Gho and Schweisguth, 1998; Lu et al., 1999; Bellaïche et al., 2004) (Figure 1B and C), the division of SOP itself, occurs along this axis forming two distinct pII daughters: pIIb (the anterior daughter) and pIIa (the posterior daughter). These daughters then divide to produce the neuron and sheath cells (pIIb daughters), and the socket and hair cells (pIIa daughters) (Knoblich, 2008). Like the SOP division, the pIIa divides in the antero-posterior axis; however, the division of pIIb, and the division of its daughter pIIIb, are neuroblast-like divisions that align along the apical-basal axis (Roegiers et al., 2001).

The most striking difference between the division of SOPs and that of NBs is the absence of a role for Inscuteable in the former (Figure 1). This dramatically changes the localization of the core polarity complexes. The Par complex localizes to the posterior end of the SOP while $G_{\alpha i}$ and Pins localize to the anterior cortex (Lu et al., 1999; Bellaïche et al., 2001b, 2004; Roegiers et al., 2001). The distribution of these polarity complexes is important for the localization of Partner of Numb (Pon) (Bellaïche et al., 2004) and, of course, Numb (Bellaïche et al., 2001b). Numb does not function as a fate determinant in NBs and their progeny; however, it plays an important role in SOP daughter fate specification. Numb, in response to Pon, localizes to the anterior side of the SOP, and after division it is inherited only by the anterior daughter pIIb. This causes pIIb and pIIa to adopt different fates by affecting signaling between these cells (Rhyu et al., 1994; Bellaïche et al., 2001b). This role of Numb will be discussed in more detail below.

The SOP has an interesting problem related to orientation of its spindle. Though SOP division is symmetrical with respect to size of the daughter cells (making spindle displacement along the antero-posterior axis unnecessary), rotational spindle movement is essential for proper segregation of Numb (Bellaïche et al., 2004). Furthermore, SOP spindles must align not only within the plane of the epithelial sheet (Figure 1C), but also along the antero-posterior axis within this plane (Figure 1B). These movements are guided by the localization of the Par complex, the Pins/$G_{\alpha i}$ complex and their respective interactions with microtubules by association with Mud (Bellaïche et al., 2004). The polarity complexes are localized according to signals provided by the planar-cell-polarity pathway, which will be discussed later.

Signaling in ACD

The initial polarization of a cell is a necessary step taken toward asymmetric division. We have seen a few examples of how cell polarity is translated into unequal segregation of fate determinants into daughter cells, but I will now discuss how the complexes providing polarity information prior to ACD are localized in the first place. The following is a more detailed discussion of the external signals that guide the polarization of the ACDs in the first division of the *C. elegans* zygote and in the division of the *Drosophila* SOP. I will also discuss Notch signaling as it relates to the fate differences between daughters of *Drosophila* SOP divisions.

Sperm as a polarity signal for the one-cell C. elegans embryo
I have discussed the importance of Par complex localization to the anterior cortex prior to the ACD of the one-cell *C. elegans* embryo, and the complementary localization of PAR-1 and PAR-2 to the posterior (Figure 3). I will now describe how this polarity is established.

Initially, PAR-3/PAR-6/PKC-3 are found throughout the cortex of the worm oocyte (Cuenca et al., 2003). The cortex is also covered in an actomyosin sock that becomes very dynamic after fertilization. After sperm entry into the oocyte the cortical surface of the oocyte contracts and the actomyosin mesh begins to retreat from the entry site (Goldstein and Hird, 1996; Wallenfang and Seydoux, 2000; Munro et al., 2004). The localization domain of the Par complex recedes concomitantly with the actomyosin network until the complex ultimately becomes concentrated at the anterior end of the embryo. Simultaneously, the posterior cortex becomes smooth as PAR-1 and PAR-2 localize to the anterior cortical domain that is no longer inhabited by the Par complex (Munro et al., 2004).

The precise signal that the sperm provides appears to be its centrosome (Goldstein and Hird, 1996; O'Connell et al., 2000; Wallenfang and Seydoux, 2000; Cowan and Hyman, 2004). Cortical contraction begins when the centrosome locates to the posterior pole (Cuenca et al., 2003; Cowan and Hyman, 2004; Munro et al., 2004). At least part of the centrosomal signal to the cortex is involved in excluding ECT-2, a Rho-GEF, from the posterior cortex. Exclusion of ECT-2 leads to asymmetric localization of RHO-1 to the anterior cytoplasm of the embryo. Anterior localization of RHO-1 is important for the anteriorly directed flow of the actomyosin network (Motegi and Sugimoto, 2006). Polarization of the embryo can occur even after depletion of γ-tubulin, which seems to prevent the formation of centrosomal microtubules (Cowan and Hyman, 2004), strongly suggesting that it is the centrosome itself that is required to initiate these dynamic movements of the actomyosin network.

PCP signaling in the Drosophila SOP
The planar-cell-polarity (PCP) signaling pathway directs global orientation of cells within an epithelial sheet. One example of this is seen in the *Drosophila* wing. Cells of the wing epithelium are endowed with a single hair. All of the hairs are oriented toward the distal end of the wing, suggesting that proximal-distal information is communicated across the entire wing structure (Goodrich and Strutt, 2011). Indeed, planar-cell-polarity signaling components are arranged along the proximal-distal axis within each cell. The seven-pass transmembrane receptor Frizzled (Fz) localizes to the distal end of cells while the four-pass transmembrane protein Van Gogh (Vang) is found at the proximal side (Tree et al., 2002; Chen et al., 2008; Strutt and Strutt, 2008) (Figure 1B and C). These recruit additional cytosolic proteins—Dishevelled (Dsh) and Prickle (Pk), respectively (Axelrod et al., 1998; Axelrod, 2001; Tree et al., 2002) (Figure 1B and C). In the absence of any of these proteins, uniform orientation of hairs is lost (Wong and Adler, 1993). The extra-cellular portions of Fz and Vang interact (Wu and Mlodzik, 2008); this is how polarity across the epithelial sheet is maintained. The Fz receptor on the distal side of a given cell interacts with Vang that is found in the proximal side of the neighboring cell. The Vang and Pk at the proximal side of the neighboring cell restrict Fz and Dsh to its distal end, where Fz interacts with Vang in the next cell over. In this manner all of the cells of the sheet are aligned within the proximal-distal axis.

The SOP also divides within the plane of an epithelial sheet (Morin and Bellaïche, 2011). Fz and Vang are located at the posterior and anterior sides of the SOP, respectively (Gho and Schweisguth, 1998; Bellaïche et al., 2001a, 2004). Pins and $G_{\alpha i}$ localize with Vang and Pk to the anterior side of the SOP while the Par complex localizes to the posterior side with Fz and Dsh (Bellaïche et al., 2001b) (Figure 1C). In *pins* mutants the spindle tips to assume a more apical-basal orientation, while the spindle assumes a more planar alignment when either Fz or Dsh is missing (David et al., 2005). This suggests that Pins promotes planar alignment of the spindle while Fz and Dsh antagonize the function of Pins in planar spindle alignment.

Though Pins plays a role in planar alignment, it does not appear to be important in antero-posterior spindle alignment (David et al., 2005). However, Fz and Dsh are indispensable for this alignment. In *fz* and *dsh* mutants antero-posterior alignment is lost (David et al., 2005). Alignment is achieved through an interaction between Dsh and the C-terminus of Mud, which interacts with the microtubules of the spindle (Ségalen et al., 2010). Mud is a central component for both planar and antero-posterior alignments as it also interacts with Pins (Ségalen et al., 2010) (Figure 1B and C).

PCP components are essential for aligning the SOP spindle. They also assure that polarity proteins are localized at what will become the divisional poles of SOP (Bellaïche et al., 2001b). Though Pins and the Par complex do not seem to play a role in the antero-posterior alignment of the spindle, it is essential that they be polarized at the anterior and posterior poles of the cell to ensure that Numb, an inhibitor of Notch signaling, is properly segregated to one daughter and not the other (Rhyu et al., 1994; Bellaïche et al., 2001b) (Figure 1B and C). I'll now discuss the role of Notch signaling in generating fate differences between daughters of SOP divisions.

Notch signaling in Drosophila SOP divisions

Notch is a transmembrane transcription factor that acts as a receptor for the Delta/Serrate/LAG-2 (DSL) family of proteins (Fehon et al., 1990). Ligand binds Notch triggering multiple cleavages of the intracellular portion of the receptor, which then travels to the nucleus where it modifies gene transcription (Jarriault et al., 1995; Kopan et al., 1996). Notch signaling is especially important during development of the *Drosophila* nervous system. During the initial specification of neuroblasts cells in the neuroectoderm signal to repress the neuroblast fate in their neighbors. These cells then differentiate as NBs and delaminate from the epithelium (Greenspan, 1990). I will not discuss further how Notch signaling is involved in this early step in NB development, but rather how Notch signaling guides fate choices of SOP progeny.

In the SOP, pIIb (the anterior daughter) inherits Numb—for reasons discussed above (Rhyu et al., 1994; Bellaïche et al., 2001b; Schaefer et al., 2001) (Figure 1B and C). Numb acts as an inhibitor of Notch signaling in this context, therefore, though Notch is present in both cells, signaling occurs only in the posterior daughter pIIa. In *numb* mutants both daughters assume a pIIa-like fate, and when Numb protein is expressed in both cells they both assume a pIIb-like fate (Rhyu et al., 1994).

In the developing *Drosophila* CNS a four-pass transmembrane protein called Sanpodo is required for Notch signaling (Skeath and Doe, 1998). It is likely that Sanpodo is also required for Notch signaling in SOP daughters as regulation of Sanpodo by Numb has been shown to be

important for proper development of the sensory organ. A component of the AP-2 complex—a complex required for targeting transmembrane proteins for endocytosis—α-Adaptin binds Numb and is required for endocytosis of Sanpodo in pIIb cells. In Numb or α-Adaptin mutants Sanpodo is found at the membrane of both pIIb and pIIa (Hutterer and Knoblich, 2005). Furthermore, *α-adaptin* mutants that are unable to bind Numb have similar phenotypes to *numb* mutants in that both SOP daughters assume a pIIa fate (Berdnik et al., 2002). Oddly, it has also been show that *numb* mutant SOP phenotypes can be rescued with Numb transgenes lacking the motifs required for it to bind endocytic proteins, including α-Adaptin (Tang et al., 2005). Despite these seemingly contradictory results, it is very likely that Numb regulates Notch by an endocytosis-dependent mechanism.

ACD in the Q Lineage of *C. elegans*

The nervous system of *Drosophila* and the division of the *C. elegans* zygote have proved to be excellent models for the study of ACD. We now have a very clear picture of how cells assign and maintain polarity, segregate fate determinants prior to division and align their mitotic spindles to allow for asymmetric inheritance of these determinants. We also have an excellent understanding of how various external signals direct these processes. Though many of these themes of ACD are repeated in multiple organisms and developmental contexts, there are still asymmetric divisions that occur by unknown mechanisms. I will now describe more recent work aimed at trying to understand the ACDs of the Q lineage of *C. elegans* (Figure 4).

The neurons of the *C. elegans* nervous system are derived from asymmetric divisions (Sulston and Horvitz, 1977; Sulston et al., 1983). The divisions of the cells Q.a and Q.p—daughters of the Q neuroblast—are two examples of asymmetrically dividing cells that give rise to neurons and apoptotic cells. There are actually two Q neuroblasts in each worm, one on the right side of the worm and one on the left, which divide post-embryonically to ultimately form the mechanosensory neurons AVM or PVM, the interneurons SDQR or SDQL and the oxygen-sensing neurons AQR or PQR. The division of the Q cell generates two sisters Q.a and Q.p. These cells divide, giving rise to daughters that are different in size and fate. In both cases, the smaller cell undergoes apoptosis. In Q.a the larger cell differentiates into the AQR or PQR neuron. In Q.p the surviving daughter is a precursor that divides once more to form the A/PVM and the SDQL/R neurons (Sulston and Horvitz, 1977) (Figure 4).

PIG-1: ortholog of human MELK

Several proteins are known to affect the divisions of the Q lineage, one of which is PIG-1. PIG-1 is a serine/threonine kinase, and is the *C. elegans* ortholog of human Maternal Embryonic Leucine-zipper Kinase (MELK). This kinase functions autonomously in the Q lineage. In *pig-1* mutants, the divisions of Q.p and Q.a—normally asymmetric with respect to the size of the daughters—are symmetric. This defect is well correlated with the *numb*er of mechanosensory neurons and interneurons that the Q.p lineage produces; in *pig-1* mutants, each Q.p division produces extra neurons of each type (Cordes et al., 2006) (Figure 5). This finding suggests that the Q.p daughter that normally dies now, in the mutants, takes the fate of its sister, divides and produces additional neurons. This was observed directly in time-lapse recordings of the divisions. This is in contrast to cell-death mutants (*ced-3*) where both sisters survive, but only

one divides to form neurons (Cordes et al., 2006). These observations suggest a role for PIG-1 in regulating the mitotic fate of Q.p daughters independent of the cell-death fate.

PIG-1 has also been shown to be involved in caspase-independent cell death. When caspases (the downstream effectors of the apoptosis pathway) are missing, cells that normally undergo apoptosis shortly after being generated, were shown to be extruded from the embryo and to die. In PIG-1 these cells did not die and were retained by the embryo. A mechanism was proposed in which PIG-1 normally prevents the cells from expressing adhesion molecules at there surfaces. The kinases LKB1 and PAR-4 were also shown to have positive effects on the ability of these cells to avoid extrusion (Denning et al., 2012). Work in our lab has also shown a role for these kinases in regulating apoptosis in the Q lineage (Jason Chien, unpublished).

Arf small GTPase cycles

Two additional proteins, CNT-2 and GRP-1, are required for ACD in the Q lineage and are thought to regulate Arfs, proteins that cycle between GTP- and GDP-bound states. CNT-2 is an Arf GTPase-activating protein of the AGAP family (Kahn et al., 2008; Singhvi et al., 2011). Its GAP domain is necessary for its function in the Q lineage, suggesting that it regulates an Arf cycle important for ACD (Singhvi et al., 2011). GRP-1 is a member of the cytohesin family of Arf GEFS and is required for fate-specification of Q descendants (Shaun Cordes, unpublished). Like other cytohesins, GRP-1 has a SEC7 domain that is required for ACD in the Q lineage. There is evidence suggesting that GRP-1 functions at the membrane. The SEC7 domain rescues completely the *grp-1* extra-cell phenotype when coupled translationally with an exogenous Pleckstrin Homology (PH) domain (a domain that interacts directly with particular lipids of the inner leaflet of the plasma membrane) (Shaun Cordes, unpublished).

Like PIG-1, CNT-2 and GRP-1 have been shown to act autonomously in the lineage (Singhvi et al., 2011; Shaun Cordes, unpublished). In *cnt-2* and *grp-1* mutants, Q.p daughters are more symmetric in size than in wild-type animals. As is seen in *pig-1* mutants, Q.pp adopts the fate of Q.pa leading to the presence of extra mechanosensory neurons, A/PVM, and extra SDQ interneurons (Figure 5). Not surprisingly, in worms with mutations in some of the genes that code for Arf proteins, extra neurons derived from Q are present. Specifically, mutations in *arf-1* and *arf-6* cause an extra-cell phenotype. Mutations in *arf-1* also suppress the *cnt-2* extra-cell phenotype, suggesting that the GTPase is constitutively active in *cnt-2* mutants and that a normal Arf cycle is necessary for the ability of Q-derived neurons to express their markers (Singhvi et al., 2011). Additional evidence suggests that GRP-1 interacts with an Arf GTPase. Double mutants between *arf-1* and *grp-1* have a more penetrant extra-cell phenotype while *arf-6* does not enhance the *grp-1* extra-cell phenotype suggesting that GRP-1 and ARF-6 function in the same cycle (Shaun Cordes, unpublished). These genetic interactions also hint that GRP-1 and CNT-2 function in separate Arf cycles, though this is not necessarily supported by other genetic evidence.

PIG-1 and GRP-1 genetic pathways

There appear to be two genetic pathways involved in Q lineage ACD: one containing *grp-1*, the other *pig-1*. As stated above, *grp-1* and *cnt-2* seem, genetically, to be in separate Arf cycles; however, *grp-1 cnt-2* double mutants look like *cnt-2* suggesting that they act in the same genetic pathway. Furthermore *cnt-2; pig-1* mutants also look like *cnt-2*. The actual genetic position of

cnt-2 is yet to be determined. We do know that placing *grp-1* and *pig-1* together has an additive effect on cell *numb*er. This is the evidence for *grp-1* and *pig-1* acting in separate pathways. Though there is support for these parallel pathways, the genetic interactions with *cnt-2* suggest that the genetic hierarchy governing ACD in the Q lineage is likely to be more complex.

NMY-2-dependent ACD

Both the Q.a and Q.p daughters of the Q neuroblast divide asymmetrically with respect to size. The posterior daughter of Q.p is smaller than the anterior daughter. This is thought to be achieved by a posterior placement of the mitotic spindle prior to division (Ou et al., 2010). The posterior daughter of Q.a, however, is larger than the anterior daughter.

In lieu of asymmetric spindle displacement, a novel mechanism involving NMY-2, which is the worm non-muscle myosin II ortholog, generates daughter-cell size asymmetry. During Q.a division, NMY-2 accumulates at the cortex of the smaller anterior daughter. NMY-2 then restricts the expansion of the volume of the anterior cell, generating asymmetry. It was also shown that locally inactivating NMY-2 (and perhaps other proteins) at the cortex of the anterior cell leads to a more symmetric division and a loss of the apoptotic fate in the anterior daughter (Ou et al., 2010).

Goals of the Current Project: The Role of TOE-2 and Wnt Signaling in Regulating Neuronal Polarity

Despite the thorough understanding of ACD that has been acquired over the past few decades, there are still mechanisms of ACD that are not well understood. In particular, how the apoptotic fate is assigned to some cells while others survive to terminally differentiate. In order to find genes that regulate apoptosis in the Q.p lineage, the lab has conducted forward-genetic screens looking for mutants that produce extra A/PVM mechanosensory neurons (Figure 5).

One such mutant, *gm396,* was found to have extra and missing neurons. The goal my work was to identify the location of the *gm396* mutation and to understand how the gene product functions in regulating apoptosis in the Q.p lineage and how this relates to what we already know about this process (Figure 4). In an attempt to explain the missing cell phenotype of *gm396* mutants I found that other ACDs in the Q lineage are also affected (Figure 4). We now know that *gm396* results from a missense mutation in *toe-2*, a gene that codes for a DEP domain-containing protein with no previously known function. The following chapter describes my characterization of the role TOE-2 plays in regulating apoptosis in the Q.p lineage, and in regulating ACD in the Q lineage, of *C. elegans*.

In chapter 3 I will discuss neuronal polarity of the PLM mechanosensory neuron as another aspect of asymmetric cell polarization. In particular, I will describe the antagonistic function of two Frizzled receptors, LIN-17 and MIG-1.

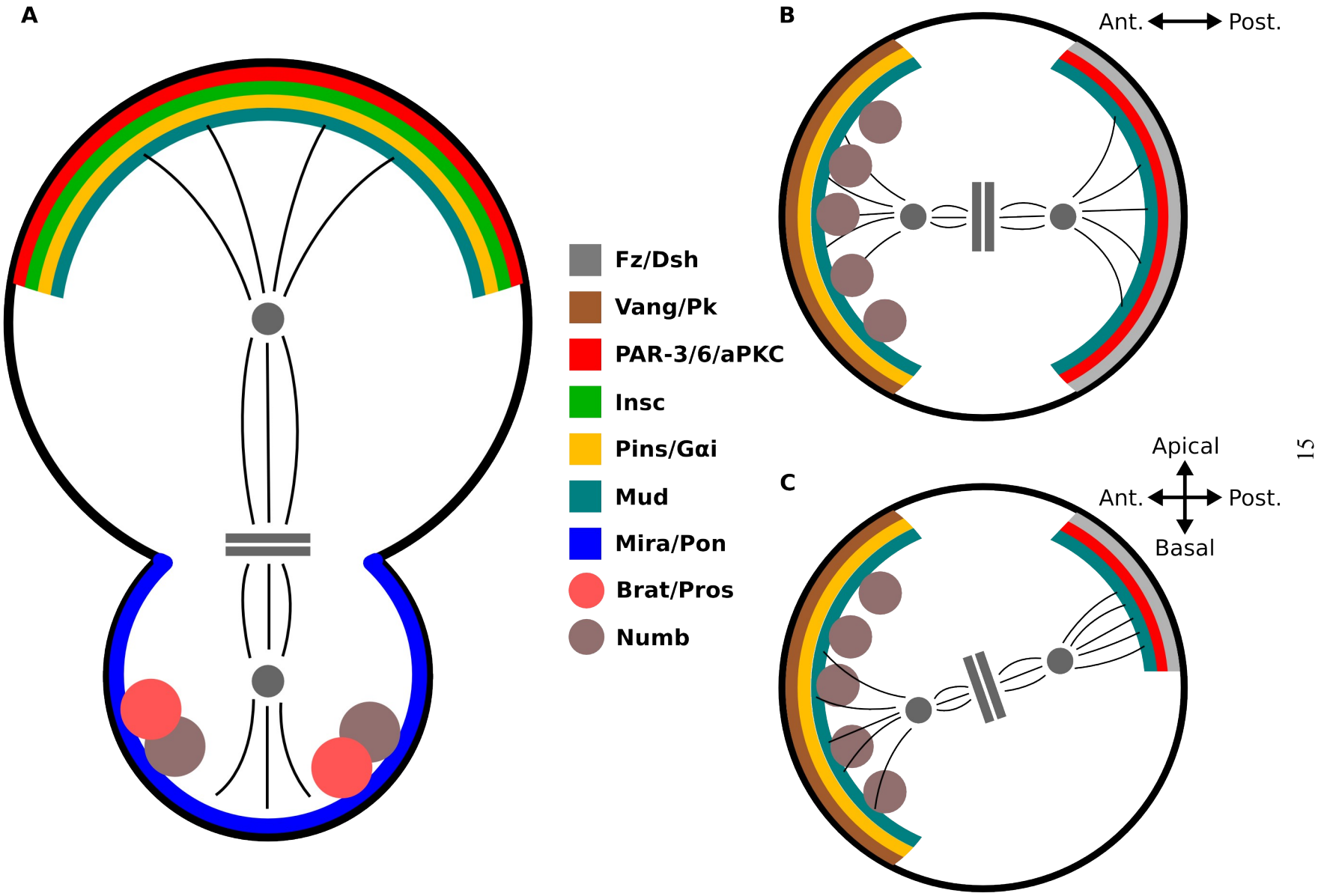
A
B
Ant.
Post.
C
Apical
Ant.
Post.
Basal
Fz/Dsh
Vang/Pk
PAR-3/6/aPKC
Insc
Pins/Gαi
Mud
Mira/Pon
Brat/Pros
Numb

Figure 1: *Drosophila* neuroblast and sensory organ precursor divisions. (A) The Par complex, Pins and $G_{\alpha i}$ localize to the apical (top) membrane of the neuroblast. This co-localization is mediated by Inscuteable (Schaefer et al., 2000; Yu et al., 2000). Pins interacts with Mud, which mediates the connection between Pins and astral microtubules (Cabernard and Doe, 2009). Miranda and Pon localize to the basal membrane of the dividing neuroblast. Their localization is required for the basal localization of determinants Pros, Brat and Numb (Fuerstenberg et al., 1998; Lee et al., 2006b). (B) An apical view of the SOP: Vang and Prickle localize at the anterior membrane while Fzs and Dsh localize at the posterior. The Par complex and Pins/$G_{\alpha i}$ localize to opposite sides of the cell because Inscuteable is not present to mediate their interaction (Lu et al., 1999; Bellaïche et al., 2001a; Roegiers et al., 2001). The Par complex localizes to the posterior side with Dsh. Pins/$G_{\alpha i}$ localize to the anterior side with Pk. Mud is required throughout the cortex for proper spindle orientation (Ségalen et al., 2010). Numb localizes to the anterior side of the SOP and inherited only by the daughter cell pIIb (Rhyu et al., 1994; Bellaïche et al., 2001a; Schaefer et al., 2001). (C) The SOP viewed from the side: Pins is necessary for keeping the mitotic spindle within the plane of the epithelium (David et al., 2005). Fz and Dsh have the opposite function in that they pull the spindle toward a more apical-basal orientation (David et al., 2005). Mud is critical for the interaction between ploarity complexes at the membrane and the microtubules (Ségalen et al., 2010).

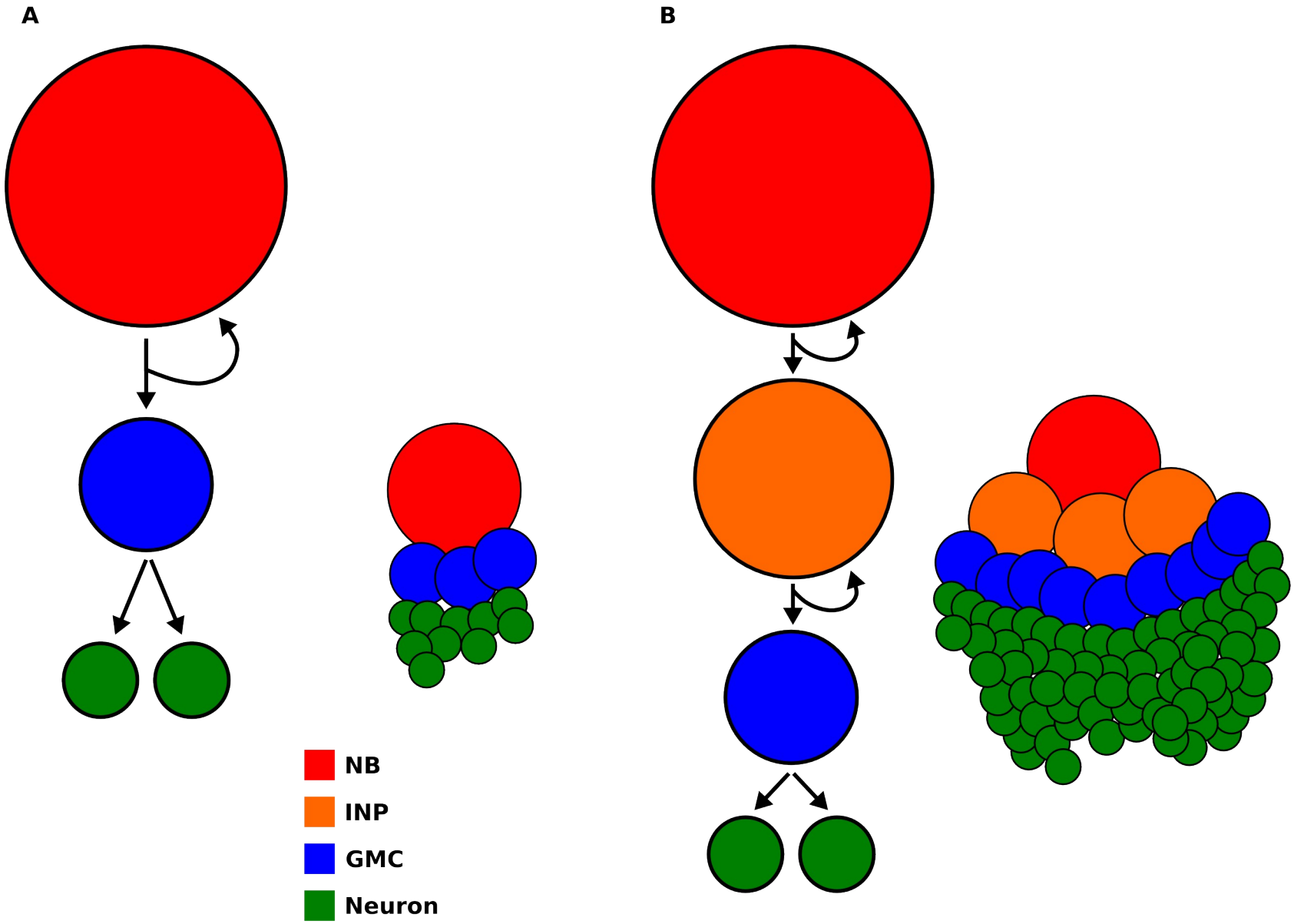
A
B
NB
INP
GMC
Neuron

Figure 2: *Drosophila* neuroblast type I and type II divisions. (A) Embryonic neuroblasts (NB) divide, giving rise to a ganglion mother cell (GMC) and a neural stem cell that retains the NB fate. The GMC divides once, giving rise to neurons and glia. (Betschinger and Knoblich, 2004; Gönczy, 2008; Knoblich, 2010; Morin and Bellaïche, 2011). (B) In larval neuroblast divisions, the NBs give rise to an intermediate neural precursor (INP). INPs divide to form a GMC and another INP cell that retains mitotic potential. INPs give rise to multiple GMCs (reviewed in Homem and Knoblich, 2012).

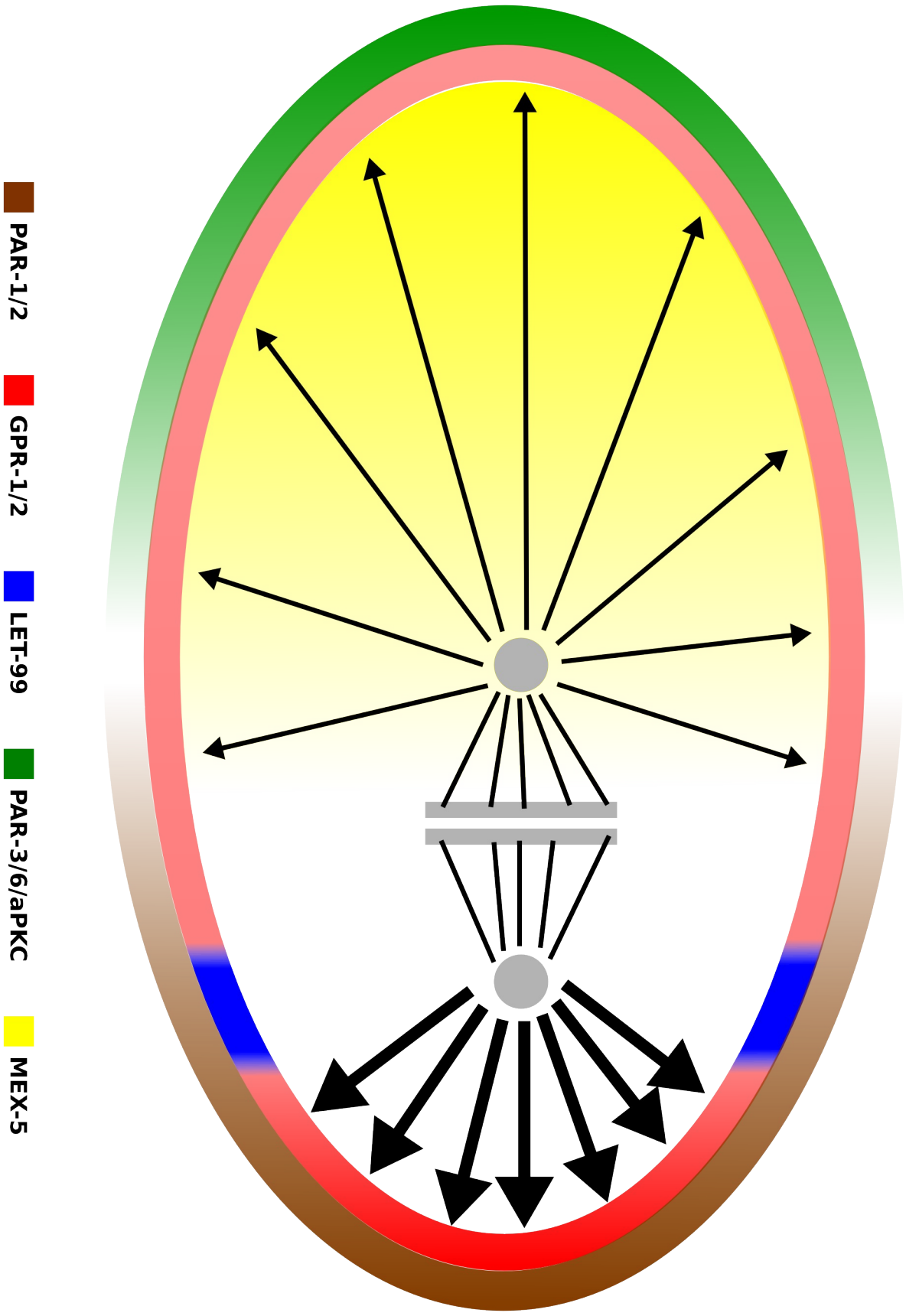
PAR-1/2
GPR-1/2
LET-99
PAR-3/6/aPKC
MEX-5

Figure 3: Asymmetric division in the one-cell *C. elegans* embryo. The embryo is shown anterior side to the left. The Par complex and additional Pars, PAR-1 and PAR-2, segregate to the anterior and posterior poles of the embryo, respectively (Kemphues et al., 1988; Etemad-Moghadam et al., 1995; Rose and Kemphues, 1998a). GPR-1/2 localize throughout the cortex on the anterior and posterior sides (Colombo et al., 2003; Gotta et al., 2003; Srinivasan et al., 2003; Afshar et al., 2004). LET-99 restricts GPR-1/2 from localizing to the posterior-lateral region of the cortex and leads to their concentration at the posterior pole (Tsou et al., 2002, 2003). MEX-5 forms an anterior-high, posterior-low concentration gradient because it is phosphorylated by PAR-1 at the posterior end of the embryo (Tenlen et al., 2008; Daniels et al., 2010). The anterior localization of MEX-5 restrricts PIE-1 to the posterior daughter of the first embryonic division (DeRenzo et al., 2003).

A/PQR
A/PVM
SDQR/L
Q

Figure 4: The Q lineage. The Q neuroblast divides to form anterior and posterior daughters Q.a and Q.p. Each daughter divides again, giving rise to a larger cell and a smaller cell that dies. The larger daughter of Q.a differentiates to become the AQR oxygen-sensing neuron. The larger daughter of Q.p divides again, giving rise to an A/PVM mechanosensory neuron and an SDQ interneuron (Sulston and Horvitz, 1977).

A

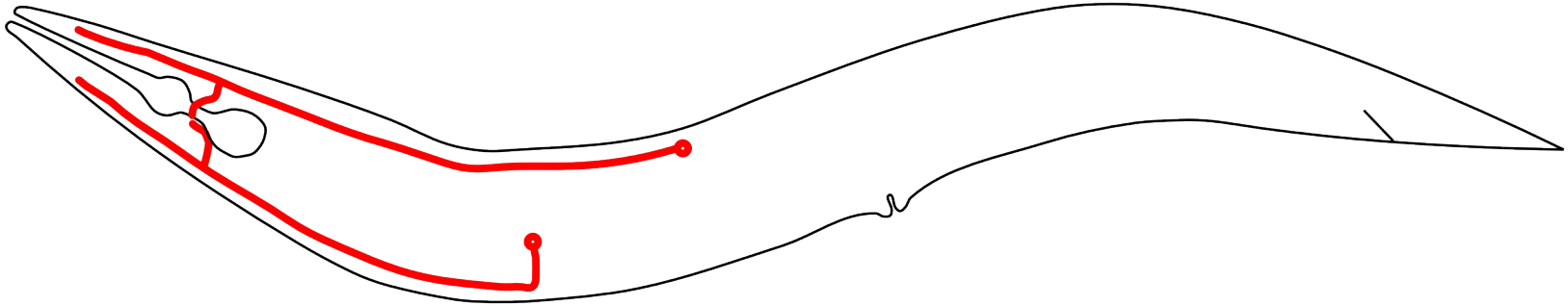

B

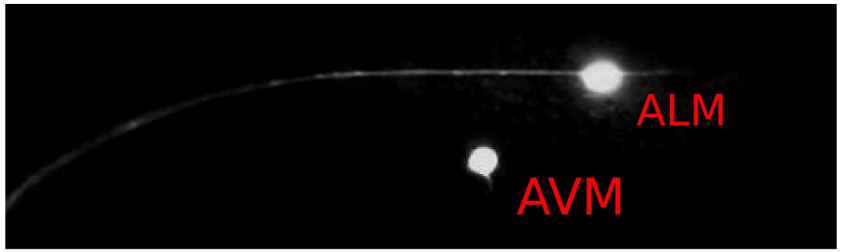

C

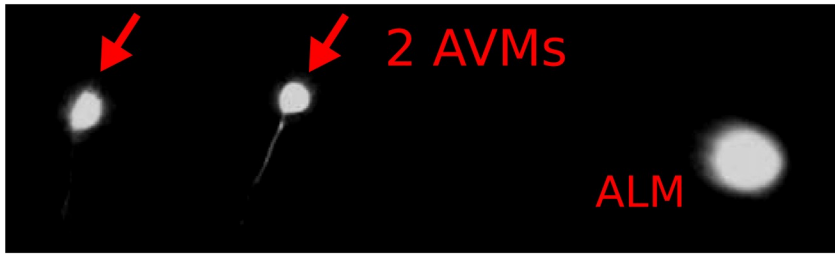

Figure 5: The extra-neuron phenotype of *toe-2* mutants. (A) The worm faces left in the diagram. The ALM and AVM mechanosensory neurons are shown in red. (B) Normally, there is one AVM mechanosensory neuron. (C) In *toe-2* mutants, and others (Cordes et al., 2006; Singhvi et al., 2011), extra AVMs are present.

REFERENCES

Afshar, K., Willard, F.S., Colombo, K., Johnston, C.A., McCudden, C.R., Siderovski, D.P., and Gönczy, P. (**2004**). RIC-8 is required for GPR-1/2-dependent Galpha function during asymmetric division of C. elegans embryos. Cell *119*, 219–230.

Atwood, S.X., and Prehoda, K.E. (**2009**). aPKC phosphorylates Miranda to polarize fate determinants during neuroblast asymmetric cell division. Curr. Biol. *19*, 723–729.

Axelrod, J.D. (**2001**). Unipolar membrane association of Dishevelled mediates Frizzled planar cell polarity signaling. Genes Dev. *15*, 1182–1187.

Axelrod, J.D., Miller, J.R., Shulman, J.M., Moon, R.T., and Perrimon, N. (**1998**). Differential recruitment of Dishevelled provides signaling specificity in the planar cell polarity and Wingless signaling pathways. Genes Dev. *12*, 2610–2622.

Batchelder, C., Dunn, M.A., Choy, B., Suh, Y., Cassie, C., Shim, E.Y., Shin, T.H., Mello, C., Seydoux, G., and Blackwell, T.K. (**1999**). Transcriptional repression by the Caenorhabditis elegans germ-line protein PIE-1. Genes Dev. *13*, 202–212.

Bellaïche, Y., Beaudoin-Massiani, O., Stuttem, I., and Schweisguth, F. (**2004**). The planar cell polarity protein Strabismus promotes Pins anterior localization during asymmetric division of sensory organ precursor cells in Drosophila. Development *131*, 469–478.

Bellaïche, Y., Gho, M., Kaltschmidt, J.A., Brand, A.H., and Schweisguth, F. (**2001a**). Frizzled regulates localization of cell-fate determinants and mitotic spindle rotation during asymmetric cell division. Nat. Cell Biol. *3*, 50–57.

Bellaïche, Y., Radovic, A., Woods, D.F., Hough, C.D., Parmentier, M.L., O'Kane, C.J., Bryant, P.J., and Schweisguth, F. (**2001b**). The Partner of Inscuteable/Discs-large complex is required to establish planar polarity during asymmetric cell division in Drosophila. Cell *106*, 355–366.

Berdnik, D., Török, T., González-Gaitán, M., and Knoblich, J.A. (**2002**). The endocytic protein alpha-Adaptin is required for numb-mediated asymmetric cell division in Drosophila. Dev. Cell *3*, 221–231.

Betschinger, J., and Knoblich, J.A. (**2004**). Dare to be different: asymmetric cell division in Drosophila, C. elegans and vertebrates. Curr. Biol. *14*, R674–685.

Betschinger, J., Mechtler, K., and Knoblich, J.A. (**2006**). Asymmetric segregation of the tumor suppressor brat regulates self-renewal in Drosophila neural stem cells. Cell *124*, 1241–1253.

Bowman, S.K., Neumüller, R.A., Novatchkova, M., Du, Q., and Knoblich, J.A. (**2006**). The Drosophila NuMA Homolog Mud regulates spindle orientation in asymmetric cell division. Dev. Cell *10*, 731–742.

Cabernard, C., and Doe, C.Q. (**2009**). Apical/basal spindle orientation is required for neuroblast homeostasis and neuronal differentiation in Drosophila. Dev. Cell *17*, 134–141.

Cabernard, C., Prehoda, K.E., and Doe, C.Q. (**2010**). A spindle-independent cleavage furrow positioning pathway. Nature *467*, 91–94.

Chen, W.-S., Antic, D., Matis, M., Logan, C.Y., Povelones, M., Anderson, G.A., Nusse, R., and Axelrod, J.D. (**2008**). Asymmetric homotypic interactions of the atypical cadherin flamingo mediate intercellular polarity signaling. Cell *133*, 1093–1105.

Chia, W., and Yang, X. (**2002**). Asymmetric division of Drosophila neural progenitors. Curr. Opin. Genet. Dev. *12*, 459–464.

Colombo, K., Grill, S.W., Kimple, R.J., Willard, F.S., Siderovski, D.P., and Gönczy, P. (**2003**). Translation of polarity cues into asymmetric spindle positioning in Caenorhabditis elegans embryos. Science *300*, 1957–1961.

Conklin, E.G. (**1905**). The Organization and Cell-lineage of the Ascidian Egg. J. Acad. Nat. Sci. Philadelphia *13*, 1–119.

Cordes, S., Frank, C.A., and Garriga, G. (**2006**). The C. elegans MELK ortholog PIG-1 regulates cell size asymmetry and daughter cell fate in asymmetric neuroblast divisions. Development *133*, 2747–2756.

Cowan, C.R., and Hyman, A.A. (**2004**). Centrosomes direct cell polarity independently of microtubule assembly in C. elegans embryos. Nature *431*, 92–96.

Cuenca, A.A., Schetter, A., Aceto, D., Kemphues, K., and Seydoux, G. (**2003**). Polarization of the C. elegans zygote proceeds via distinct establishment and maintenance phases. Development *130*, 1255–1265.

Daniels, B.R., Dobrowsky, T.M., Perkins, E.M., Sun, S.X., and Wirtz, D. (**2010**). MEX-5 enrichment in the C. elegans early embryo mediated by differential diffusion. Development *137*, 2579–2585.

Daniels, B.R., Perkins, E.M., Dobrowsky, T.M., Sun, S.X., and Wirtz, D. (**2009**). Asymmetric enrichment of PIE-1 in the Caenorhabditis elegans zygote mediated by binary counterdiffusion. J. Cell Biol. *184*, 473–479.

Darwin, C. (**1859**). Chapter IV. In On the Origin of Species, (London: John Murray), p. 123.

David, N.B., Martin, C.A., Segalen, M., Rosenfeld, F., Schweisguth, F., and Bellaïche, Y. (**2005**). Drosophila Ric-8 regulates Galphai cortical localization to promote Galphai-dependent planar orientation of the mitotic spindle during asymmetric cell division. Nat. Cell Biol. *7*, 1083–1090.

Denning, D.P., Hatch, V., and Horvitz, H.R. (**2012**). Programmed elimination of cells by caspase-independent cell extrusion in C. elegans. Nature *488*, 226–230.

DeRenzo, C., Reese, K.J., and Seydoux, G. (**2003**). Exclusion of germ plasm proteins from somatic lineages by cullin-dependent degradation. Nature *424*, 685–689.

Doe, C.Q., Chu-LaGraff, Q., Wright, D.M., and Scott, M.P. (**1991**). The prospero gene specifies cell fates in the Drosophila central nervous system. Cell *65*, 451–464.

Draper, B.W., Mello, C.C., Bowerman, B., Hardin, J., and Priess, J.R. (**1996**). MEX-3 is a KH domain protein that regulates blastomere identity in early C. elegans embryos. Cell *87*, 205–216.

Edgar, L.G., Carr, S., Wang, H., and Wood, W.B. (**2001**). Zygotic expression of the caudal homolog pal-1 is required for posterior patterning in Caenorhabditis elegans embryogenesis. Dev. Biol. *229*, 71–88.

Etemad-Moghadam, B., Guo, S., and Kemphues, K.J. (**1995**). Asymmetrically distributed PAR-3 protein contributes to cell polarity and spindle alignment in early C. elegans embryos. Cell *83*, 743–752.

Fehon, R.G., Kooh, P.J., Rebay, I., Regan, C.L., Xu, T., Muskavitch, M.A., and Artavanis-Tsakonas, S. (**1990**). Molecular interactions between the protein products of the neurogenic loci Notch and Delta, two EGF-homologous genes in Drosophila. Cell *61*, 523–534.

Fuerstenberg, S., Peng, C.Y., Alvarez-Ortiz, P., Hor, T., and Doe, C.Q. (**1998**). Identification of Miranda protein domains regulating asymmetric cortical localization, cargo binding, and cortical release. Mol. Cell. Neurosci. *12*, 325–339.

Gho, M., and Schweisguth, F. (**1998**). Frizzled signalling controls orientation of asymmetric sense organ precursor cell divisions in Drosophila. Nature *393*, 178–181.

Ghosh, D., and Seydoux, G. (**2008**). Inhibition of transcription by the Caenorhabditis elegans germline protein PIE-1: genetic evidence for distinct mechanisms targeting initiation and elongation. Genetics *178*, 235–243.

Goldstein, B., and Hird, S.N. (**1996**). Specification of the anteroposterior axis in Caenorhabditis elegans. Development *122*, 1467–1474.

Gönczy, P. (**2008**). Mechanisms of asymmetric cell division: flies and worms pave the way. Nat. Rev. Mol. Cell Biol. *9*, 355–366.

Goodrich, L.V., and Strutt, D. (**2011**). Principles of planar polarity in animal development. Development *138*, 1877–1892.

Gotta, M., and Ahringer, J. (**2001**). Distinct roles for Galpha and Gbetagamma in regulating spindle position and orientation in Caenorhabditis elegans embryos. Nat. Cell Biol. *3*, 297–300.

Gotta, M., Dong, Y., Peterson, Y.K., Lanier, S.M., and Ahringer, J. (**2003**). Asymmetrically distributed C. elegans homologs of AGS3/PINS control spindle position in the early embryo. Curr. Biol. *13*, 1029–1037.

Greenspan, R.J. (**1990**). The Notch gene, adhesion, and developmental fate in the Drosophila embryo. New Biol. *2*, 595–600.

Griffin, E.E., Odde, D.J., and Seydoux, G. (**2011**). Regulation of the MEX-5 gradient by a spatially segregated kinase/phosphatase cycle. Cell *146*, 955–968.

Hirata, J., Nakagoshi, H., Nabeshima, Y., and Matsuzaki, F. (**1995**). Asymmetric segregation of the homeodomain protein Prospero during Drosophila development. Nature *377*, 627–630.

Homem, C.C.F., and Knoblich, J.A. (**2012**). Drosophila neuroblasts: a model for stem cell biology. Development *139*, 4297–4310.

Horvitz, H.R., and Herskowitz, I. (**1992**). Mechanisms of asymmetric cell division: two Bs or not two Bs, that is the question. Cell *68*, 237–255.

Huang, N.N., Mootz, D.E., Walhout, A.J.M., Vidal, M., and Hunter, C.P. (**2002**). MEX-3 interacting proteins link cell polarity to asymmetric gene expression in Caenorhabditis elegans. Development *129*, 747–759.

Hung, T.J., and Kemphues, K.J. (**1999**). PAR-6 is a conserved PDZ domain-containing protein that colocalizes with PAR-3 in Caenorhabditis elegans embryos. Development *126*, 127–135.

Hunter, C.P., Harris, J.M., Maloof, J.N., and Kenyon, C. (**1999**). Hox gene expression in a single Caenorhabditis elegans cell is regulated by a caudal homolog and intercellular signals that inhibit wnt signaling. Development *126*, 805–814.

Hunter, C.P., and Kenyon, C. (**1996**). Spatial and temporal controls target pal-1 blastomere-specification activity to a single blastomere lineage in C. elegans embryos. Cell *87*, 217–226.

Hutterer, A., and Knoblich, J.A. (**2005**). Numb and alpha-Adaptin regulate Sanpodo endocytosis to specify cell fate in Drosophila external sensory organs. EMBO Rep. *6*, 836–842.

Ikeshima-Kataoka, H., Skeath, J.B., Nabeshima, Y., Doe, C.Q., and Matsuzaki, F. (**1997**). Miranda directs Prospero to a daughter cell during Drosophila asymmetric divisions. Nature *390*, 625–629.

Izumi, Y., Ohta, N., Hisata, K., Raabe, T., and Matsuzaki, F. (**2006**). Drosophila Pins-binding protein Mud regulates spindle-polarity coupling and centrosome organization. Nat. Cell Biol. *8*, 586–593.

Jan, Y.N., and Jan, L.Y. (**2001**). Asymmetric cell division in the Drosophila nervous system. Nat. Rev. Neurosci. *2*, 772–779.

Jarriault, S., Brou, C., Logeat, F., Schroeter, E.H., Kopan, R., and Israel, A. (**1995**). Signalling downstream of activated mammalian Notch. Nature *377*, 355–358.

Kahn, R.A., Bruford, E., Inoue, H., Logsdon, J.M., Jr, Nie, Z., Premont, R.T., Randazzo, P.A., Satake, M., Theibert, A.B., Zapp, M.L., et al. (**2008**). Consensus nomenclature for the human ArfGAP domain-containing proteins. J. Cell Biol. *182*, 1039–1044.

Kemphues, K.J., Priess, J.R., Morton, D.G., and Cheng, N.S. (**1988**). Identification of genes required for cytoplasmic localization in early C. elegans embryos. Cell *52*, 311–320.

Knoblich, J.A. (**2008**). Mechanisms of asymmetric stem cell division. Cell *132*, 583–597.

Knoblich, J.A. (**2010**). Asymmetric cell division: recent developments and their implications for tumour biology. Nat. Rev. Mol. Cell Biol. *11*, 849–860.

Kopan, R., Schroeter, E.H., Weintraub, H., and Nye, J.S. (**1996**). Signal transduction by activated mNotch: importance of proteolytic processing and its regulation by the extracellular domain. Proc. Natl. Acad. Sci. U.S.A. *93*, 1683–1688.

Kuwada, J.Y., and Goodman, C.S. (**1985**). Neuronal determination during embryonic development of the grasshopper nervous system. Dev. Biol. *110*, 114–126.

Lee, C.-Y., Andersen, R.O., Cabernard, C., Manning, L., Tran, K.D., Lanskey, M.J., Bashirullah, A., and Doe, C.Q. (**2006a**). Drosophila Aurora-A kinase inhibits neuroblast self-renewal by regulating aPKC/Numb cortical polarity and spindle orientation. Genes Dev. *20*, 3464–3474.

Lee, C.-Y., Wilkinson, B.D., Siegrist, S.E., Wharton, R.P., and Doe, C.Q. (**2006b**). Brat Is a Miranda Cargo Protein that Promotes Neuronal Differentiation and Inhibits Neuroblast Self-Renewal. Developmental Cell *10*, 441–449.

Li, L., and Vaessin, H. (**2000**). Pan-neural Prospero terminates cell proliferation during Drosophila neurogenesis. Genes Dev. *14*, 147–151.

Lu, B., Usui, T., Uemura, T., Jan, L., and Jan, Y.N. (**1999**). Flamingo controls the planar polarity of sensory bristles and asymmetric division of sensory organ precursors in Drosophila. Curr. Biol. *9*, 1247–1250.

Matsuzaki, F., Ohshiro, T., Ikeshima-Kataoka, H., and Izumi, H. (**1998**). miranda localizes staufen and prospero asymmetrically in mitotic neuroblasts and epithelial cells in early Drosophila embryogenesis. Development *125*, 4089–4098.

Mello, C.C., Schubert, C., Draper, B., Zhang, W., Lobel, R., and Priess, J.R. (**1996**). The PIE-1 protein and germline specification in C. elegans embryos. Nature *382*, 710–712.

Merdes, A., Ramyar, K., Vechio, J.D., and Cleveland, D.W. (**1996**). A complex of NuMA and cytoplasmic dynein is essential for mitotic spindle assembly. Cell *87*, 447–458.

Miller, K.G., and Rand, J.B. (**2000**). A role for RIC-8 (Synembryn) and GOA-1 (G(o)alpha) in regulating a subset of centrosome movements during early embryogenesis in Caenorhabditis elegans. Genetics *156*, 1649–1660.

Morin, X., and Bellaïche, Y. (**2011**). Mitotic spindle orientation in asymmetric and symmetric cell divisions during animal development. Dev. Cell *21*, 102–119.

Motegi, F., and Sugimoto, A. (**2006**). Sequential functioning of the ECT-2 RhoGEF, RHO-1 and CDC-42 establishes cell polarity in Caenorhabditis elegans embryos. Nat. Cell Biol. *8*, 978–985.

Munro, E., Nance, J., and Priess, J.R. (**2004**). Cortical flows powered by asymmetrical contraction transport PAR proteins to establish and maintain anterior-posterior polarity in the early C. elegans embryo. Dev. Cell *7*, 413–424.

Nguyen-Ngoc, T., Afshar, K., and Gönczy, P. (**2007**). Coupling of cortical dynein and G alpha proteins mediates spindle positioning in Caenorhabditis elegans. Nat. Cell Biol. *9*, 1294–1302.

O'Connell, K.F., Maxwell, K.N., and White, J.G. (**2000**). The spd-2 gene is required for polarization of the anteroposterior axis and formation of the sperm asters in the Caenorhabditis elegans zygote. Dev. Biol. *222*, 55–70.

Ou, G., Stuurman, N., D'Ambrosio, M., and Vale, R.D. (**2010**). Polarized myosin produces unequal-size daughters during asymmetric cell division. Science *330*, 677–680.

Parmentier, M.L., Woods, D., Greig, S., Phan, P.G., Radovic, A., Bryant, P., and O'Kane, C.J. (**2000**). Rapsynoid/partner of inscuteable controls asymmetric division of larval neuroblasts in Drosophila. J. Neurosci. *20*, RC84.

Peng, C.Y., Manning, L., Albertson, R., and Doe, C.Q. (**2000**). The tumour-suppressor genes lgl and dlg regulate basal protein targeting in Drosophila neuroblasts. Nature *408*, 596–600.

Reese, K.J., Dunn, M.A., Waddle, J.A., and Seydoux, G. (**2000**). Asymmetric segregation of PIE-1 in C. elegans is mediated by two complementary mechanisms that act through separate PIE-1 protein domains. Mol. Cell *6*, 445–455.

Rhyu, M.S., Jan, L.Y., and Jan, Y.N. (**1994**). Asymmetric distribution of numb protein during division of the sensory organ precursor cell confers distinct fates to daughter cells. Cell *76*, 477–491.

Roegiers, F., Younger-Shepherd, S., Jan, L.Y., and Jan, Y.N. (**2001**). Two types of asymmetric divisions in the Drosophila sensory organ precursor cell lineage. Nat. Cell Biol. *3*, 58–67.

Rose, L.S., and Kemphues, K. (**1998a**). The let-99 gene is required for proper spindle orientation during cleavage of the C. elegans embryo. Development *125*, 1337–1346.

Rose, L.S., and Kemphues, K.J. (**1998b**). Early patterning of the C. elegans embryo. Annu. Rev. Genet. *32*, 521–545.

Schaefer, M., Petronczki, M., Dorner, D., Forte, M., and Knoblich, J.A. (**2001**). Heterotrimeric G proteins direct two modes of asymmetric cell division in the Drosophila nervous system. Cell *107*, 183–194.

Schaefer, M., Shevchenko, A., Shevchenko, A., and Knoblich, J.A. (**2000**). A protein complex containing Inscuteable and the Galpha-binding protein Pins orients asymmetric cell divisions in Drosophila. Curr. Biol. *10*, 353–362.

Schober, M., Schaefer, M., and Knoblich, J.A. (**1999**). Bazooka recruits Inscuteable to orient asymmetric cell divisions in Drosophila neuroblasts. Nature *402*, 548–551.

Schroer, T.A., Steuer, E.R., and Sheetz, M.P. (**1989**). Cytoplasmic dynein is a minus end-directed motor for membranous organelles. Cell *56*, 937–946.

Schubert, C.M., Lin, R., de Vries, C.J., Plasterk, R.H., and Priess, J.R. (**2000**). MEX-5 and MEX-6 function to establish soma/germline asymmetry in early C. elegans embryos. Mol. Cell *5*, 671–682.

Ségalen, M., Johnston, C.A., Martin, C.A., Dumortier, J.G., Prehoda, K.E., David, N.B., Doe, C.Q., and Bellaïche, Y. (**2010**). The Fz-Dsh planar cell polarity pathway induces oriented cell division via Mud/NuMA in Drosophila and zebrafish. Dev. Cell *19*, 740–752.

Shen, C.P., Jan, L.Y., and Jan, Y.N. (**1997**). Miranda is required for the asymmetric localization of Prospero during mitosis in Drosophila. Cell *90*, 449–458.

Shen, C.P., Knoblich, J.A., Chan, Y.M., Jiang, M.M., Jan, L.Y., and Jan, Y.N. (**1998**). Miranda as a multidomain adapter linking apically localized Inscuteable and basally localized Staufen and Prospero during asymmetric cell division in Drosophila. Genes Dev. *12*, 1837–1846.

Siegrist, S.E., and Doe, C.Q. (**2005**). Microtubule-induced Pins/Galphai cortical polarity in Drosophila neuroblasts. Cell *123*, 1323–1335.

Siller, K.H., Cabernard, C., and Doe, C.Q. (**2006**). The NuMA-related Mud protein binds Pins and regulates spindle orientation in Drosophila neuroblasts. Nat. Cell Biol. *8*, 594–600.

Siller, K.H., and Doe, C.Q. (**2009**). Spindle orientation during asymmetric cell division. Nature Cell Biology *11*, 365–374.

Singhvi, A., Teuliere, J., Talavera, K., Cordes, S., Ou, G., Vale, R.D., Prasad, B.C., Clark, S.G., and Garriga, G. (**2011**). The Arf GAP CNT-2 regulates the apoptotic fate in C. elegans asymmetric neuroblast divisions. Curr. Biol. *21*, 948–954.

Skeath, J.B., and Doe, C.Q. (**1998**). Sanpodo and Notch act in opposition to Numb to distinguish sibling neuron fates in the Drosophila CNS. Development *125*, 1857–1865.

Sonoda, J., and Wharton, R.P. (**2001**). Drosophila Brain Tumor is a translational repressor. Genes Dev. *15*, 762–773.

Spana, E.P., and Doe, C.Q. (**1995**). The prospero transcription factor is asymmetrically localized to the cell cortex during neuroblast mitosis in Drosophila. Development *121*, 3187–3195.

Spencer, H. (**1864**). Part II: Chapter II: Development. In The Principles of Biology, (Edinburgh: Williams and Norgate), pp. 141–142.

Spencer, H. (**1898a**). First Principles (New York: D. Appleton and Company).

Spencer, H. (**1898b**). Part II: Chapter XV. In First Principles, (New York: D. Appleton and Company), pp. 344–347.

Srinivasan, D.G., Fisk, R.M., Xu, H., and van den Heuvel, S. (**2003**). A complex of LIN-5 and GPR proteins regulates G protein signaling and spindle function in C elegans. Genes Dev. *17*, 1225–1239.

Strutt, H., and Strutt, D. (**2008**). Differential stability of flamingo protein complexes underlies the establishment of planar polarity. Curr. Biol. *18*, 1555–1564.

Sulston, J.E., and Horvitz, H.R. (**1977**). Post-embryonic cell lineages of the nematode, Caenorhabditis elegans. Dev. Biol. *56*, 110–156.

Sulston, J.E., Schierenberg, E., White, J.G., and Thomson, J.N. (**1983**). The embryonic cell lineage of the nematode Caenorhabditis elegans. Dev. Biol. *100*, 64–119.

Tabuse, Y., Izumi, Y., Piano, F., Kemphues, K.J., Miwa, J., and Ohno, S. (**1998**). Atypical protein kinase C cooperates with PAR-3 to establish embryonic polarity in Caenorhabditis elegans. Development *125*, 3607–3614.

Takesono, A., Cismowski, M.J., Ribas, C., Bernard, M., Chung, P., Hazard, S., 3rd, Duzic, E., and Lanier, S.M. (**1999**). Receptor-independent activators of heterotrimeric G-protein signaling pathways. J. Biol. Chem. *274*, 33202–33205.

Tang, H., Rompani, S.B., Atkins, J.B., Zhou, Y., Osterwalder, T., and Zhong, W. (**2005**). Numb proteins specify asymmetric cell fates via an endocytosis- and proteasome-independent pathway. Mol. Cell. Biol. *25*, 2899–2909.

Tenlen, J.R., Molk, J.N., London, N., Page, B.D., and Priess, J.R. (**2008**). MEX-5 asymmetry in one-cell C. elegans embryos requires PAR-4- and PAR-1-dependent phosphorylation. Development *135*, 3665–3675.

Tree, D.R.P., Shulman, J.M., Rousset, R., Scott, M.P., Gubb, D., and Axelrod, J.D. (**2002**). Prickle mediates feedback amplification to generate asymmetric planar cell polarity signaling. Cell *109*, 371–381.

Tsou, M.-F.B., Hayashi, A., DeBella, L.R., McGrath, G., and Rose, L.S. (**2002**). LET-99 determines spindle position and is asymmetrically enriched in response to PAR polarity cues in C. elegans embryos. Development *129*, 4469–4481.

Tsou, M.-F.B., Hayashi, A., and Rose, L.S. (**2003**). LET-99 opposes Gα/GPR signaling to generate asymmetry for spindle positioning in response to PAR and MES-1/SRC-1 signaling. Development *130*, 5717–5730.

Uemura, T., Shepherd, S., Ackerman, L., Jan, L.Y., and Jan, Y.N. (**1989**). numb, a gene required in determination of cell fate during sensory organ formation in Drosophila embryos. Cell *58*, 349–360.

Wallenfang, M.R., and Seydoux, G. (**2000**). Polarization of the anterior-posterior axis of C. elegans is a microtubule-directed process. Nature *408*, 89–92.

Wang, C., Li, S., Januschke, J., Rossi, F., Izumi, Y., Garcia-Alvarez, G., Gwee, S.S.L., Soon, S.B., Sidhu, H.K., Yu, F., et al. (**2011**). An ana2/ctp/mud complex regulates spindle orientation in Drosophila neuroblasts. Dev. Cell *21*, 520–533.

Wang, H., Somers, G.W., Bashirullah, A., Heberlein, U., Yu, F., and Chia, W. (**2006**). Aurora-A acts as a tumor suppressor and regulates self-renewal of Drosophila neuroblasts. Genes Dev. *20*, 3453–3463.

Waring, D.A., and Kenyon, C. (**1991**). Regulation of cellular responsiveness to inductive signals in the developing C. elegans nervous system. Nature *350*, 712–715.

Willard, F.S., Kimple, R.J., and Siderovski, D.P. (**2004**). Return of the GDI: the GoLoco motif in cell division. Annu. Rev. Biochem. *73*, 925–951.

Wodarz, A., Ramrath, A., Grimm, A., and Knust, E. (**2000**). Drosophila atypical protein kinase C associates with Bazooka and controls polarity of epithelia and neuroblasts. J. Cell Biol. *150*, 1361–1374.

Wodarz, A., Ramrath, A., Kuchinke, U., and Knust, E. (**1999**). Bazooka provides an apical cue for Inscuteable localization in Drosophila neuroblasts. Nature *402*, 544–547.

Wong, L.L., and Adler, P.N. (**1993**). Tissue polarity genes of Drosophila regulate the subcellular location for prehair initiation in pupal wing cells. J. Cell Biol. *123*, 209–221.

Wu, J., and Mlodzik, M. (**2008**). The frizzled extracellular domain is a ligand for Van Gogh/Stbm during nonautonomous planar cell polarity signaling. Dev. Cell *15*, 462–469.

Yu, F., Morin, X., Cai, Y., Yang, X., and Chia, W. (**2000**). Analysis of partner of inscuteable, a novel player of Drosophila asymmetric divisions, reveals two distinct steps in inscuteable apical localization. Cell *100*, 399–409.

Zhang, F., Barboric, M., Blackwell, T.K., and Peterlin, B.M. (**2003**). A model of repression: CTD analogs and PIE-1 inhibit transcriptional elongation by P-TEFb. Genes Dev. *17*, 748–758.

CHAPTER 2

THE ROLE OF TOE-2 IN APOPTOSIS AND ASYMMETRIC CELL DIVISION

Contributions to this chapter:
Karla Talavera isolated *gm396* in the forward-genetic screen for mutants with extra neurons and generated the SNP-mapping data for *gm396*. Jérôme Teulière and Jason Chien generated the *gmIs81* transgene. Jérôme Teulière provided the cell-number data for *zdIs5; pig-1(gm301)* and *ced-3(n717); gmIs81*. Te-Wen Lo generated and injected the mRNA used in the TALENs experiments.

SUMMARY

While we understand how cells die in *C. elegans*, we know much less about how cells are instructed to adopt the apoptotic fate. To address this issue, we study the Q.p neuroblast, which divides to produce a larger anterior cell and a smaller posterior cell that dies. The surviving Q.p daughter divides again to form the neurons A/PVM and SDQ. We conducted a forward-genetic screen for mutants with extra A/PVMs in order to identify genes that regulate the apoptotic fate. I identified a mutation in the gene *toe-2*, which encodes a target of the worm ERK ortholog, MPK-1. I found that TOE-2 not only regulates the apoptotic fate of the posterior Q.p daughter, but it also plays a role in the asymmetric division of Q, the mother of Q.p. I found that TOE-2 functions autonomously in the Q lineage where it regulates several asymmetric cell divisions (ACDs). I also show that, during Q lineage cell divisions, TOE-2 localizes to centrosomes, to the posterior cortex and at the site where the cleavage furrow will form.

INTRODUCTION

In 1842, Carl Christoph Vogt first described what we now call apoptosis in his study of the development of *Alytes obstetricans*, the common midwife toad. During a study of the developing spinal column he became curious about whether the cells of the notochord transformed to become the cartilaginous tissue that formed the vertebrae or whether the notochord was destroyed to make way for new vertebral tissue. He observed that these were distinct tissues and that as the newly developing vertebral tissue encroached upon the cells of the notochord these cells shrunk until ultimately, they were "absorbed" (Vogt, 1842). And he seems to have left it at that. Thanks to a renewed interest in apoptosis during the 20th century, we now know much more about the process at the cytological and molecular levels.

At the cellular level, apoptosis is characterized by condensation of chromatin in the nucleus and a reduction in the amount of cytoplasm in the cell. As a consequence organelles become tightly packed until the cell begins to fragment in a process called "budding," which leads to the formation of multiple apoptotic bodies that contain organelles and bits of nuclear membrane and chromatin (reviewed in Elmore, 2007). The outer leaflets of apoptotic body plasma membranes contain phosphatidylserine (PS), a component of phospholipids that is usually kept on the cytoplasmic side of the membrane. The exposure of PS to the extracellular environment acts as a recognition signal and trigger to cells that will engulf the apoptotic bodies (Fadok et al., 1992; Bratton et al., 1997).

The genes that encode the central components of the apoptotic pathway were first discovered in *C. elegans* (Ellis and Horvitz, 1986; Hengartner et al., 1992; Hengartner and Horvitz, 1994; Conradt and Horvitz, 1998). Mammalian orthologs exist for all of the genes in the pathway (Yuan et al., 1993; Zou et al., 1997; Bouillet and Strasser, 2002), though there are some differences in the ways the apoptotic pathways of *C. elegans* and mammals function.

Caspases are the ultimate downstream components of the pathway and initiate the various cellular processes involved in apoptosis of the cell (e.g. DNA fragmentation and export of proteins from the mitochondrion) (reviewed in Elmore, 2007). Forming a family of cysteine proteases, caspases exist in procaspase and activated forms and promote apoptosis by cleaving

specific substrates involved in cellular processes. Some caspases have autocatalytic activity, which converts the caspase proenzyme to an active protease that can cleave other caspases to initiate a cascade (reviewed in Elmore, 2007). Multiple caspases have been identified in *C. elegans* and have been shown to be able to enzymatically cleave one another (Shaham, 1998) though only *ced-3* has been shown to have a clear role in apoptosis. In mammals, caspases are divided into two groups: initiator and effector caspases. Caspases 3, 6 and 7 are effector caspases, whose activity ultimately leads to apoptosis; however, they must be cleaved by initiator caspases before becoming active (Elmore, 2007; Verbrugge et al., 2010).

Apaf-1 (CED-4 in worms) is required for activation of the auto-catalytic activity of the caspases. In the current model, the Bcl-2 ortholog CED-9 binds and sequesters CED-4 to the cytoplasmic surface of mitochondria (Chinnaiyan et al., 1997; Spector et al., 1997; Wu et al., 1997; Chen et al., 2000). CED-3 is only activated when the BH3-only ortholog EGL-1 competes with CED-4 for binding of CED-9, leading to release CED-4 from the mitochondrial surface and subsequent activation of the CED-3 caspase (Conradt and Horvitz, 1998; del Peso et al., 1998; Chen et al., 2000; Parrish et al., 2000; Yan et al., 2004).

In mammals Apaf-1 and the initiator caspase, Caspase 9, form a complex called the apoptosome (Hill et al., 2004). In the apoptosome, Caspase 9 auto-activates, and active Caspase 9 then cleaves the effector procaspases 3, 6 and 7 (reviewed in Verbrugge et al., 2010). Apoptosome activity is also regulated by factors released from mitochondria. The active version of the BH3-only protein Bid induces homo-oligomerization of the proapoptotic Bcl-2 family members Bak and Bax, which promote release of Cytochrome C from within the mitochondrion (Wei et al., 2001). Cytochrome C binds Apaf-1 promoting assembly of the apoptosome (Liu et al., 1996; Li et al., 1997; Zou et al., 1997; Wei et al., 2001; Hill et al., 2004). The Bcl-2 family members play a more complicated role in mammalian apoptosis than they do in worms because there are proapoptotic Bcl-2 family members (e.g. Bak and Bax, as well as anti-apoptotic family members. Bcl-2 and Bcl-X play an antiapoptotic role in mammals, just as their ortholog CED-9 does in worms; however, while Bcl-2 and Bcl-X seem to inhibit Apaf-1 directly by binding via a third protein Aven (Chau et al., 2000), the antiapoptotic Bcl-2 proteins may also prevent release of Cytochrome C from the mitochondrion, though an *in vitro* study provides conflicting evidence in this regard (Newmeyer et al., 2000).

Though the mitochondrion plays a prominent role in the intrinsic apoptosis pathway, initiator caspases can directly activate effector caspases in response to external signals. Within the context of apoptosis, the death receptors CD95 and TRAIL-receptors R1 and R2 are the most well studied members of the tumor necrosis factor (TNF) receptor gene superfamily (reviewed in Locksley et al., 2001). Upon ligand binding, these receptors trimerize and associate via their death domains (DD). An adaptor FADD then binds the receptor complex via its own DD. FADD also has a death effector domain (DED), which is also found in initiator caspases (e.g. Caspases 8, 10), and promotes protein-protein binding. The complex formed by death receptors, FADD and initiator caspases is termed the death-inducing signaling complex, or DISC. Within the DISC, initiator caspases are activated and then directly activate effector caspases leading to apoptosis (reviewed in Ashkenazi and Dixit, 1998 and Verbrugge et al., 2010). DISCs can also function via the mitochondrion by cleaving and activating the BH3-only protein Bid. The extrinsic apoptosis pathway seems to function primarily in the development of the adaptive

immune system of mammals to prevent the development of self-reactive immune cells and to remove cells that accumulate after an immune response (reviewed in Elmore, 2007). Death receptor function is conserved, at least in *Drosophila* (Moreno et al., 2002), in spite of the fly's lack of an adaptive immune system, but *C. elegans* has no known TNF receptor orthologs.

Though there is no evidence in the literature that points to a signaling event that specifies the apoptotic fate of cells in *C. elegans*, we do know of some transcription factors upstream of EGL-1 that lead cells down the road to apoptosis. The hermaphrodite-specific neuron (HSN), dies in males, but survives in hermaphrodites. Survival is ensured by the action of TRA-1, a Zn-finger DNA-binding protein that represses *egl-1* expression (Hodgkin, 1987; Zarkower and Hodgkin, 1992; Conradt and Horvitz, 1999). Another neuron, the NSM, is a motor neuron whose sister cell undergoes apoptosis. The Helix-Loop-Helix (HLH) transcriptional activators HLH-2 and -3 are partially required for EGL-1-dependent apoptosis in the NSM sister (Krause et al., 1997; Thellmann et al., 2003), and when CES-1, a transcriptional repressor, is overexpressed it prevents the death of NSM sisters suggesting that it could negatively regulate EGL-1 (Metzstein et al., 1996; Metzstein and Horvitz, 1999; Thellmann et al., 2003). The reason the NSM sisters normally die, in spite of the antiapoptotic effects of CES-1, might be because the basic leucine zipper (bZIP) protein CES-2 represses expression of CES-1 (Metzstein and Horvitz, 1999).

It is clear that the apoptotic fate in these cells is specified by transcriptional programs, but apart from HSNs, we still know very little about how these programs are initiated. It is likely that, at some level in the cell lineage, the apoptosis pathway is integrated with signal transduction. It has been shown that Wnt signaling is involved in generating distinct transcriptional outputs that lead to the differentiation of sister neurons SMDD and AIY(Bertrand and Hobert, 2009). Preliminary results from our lab indicate that Frizzleds (Fz) *lin-17* and *mom-5* regulate the apoptotic fate in the Q lineage (unpublished data from Pan, Teulière).

Fzs are seven-pass transmembrane receptors involved in planar cell polarity (PCP) (reviewed in Simons and Mlodzik, 2008), canonical (reviewed in Macdonald et al., 2007) and non-canonical (reviewed in Semenov et al., 2007) Wnt signaling pathways. Dishevelled (Dsh) is an important transduction molecule acting downstream of Fz in PCP, canonical and non-canonical Wnt pathways. Dsh proteins have a characteristic domain architecture consisting of the DIX, PDZ and DEP domains. The DIX domain is important for binding of Dsh to Axin, a negative regulator of β-catenin in the canonical Wnt signaling pathway (Kishida et al., 1999; Itoh et al., 2000; Julius et al., 2000), while the PDZ domain is a protein-protein interaction domain involved in complex formation (Hung and Sheng, 2002).

The DEP domain (named for the first proteins in which the domain was recognized: Dsh, EGL-10 and Pleckstrin) of Dsh is required for function in various signaling pathways and developmental contexts. For example the DEP domain mediates an indirect interaction with Rho family GTP-ase, RhoA, via Daam1 during *Xenopus* gastrulation (Habas et al., 2001). Dsh promotes phosphorylation of c-Jun in the JNK pathway downstream of PCP signaling in developing *Drosophila* ommatidia (Boutros et al., 1998), and this requires the DEP domain. It has also been shown that Dsh, through its DEP domain, interacts with the μ2 subunit of the Clathrin AP-2 adaptor (Yu et al., 2010). This interaction leads to the endocytosis of Fzs during vertebrate development and is thought to be an important step in non-canonical Wnt signaling.

More generally DEP domains are thought to promote localization to the plasma membrane (Axelrod et al., 1998; Wong et al., 2000). From a study of DEP domain structure it was clear that a patch of basic amino acid residues clusters at an exposed surface of the DEP domain (Wong et al., 2000). This patch is likely to mediate an electrostatic interaction with negatively charged phospholipids found on the inner leaflet of the plasma membrane (Wong et al., 2000). This localization allows DEP domain-containing proteins to regulate signals sent from cell surface receptors to downstream effectors. For example, regulator of G protein signaling proteins (RGSs) are homologs of EGL-10 that regulate heterotrimeric GTPases. These G proteins are typically located on the cytoplasmic surface of the plasma membrane (reviewed in Marrari et al., 2007) and are involved in transducing signals from various extra-cellular factors (e.g. neurotransmitters, chemokines and hormones). These factors stimulate G-protein coupled receptors (GPCR) that then pass the signal to the GTPases (Neves et al., 2002). More specifically, stimulated GPCRs promote the exchange of GTP for GDP within the Gα subunit of the GTPase. In the GTP-bound form, Gα dissociates from Gβγ and the separate subunits are then free to transduce signals to downstream effectors. Hydrolysis of GTP to GDP by Gα causes reassociation of the G protein subunits and cessation of transduction (Oldham and Hamm, 2006).

RGSs are G protein activating proteins (GAP) that modulate G protein signaling by enhancing the hydrolytic activity of Gα, thereby reducing the time during which the G protein subunits are dissociated from one another (Chen and Hamm, 2006). In addition to their interaction with G proteins, the RGSs likely bind, via their DEP domains, GPCRs. The yeast RGS Sst2 binds the C-terminal tail of the GPCR Ste2 in this way, and this association seems also to be regulated. Upon phosphorylation, Sst2 dissociates from Ste2, allowing for recycling of Sst2 from endocytosed receptors, but also potentially allowing for further regulation of signaling by relieving the attenuation of G protein transduction that was a consequence of Sst2 GAP activity (Ballon et al., 2006).

We have discussed the signaling functions of the most well-understood DEP domain-containing proteins; however, the DEP domain is found in multiple proteins of unknown function. It is likely that these proteins localize at the plasma membrane. Further inquiry may reveal novel roles for these proteins in signal transduction.

TOE-2 is a poorly understood DEP domain-containing protein that encodes a target of the worm ERK ortholog, MPK-1. MPK-1 is involved in multiple developmental processes including vulval development (Lackner et al., 1994; Lackner and Kim, 1998; Pellegrino et al., 2011), cell polarity (Spilker et al., 2009) and germline development (Arur et al., 2009; Rutkowski et al., 2011). MPK-1 plays an antiapoptotic role in the germline. A weak loss-of-function mutant for *mpk-1* has increased germline apoptosis. RNAi against *toe-2* was shown to enhance the phenotype of the *mpk-1* mutant. It was later shown that TOE-2 is indeed an MPK-1 substrate (Arur et al., 2009). However, beyond the genetic analysis in the germline, nothing is known about how TOE-2 regulates apoptosis.

I have discovered a role for TOE-2 in regulating the apoptotic fate in the *C. elegans* Q neuroblast lineage. I found that TOE-2 functions autonomously in the Q lineage and is required for proper asymmetric cell divisions (ACDs), including those that produce apoptotic cells. I observed that TOE-2 localizes during mitosis to centrosomes and at the cortex at the site where the cleavage

furrow will form. Preliminary results indicate that TOE-2 may also localize asymmetrically in Q and Q.p neuroblasts just before division. These results, together with our current understanding of the function of the DEP domain, suggest the possibility that TOE-2 is involved in integrating signaling at the plasma membrane with the intrinsic apoptosis pathway.

MATERIALS AND METHODS

Strains and Genetics
Worms were cultured as previously described (Brenner, 1974). All experiments were conducted using worms cultured at 20°C unless otherwise noted.

LG I: *zdIs5[Pmec-4::GFP; lin-15(+)]* (Clark and Chiu, 2003)

LG II: *toe-2(gm396, gm407, gm408)* (this study), *toe-2(ok2807)* (*C. elegans* Gene Knockout Project at OMRF), *rrf-3(pk1426)* (Simmer et al., 2002)

LG III: *mpk-1(ga111)* (Leacock and Reinke, 2006)

LGIV: *ced-3(n2436)* (Shaham et al., 1999), *ced-3(n717)* (Ellis and Horvitz, 1986), *pig-1(gm301)* (Cordes et al., 2006)

LGX: *gmIs81[Pmec-4::mcherry; Pflp-12::EBFP2; Pgcy-32::gfp; Pegl-17::gfp]* (Jérôme Teulière and Jason Chien, unpublished)

Unmapped: *gmIs86[Pegl-17::toe-2a::gfp; Pmyo-2::mcherry]* (this study)

Extra-chromosomal arrays: *gmEx674[Pmab-5::toe-2a::mcherry; Pmyo-2::gfp]*, *gmEx675[Pmab-5::toe-2a::mcherry; Pmyo-2::gfp]*, *gmEx678[Pegl-17::toe-2a::gfp; Pmyo-2::mcherry]*, *gmEx681[Pegl-17::Δdep-toe-2a::gfp; Pmyo-2::mcherry]*, *unnamed[Ptoe-2::gfp; pRF4]* (all from this study)

Molecular biology and transgene construction
The *toe-2* cDNA was isolated from a random-hexamer primed cDNA library using the primers ATGAGTTCGTCTCGTCACTTCA and TTATATCATTCCTGGGAAAAAGTCGTT. The pcr fragment was then subcloned into the pCR2.1 TOPO vector. The sequence in the cDNA that encodes the DEP domain was removed from the cDNA using the primers CTCAAGCACGATCCCAGTTCTCTGAATCATTATATATTGTG and CACAATATATAATGATTCAGAGAACTGGGATCGTGCTTGAG with the Quick Change II site-directed mutagenesis kit (Agilent Technologies).

The transgenic constructs were generated from pre-existing multi-site Gateway entry clones and entry clones made using the *toe-2* cDNAs described above. Transgenes were generated by injecting construct and co-injection marker DNA into the gonad of young adult worms (Mello et al., 1991).

EMS mutagenesis screen
We mutagenized *zdIs5[Pmec-4::gfp]*; *ced-3(n2436)* hermaphrodites with 50 mM ethylmethylsulfonate (EMS) and screened F2 progeny for mutants with extra A/PVMs at a frequency above the background frequency of non-mutagenized *zdIs5; ced-3(n2436)* worms.

gm396 SNP mapping
Using the Hawaiian isolate (CB4856) of *C. elegans* for single-nucleotide polymorphism (SNP) mapping, we placed *gm396* between snp_C34F11[2] and snp_T24B8[1] on LG II (Wicks et al., 2001).

Whole-genome sequencing
Mutant worms were cultured on four large NG agar plates until starved. I then washed the worms from the plates with M9 and rinsed the worms two more times in M9. Worms were then washed once in NTE buffer (100mM NaCl; 50mM Tris; 20mM EDTA). Worms were pelleted and the pellet was frozen at -80°C for 24 hours. I then added 1X lysis buffer (NTE; 0.5% SDS) containing 100 μg/mL Proteinase K to the pellet and rocked at 65°C for one hour. Fresh Proteinase K was added at the previous concentration and the worms rocked at 65°C for one more hour.

One volume of 25:24:1 phenol:chloroform:isoamyl alcohol was added and the whole was vortexed. The solution was centrifuged for three minutes at 4,000 rpm. The aqueous (top) phase was extracted and saved. This extraction procedure was repeated once more with the extracted aqueous layer.

In order to precipitate the DNA, two volumes of 100% ethanol were added to the extracted solution and mixed. The solution was centrifuged for thirty minutes at 4°C. The pellet was allowed to air dry and then was dissolved in 400 μL TE (Qiagen EB). RNase A was added at 20 μg/mL and the solution incubated for thirty minutes at 37°C. The phenol:chloroform extraction was repeated once more. I then added 1/10 volume of 3M sodium acetate and 2.5 volumes 100% ethanol and mixed. The solution was centrifuged for thirty minutes at 4°C. The pellet was washed with 70% ethanol and the pellet was allowed to dry for approximately ten minutes. The pellet was dissolved in 400 μL TE.

Genomic DNA (approximately 5 mg) was sheared to an average length of 300 base pairs with a Covaris S2 instrument and prepared for paired-end sequencing using the Illumina paired-end sample preparation guide. 100 base-pair single reads were obtained using an Illumina Genome Analyzer IIx. Sequencing data were analyzed using MAQ and custom Perl scripts as described in (Gerhold et al., 2011).

RNAi knockdown of toe-2
RNAi was performed by feeding worms individual bacterial clones from the library constructed in the Vidal Lab (Rual et al., 2004). RNAi against *toe-2* was done with the clone containing mv_C56E6.3. The negative control was a clone containing empty vector (L4440) in the bacterial host HT115 (Timmons et al., 2001).

Protein sequence data-mining
The location of the DEP domain of TOE-2 was confirmed using the Conserved Domain Search Service at NCBI. The D and DEF ERK docking site motifs were described previously (Arur et al., 2009).

Zeiss imaging and scoring
Worms were anesthetized in 1.25 mM levamisole. A Zeiss Axioskop 2 microscope was used to examine worms. Images were collected using an ORCA-ER CCD camera (Hammamatsu) and Open1ab imaging software (Improvision).

Design and use of TALENs
TAL effector nucleases (TALENs) were used, as previously described (Wood et al., 2011), to create mutant alleles of *toe-2*. A pair of TALENs was designed to recognize the sequences TGGAACAAATGCAATC and TTTCTGAGCACGGATA within the region of the *toe-2* ORF that codes for the N-terminal end of the DEP domain, just downstream of an in-frame start codon.

TALENs were made using the protocol described in Cermak et al., 2011 with a few modifications. In place of the final vector pTAL3, I used a modified version of TALEN6-101318 (a generous gift from Barbara Meyer), which was optimized for use in worms. TALEN6-101318 was modified using the primers CTCACCGGGGCCCCCCTGGAGACGACCCCAGACCAGGT and CGCCACCAGATGGTCGTTGGAGACGGCAGCCAACGCGGGA with the Quick Change II site-directed mutagenesis kit (Agilent Technologies). The DNA-recognition domain of the modified TALEN6-101318 was then replaced with the LacZ cassette of pTAL3 using the restriction enzyme Esp3I. I sequenced the DNA binding domains of the generated TALENs using the primers TAACAGCGGTAGAGGCAGTG and TCTCCTCCAGCTCGCTCTTC.

Confocal imaging and time-lapse
Time-lapse images of Q and Q.p divisions were captured at twenty second intervals on a spinning-disk (CSU-X1; Yokogawa) confocal microscope. Images were captured using an EM CCD camera (Evolve; Photometrics) and SlideBook software (Intelligent Imaging Innovations).

Cell-size asymmetry
Q.pa and Q.pp cell areas were measured in L1 larvae. Areas were measured in triplicate using ImageJ. The size ratio was calculated using average area values. Q.pa and Q.pp were imaged only when the Q.pp did not appear apoptotic, was not rounded, and was still attached to Q.pa as described in Singhvi et al., 2011.

RESULTS

Mapping of gm396 and initial characterization of the toe-2(gm396) extra-neuron phenotype
The Q.p neuroblast divides to form an anterior cell and a smaller posterior cell that dies. The larger cell divides again to form the A/PVM mechanosensory neuron and an SDQL/R interneuron (Figure 1A). Mutations in genes that positively regulate programmed cell-death

(e.g. *ced-3;* Table 1) cause the posterior Q.p to survive, and to sometimes adopt the fate of one of its nieces (e.g. A/PVM; Figure 1B).

In contrast with cell-death mutants, other mutants cause the posterior daughter of Q.p to divide like its sister (Q.pa) to produce extra neurons (Figure 1C). For example, mutations in *pig-1*—the *C. elegans* ortholog of human MELK (Cordes et al., 2006)—or the ArfGAP *cnt-2* (Singhvi et al., 2011) cause Q.pp to adopt a mitotic fate, producing neurons like its sister Q.pa. The mitotic and apoptotic fates are somewhat independent from one another such that, in a *pig-1* or *cnt-2* mutant for example, the newly adopted mitotic fate of Q.pp may be masked by its apoptotic fate. Accordingly, the penetrance of the mitotic-fate defects in these mutants is enhanced in a cell-death defective background.

To identify genes regulating asymmetric cell division in the Q.p lineage, we mutagenized *ced-3(n2436)* mutant worms carrying *zdIs5* (Clark and Chiu, 2003), a transgene that drives expression of GFP in the A/PVMs (and other lineally unrelated mechanosensory neurons) from the *mec-4* promoter, and screened for extra neurons. We isolated many mutants, including *gm396.* We used single-nucleotide polymorphism (SNP) mapping to place the causative mutation in a region on chromosome II that contains approximately 1400 genes. Then, using whole-genome sequencing, I found that *gm396* mutants carry a missense mutation within the *toe-2* locus (Figure 2A). To determine whether the mutation in *toe-2* were responsible for the extra-neuron phenotype I see in *gm396* mutants, I used RNAi against *toe-2* in *zdIs5* and *zdIs5; rrf-3(pk1426); ced-3(n2436)* worms and saw extra A/PVMs in approximately 10.5% (Figure 2B; Table 1) and 36.0% (Table 1) of lineages scored, respectively, while RNAi with the empty L4440 vector in *zdIs5; rrf-3(pk1426); ced-3(n2436)* produced extra neurons in only 2.3% of lineages scored (Table 1). RNAi against *toe-2* is more effective in worms that are mutant for *rrf-3* because mutations in *rrf-3* make cells more sensitive to RNAi (Simmer et al., 2002).

TOE-2 has a DEP domain near its N-terminus (Figure 2A). The *toe-2(gm396)* allele contains a point mutation of a T (base pair 519 of the *toe-2* ORF) to a G. In the TOE-2 protein, this changes tyrosine 159, found at the C-terminal end of the DEP domain, to an aspartate. This tyrosine is conserved in the DEP domain of *Drosophila* Dishevelled (Dsh) and is a phosphorylation target of the Abelson tyrosine kinase (dAbl), which positively regulates the activity of Dsh in the planar cell polarity pathway (Singh et al., 2010). The mutation of tyrosine to aspartate is potentially a phosphomimetic change, which raised the possibility that *toe-2(gm396)* is a gain-of-function mutation. In addition, only one additional allele of *toe-2*, *ok2807* (courtesy of the *C. elegans* Gene Knockout Consortium) (Figure 2A) was available, and this mutant had a much less penetrant extra-neuron phenotype than *toe-2(gm396)*. This difference in phenotype is likely due to the nature of the *ok2807* allele, which carries an in-frame deletion that may allow for the production of a partially functional protein; however, if *toe-2(gm396)* were a gain-of-function mutation, this could also explain the difference in penetrance between the alleles.

I addressed this issue in the following ways: first, I determined whether the *gm396* allele was dominant. Though gain-of-function alleles are not necessarily dominant, they usually are. I placed the *gm396* allele over the *mIn1* balancer chromosome and did not observe any extra A/PVM neurons in heterozygous animals (data not shown). Second, I reasoned that, if *gm396* is a gain-of-function allele, reducing the levels of TOE-2 protein produced in *toe-2(gm396)*

mutants should suppress the extra-neuron phenotype. To the contrary, I saw extra neurons in 31.3% of lineages scored in *toe-2(gm396); toe-2(RNAi)* worms compared to 24.8% seen in *toe-2(gm396)* mutant worms (Table 1). The difference is not statistically significant by the X^2 test of significance. Third, I generated additional alleles—*gm407* and *gm408*—using TALENs (Wood et al., 2011) and saw that these mutants also had extra A/PVMs at a frequency similar to that seen in the original *gm396* mutant (Figure 2B ; Table 1). The *gm407* allele contains an in-frame 6 base-pair deletion that removes phenylalanine 84 and lysine 85 in the protein. These residues reside within the DEP domain, and together with changes caused by the *gm396* allele suggest that the DEP domain is important for TOE-2 function. The *gm408* allele contains an 8 base-pair deletion that causes a frame shift, and in the protein, replaces phenylalanine 84 with the amino acid sequence: LHIRAQKI. This sequence is followed by a premature stop codon, suggesting that this allele is a molecular null. This lesion is consistent with the fact that the *toe-2(gm408ok287)* mutants have the most penetrant phenotype of any of the existing *toe-2* alleles (Figure 2B, Table 1).

Mutants for toe-2 affect multiple divisions within the Q lineage

The presence of extra A/PVMs in *zdIs5; toe-2* mutants can be explained by a defect in apoptosis where the posterior daughter of Q.p survives and expresses the A/PVM marker; however, it was unclear why the strongest *toe-2* mutants had, in addition to extra neurons, missing neurons (Figure 2B, Table 1). Missing cells could be explained by a failure of A/PVM neurons to express the marker, or by a fate transformation of the neurons or one of their progenitors. In order to better characterize the extra- and missing-cell phenotypes of *toe-2* mutants, I used the transgene *gmIs81*, which allows us to observe all of the neurons derived from the Q lineage.

Q.a, the anterior daughter of Q, like Q.p, divides asymmetrically giving rise to a larger cell and a smaller cell that dies. However, in the case of Q.a, it is the small anterior cell that dies while the larger posterior daughter differentiates to become the A/PQR oxygen-sensing neuron (Figure 3A). I saw that *toe-2* mutants affect cell fates in the Q lineage at multiple levels. As expected, I saw that in strong *toe-2* alleles the posterior daughter of Q.p survives and expresses either the A/PVM or SDQ marker (Figure 3B; Table 2; Figure 4-5). I also saw that the surviving cell sometimes adopts the mitotic fate of its sister, producing two additional neurons, one A/PVM and one SDQ (Figure 3C; Table 2; Figure 4-5). In addition to defects in the number of Q.p-derived cells, I saw that the normally apoptotic anterior daughter of Q.a sometimes survives and expresses the A/PQR marker (Figure 3D; Table 2; Figure 4-5). However, this loss of the apoptotic fate in Q.aa only accounts for roughly half of the instances where extra A/PQR neurons were observed. I also saw that extra A/PQR neurons are produced at the expense of A/PVM and SDQ neurons (Figure 3E; Table 2; Figure 4-5), which accounts for most of the missing A/PVMs that I see in *toe-2* mutants. An inability to express their markers can explain the remaining lineages with missing A/PVM and SDQ neurons (Table 2).

It is difficult to decipher whether, with respect to the Q.p lineage, *toe-2* is strictly a proapoptotic gene or whether it regulates mitotic and neuronal fates as well. It is possible that *toe-2* is merely proapoptotic and the array of defects seen in mutants (Figure 1B-C) is the default when Q.pp is allowed to survive. Alternatively, mutants for *toe-2* may allow Q.pp to survive and also independently fail to specify an underlying fate. For example, Q.pp survives and TOE-2 is not present to specify a neuronal fate, so Q.pp adopts a mitotic fate instead. To test this we first

looked at neuron numbers in *ced-3(n717); gmIs81* worms. The *n717* allele results in a strong loss of caspase function that is required for execution of apoptosis (Ellis and Horvitz, 1986). This mutation ensures that Q.pp will survive most, if not all, of the time. In this strain, I almost never (0.8% of lineages) saw Q.pp adopt the mitotic-fate and express the A/PVM and SDQ neuronal markers. However, I saw Q.pp express either the A/PVM or SDQ marker in 5.9% and 10.0% of lineages scored, respectively (Table 2). In *toe-2(gm396); ced-3(n717); gmIs81* mutants I saw Q.pp express the A/PVM or SDQ marker in 22.5% and 7.5% of lineages, but I also saw Q.pp adopting a mitotic fate in 12.6% of lineages scored. The double mutant with the weaker allele, *toe-2(ok2807); ced-3(n717); gmIs81*, had a similar distribution: I saw the A/PVM or SDQ markers expressed 16% and 4.0% of the time, respectively. I also saw Q.pp adopt the mitotic fate in 4% of lineages scored (Table 2).

Despite the fact that Q.pp survives in the *ced-3* mutant background, I still observed missing neurons in the doubles with *toe-2*. Much of this is accounted for by the transformation of Q.p to Q.a. However in the *toe-2(ok2807); ced-3(n717)* double mutant, this transformation occurred only 2.0% of the time, while it occurred in 11.9% of lineages in the *toe-2(gm396); ced-3(n717)* double mutant (Table 2). The rest of the missing Q.p-derived neurons were likely a result of living cells failing to express their respective markers. I saw only one A/PVM and no SDQ in 5.7% and 14% of lineages in *toe-2(gm396)* and *toe-2(ok2807)* doubles with *ced-3(n717)*, respectively (Table 2). I also saw one SDQ and no A/PVM in 1.2% and 2.0% of lineages scored, respectively (Table 2).

TOE-2 acts autonomously in the Q lineage and requires the DEP domain for its function. Having established that *toe-2* regulates apoptosis and ACD in the Q lineage, I wanted to know where TOE-2 functions. I first asked where TOE-2 is expressed. I drove expression of GFP from the promoter of *toe-2*, which I designated as all of the sequence 2 kb upstream of the start codon of *toe-2*. The promoter is active in many cells of the developing embryo, but is excluded from the dorsal posterior region. In adult animals expression is restricted to the spermatheca and a few cells near the anus. In early larvae, expression is seen in the seam cells, and later in P cells and there descendants (data not shown). The promoter is also active in Q; its daughters Q.a (Figure 9A) and Q.p (Figure 9B); and in the mature neurons A/PVM, SDQR/L and A/PQR (Figure 9C, only right-side neurons are shown). This expression pattern is consistent with the idea that TOE-2 plays an autonomous role in the Q lineage; however, a non-autonomous role can not be ruled out.

The expression studies show where TOE-2 is expressed, not where it functions. TOE-2 could be required outside the lineage, for example, in the generation or propagation of a polarizing signal. To test more directly whether TOE-2 functions autonomously in the Q lineage I expressed TOE-2::GFP from the promoter of *mab-5* in *toe-2(gm396)* mutants. The *mab-5* promoter is active in cells near the right and left Q cells before they migrate and its activity is required in QL for it to migrate posteriorly, however, it is not active in QR (Costa et al., 1988; Cowing and Kenyon, 1992; Salser and Kenyon, 1992). If TOE-2 were acting non-autonomously I may see rescue of the extra-cell phenotype in the Q lineages on both the right and left sides of the worm or no rescue of either side. However, if TOE-2 acts autonomously, I should see rescue on the left side, but not on the right. I compared siblings from mothers that carried *gmEx674* and *gmEx675* transgenes (independent lines of the *Pmab-5::toe-2::mCherry* transgene). In siblings that no

longer carried the transgene, I observed extra cells at a frequency similar to what I saw in *toe-2* mutants (Figure 9D, Table 1). In siblings that still carried the transgene, I saw a significant rescue on the left side, but not on the right (Figure 9D, Table 1) suggesting that TOE-2 acts autonomously within the Q lineage. I then expressed TOE-2::GFP from the promoter of *egl-17* which is expressed in both QL and QR. In this strain (*toe-2(gm396); gmEx678*), non-transgenic siblings had extra cells on both sides, but in their transgenic siblings, I saw rescue on both sides of the worm (Figure 9D, Table 1).

The DEP domain is the only recognizable domain found in TOE-2. I expressed TOE-2ΔDEP (Figure 10A) from the *egl-17* promoter (*gmEx681*) and saw that the construct did not fully rescue the extra cell phenotype of *toe-2(gm396)* mutants suggesting that the DEP domain is required for TOE-2 function in regulating cell division in the Q lineage (Figure 10B). It is possible that I did not see rescue because the *toe-2Δdep* transcript is unstable resulting in production of little or no protein. However, I saw that GFP levels and localization were similar in the Q lineages of *gmEx681[Pegl-17::toe-2Δdep::GFP]* and *gmEx678[Pegl-17::toe-2::gfp]* animals.

In addition to the DEP domain, TOE-2 has two D domains and a DEF domain. All three are docking sites for MPK-1, the worm ortholog of mammalian ERK. Both D domains are deleted in *toe-2(ok2807)* (Figure 10A), and extra neurons are seen at a very low penetrance (Figure 1B; Table 1), suggesting that MPK-1 is not playing a significant role in the divisions of the Q lineage. However, to directly assess whether MPK-1 plays a role, I looked for extra A/PVM neurons in *mpk-1(ga111)* mutant worms at 25 degrees Celsius (this allele is temperature sensitive). I also looked at the *toe-2(gm396); mpk-1(ga111)* double mutant for any enhancement of the extra-cell phenotype. I observed no extra cells in the *mpk-1(ga111)* single mutant, and loss of *mpk-1* did not enhance the extra-cell phenotype of the *toe-2(gm396)* mutant (Figure 10C; Table 1). Taken together with the low-penetrance extra-cell phenotype of the *toe-2(ok2807)* allele, these results suggest that MPK-1 plays a limited role, if any, in the development of the Q lineage.

TOE-2 localizes dynamically during division of Q and Q.p

In order to observe TOE-2 localization in the Q lineage I drove expression of a TOE-2::GFP fusion protein from the *egl-17* promoter. I observed dynamic sub-cellular localization of TOE-2::GFP in the dividing Q cell. Before division, TOE-2::GFP localizes diffusely in the cytoplasm and is highly concentrated in the nucleus. Around metaphase, TOE-2::GFP localizes to centrosomes (Figure 11, 0s). The protein remains at centrosomes throughout the rest of the division and is inherited by both daughter cells (Figure 11, 0-300s). Prior to anaphase TOE-2 localizes to the region of the cortex that will become the furrow (Figure 11, 20-40s). At this time TOE-2::GFP also appears to localize asymmetrically at the posterior cortex of the cell (Figure 11, 20s)—though the evidence supporting this aspect of the localization are preliminary and more time-lapse images need to be acquired. As anaphase continues, TOE-2 is highly concentrated within the furrow (Figure 11, 80-260s) and remains there until it eventually ends up in the midbody (Figure 11, 280-300s). During telophase, TOE-2 localizes to chromatin (Figure 11, 200-300s). After abscission of the daughter cells, TOE-2 is again diffuse in the cytoplasm and highly concentrated in the nucleus.

The localization of TOE-2 in Q.p is similar to that seen in Q. In Q.p, TOE-2 localizes to centrosomes (Figure 12, 0-220s), to the region of the cortex in which the furrow will form (Figure 12, 20-60s), within the furrow throughout the division (Figure 12, 80-280s) and later, in the midbody (Figure 12, 300s). Preliminary results from a time-lapse image suggest that TOE-2::GFP localizes asymmetrically to the posterior cortex of Q.p, as it does in Q, before the cleavage furrow forms (Figure 12, 40-140s). In contrast with the chromatin localization of TOE-2::GFP during Q division, the protein appears to be excluded from the chromatin of Q.p daughters during telophase.

The cell size asymmetry of Q.p daughters is maintained in a toe-2 mutant

Previous work in the lab has shown a correlation between the size of sister cells and their competency to execute the apoptosis pathway. Though the Q.p division is normally asymmetric with respect to size (Q.pa is much larger than Q.pp), in mutants where Q.pp survives and becomes a neuron (e.g. *pig-1* and *cnt-2*), the Q.p divides more symmetrically (Cordes et al., 2006; Singhvi et al., 2011). The localization of TOE-2 to centrosomes and the cleavage furrow suggested that TOE-2 may be involved in asymmetric placement of the cleavage furrow that produces daughter cells of relatively different sizes. This idea was tempting in particular because TOE-2 seems to localize at the cortex, between the centrosomes, even before the furrow forms. To test whether TOE-2 was functioning in this way I used *rdvIs1*, a transgene that expresses mCherry attached to proteins in chromatin and to the plasma membrane of the cells in the Q lineage. This marker allowed us to observe and measure the relative sizes of the anterior and posterior Q.p daughters in wild-type and *toe-2(gm396)* mutant animals. I reasoned that, if TOE-2 were important for asymmetric placement of the cleavage furrow, the Q.p daughters, which are usually of unequal size, would be more symmetric with respect to size in a *toe-2* mutant. To the contrary I found that cell size asymmetry between the daughters was not significantly affected (Figure 13).

toe-2 is in the pig-1 genetic pathway

The ortholog of human MELK, PIG-1, is known to regulate apoptosis and asymmetric division in the Q lineage (Cordes et al., 2006). In *pig-1(gm301)* mutants extra A/PVMs are present in 40.0% of lineages scored; however, *pig-1* mutants do not have missing neurons. In *toe-2(gm396); pig-1(gm301)* double mutants, extra A/PVMs are seen at a frequency of 36.6%. Comparison between these numbers is complicated slightly because *toe-2* mutants are also missing neurons. If lineages missing A/PVMs are ignored, *toe-2(gm396)* mutants have extra neurons in 43.4% of lineages (Figure 14), which is not a significant difference. The similarity in penetrance of the extra-cell phenotype between the *pig-1* single mutant and the *toe-2; pig-1* double mutant suggests that *toe-2* and *pig-1* function in the same genetic pathway to regulate the apoptotic fate of Q.pp.

DISCUSSION

TOE-2 normally functions in the Q lineage to promote a consistent pattern of ACD and fate assignment among terminally differentiating cells in the lineage. For example, it is clear that TOE-2 is required for proper ACD of the Q neuroblast itself. In strong loss-of-function *toe-2* mutants, the posterior daughter of Q often adopts the fate of the anterior Q daughter. This occurs

much less frequently in the weak loss-of-function mutant *toe-2(ok2807)*. One prominent difference between these groups of mutants is that in the weak loss-of-function mutant, the DEP domain is intact, while in strong loss-of-function mutants, the DEP domain is either not present —the case in *toe-2(gm408ok2807)* mutants—or is crippled, as is likely to be the case in the *toe-2(gm396)* and *toe-2(gm407)* mutants.

These findings raise questions about the function of the DEP domain in Q neuroblast ACD. DEP domains are generally thought to be important for plasma membrane localization (Axelrod et al., 1998; Wong et al., 2000), suggesting that TOE-2 functions at the membrane. A function at the membrane is consistent with the localization of TOE-2 that I observed in Q and Q.p cells; however, preliminary imaging of GFP-tagged TOE-2ΔDEP suggests that the membrane localization of TOE-2—in particular, localization to the cleavage furrow—is intact during Q division. These data come with the caveat that the tagged transgene was in a wild-type background. In this strain it is possible that endogenous TOE-2 with an intact DEP domain oligomerizes with TOE-2ΔDEP protein, allowing it to localize to the plasma membrane. This possibility can be tested by asking whether GFP-tagged TOE-2ΔDEP localizes to the membrane in *toe-2(gm408ok2807)* mutants.

If the DEP domain were not important for TOE-2 localization, then what might be its function? The DEP domain could be important for the ability of TOE-2 to mediate interaction between other proteins that regulate ACD in the Q neuroblast. Preliminary imaging of TOE-2ΔDEP in Q suggests that, while the protein still localizes to the membrane, the daughters of Q are asymmetric in size (data not shown). This localization occurs in the presence of wild-type TOE-2. If this observation can be repeated, it is possible that membrane localized TOE-2ΔDEP acts as a dominant-negative, restricting the interaction between regulators of Q division. It has been shown that the DEP domain of Sst2, an RGS in yeast, is important for binding the C-terminal tail of the GPCR Ste2 (Ballon et al., 2006). TOE-2 may complex with other membrane proteins via its DEP domain to regulate cell size during Q division.

Another curious aspect of TOE-2 localization is its presence at the cleavage furrow during Q.p divisions. TOE-2 localizes to the cortex where the cleavage furrow will form. This suggested that TOE-2 regulates the apoptotic fate by making the Q.p division more symmetrical with respect to size. There is precedence for this mechanism as analyses of mutants in both *cnt-2* (Singhvi et al., 2011) and *pig-1* (Cordes et al., 2006) have shown a correlation between defective size asymmetry of Q.p daughters and defects in apoptosis. However, I have shown that the cell-size asymmetry of the Q.p division is intact in a *toe-2* mutant (Figure 13).

Then why might TOE-2 localize to the furrow? It may not be in the furrow localization *per se*, but in the midbody, that TOE-2 function is required. The midbody is the last point of connection between cells after division and is important for the final abscission event (Mullins and Biesele, 1977; Gromley et al., 2005; Barr and Gruneberg, 2007; Steigemann et al., 2009; Kuo et al., 2011). It has been proposed that signaling molecules localize to the midbody and are exocytosed in membrane vesicles. These extracellular vesicles would then participate in intercellular signaling (Marzesco et al., 2005; Dubreuil et al., 2007). TOE-2 could be required in the midbody to facilitate the exocytosis of signaling molecules. A function at this site would be interesting because the midbody can be inherited asymmetrically after division by the cell with the older

centrosome (Kuo et al., 2011). This would provide a mechanism for asymmetric signaling between Q and Q.p daughters after division to determine their fates. An alternative, and less exciting, possibility is that TOE-2 localizes to the midbody as a disposal mechanism. Midbodies have been shown to be extruded by cells after division (Mullins and Biesele, 1977) and have also been shown to be endocytosed and degraded through autophagy (Gromley et al., 2005; Goss and Toomre, 2008; Pohl and Jentsch, 2009; Kuo et al., 2011). Perhaps, in the late stages of mitosis TOE-2 has already served its purpose and the cell is then looking to get rid of it. It has been shown that the midbody formed after Q division is extruded and engulfed by another cell (Chai et al, In press at JCB). This is consistent with the idea that TOE-2 needs to be disposed of but does not rule out the possibility of a signaling role for midbody-localized TOE-2 prior to midbody extrusion.TOE-2 may also have a function at the furrow that overlaps with the functions of other proteins, or TOE-2 furrow localization may restrict it from acting at other locations in the cell.

Apart from ACD in Q and Q.p, TOE-2 also regulates the fates of Q derived neurons and neuronal precursors. There also appears to be a pro-apoptotic role for TOE-2 in Q.pp as *toe-2* mutants have extra neurons when Q.pp survives and expresses either A/PVM or SDQ markers. Mutants for *toe-2* also have extra A/PQR neurons derived from Q.a, reflecting a pro-apoptotic function of TOE-2 in Q.aa. It will be important to observe how TOE-2 localizes in the Q.a division. An anterior cortical localization in Q.a and a confirmation of posterior localization in Q.p would suggest that asymmetric TOE-2 regulates the apoptotic fate in Q.a and Q.p.

In addition to regulating the apoptotic fate, TOE-2 seems to prevent a surviving Q.pp from taking on the mitotic fate of its sister. In a *ced-3* mutant where Q.pp always survives, the cell almost never adopts the mitotic fate of Q.pa, but in *ced-3* doubles with weak or strong loss-of-function *toe-2* mutants, adoption of the mitotic fate happens more frequently (Table 2). This finding suggests that TOE-2 is normally doing one of two things: it may be promoting a Q.pp posterior fate or restricting Q.pp from adopting the anterior Q.pa fate.

There also seems to be a bias in *toe-2* mutants as to which neuronal fate Q.pp adopts when it survives. In *ced-3*, a surviving Q.pp expresses the A/PVM marker about half as often as it expresses the SDQ marker. The opposite is true in *ced-3; toe-2* double mutants where a surviving Q.pp expresses the A/PVM marker 3 to 4 times more often than it does the SDQ marker (Table 2). Consistent with the idea that TOE-2 promotes posterior fates, the Q.pap sometimes fails to express the SDQ marker in *ced-3; toe-2* double mutants. The opposite (where Q.paa fails to express the A/PVM marker) occurs less frequently. These data suggest that, in addition to its proapoptotic function, TOE-2 regulates neuronal and mitotic fates in the Q lineage.

TOE-2 is likely to be important for development outside of the Q lineage as well. Imaging of a transcriptional GFP fusion to *toe-2* suggests functions for *toe-2* in the early embryo and in the P cells and their descendants. When expressed in P cells from a heterologous promoter, GFP-tagged TOE-2 localized to centrosomes as it does prior to division of Q and Q.p. This localization does not prove that there is a function for TOE-2 in these cells, but it is suggestive of

a general role for TOE-2 in regulating asymmetric divisions. I have observed extra neurons in other lineages. I have seen what appear to be extra URX, PLM, ALM and I4 neurons in *toe-2* mutants. Cell deaths do not occur near ALM or I4 within their respective lineages, further supporting the idea that TOE-2 is doing more than simply promoting apoptosis.

We also know, from work done by the Schedl group, that TOE-2 regulates apoptosis in the germ line (Arur et al., 2009). Mysteriously, TOE-2 and MPK-1 seem to play an anti-apoptotic role in the germ line, while TOE-2 has a proapoptotic function in the Q lineage. I can only speculate that, because TOE-2 appears to play a role in regulating multiple fates and not just the apoptotic fate, TOE-2 may act to integrate cell signaling and transcriptional outputs leading to fate decisions; however, the specificity of these outputs is provided by effectors downstream of TOE-2. This is not unprecedented: Dsh proteins play a role in PCP, canonical and non-canonical Wnt signaling, but these pathways operate in diverse developmental contexts with different transcriptional and cellular outputs (reviewed in Macdonald et al., 2007; Semenov et al., 2007; and Simons and Mlodzik, 2008).

We currently know very little about the pathways in which TOE-2 functions. I have shown that *toe-2* and *pig-1* function in the same genetic pathway to regulate the apoptotic fate in Q.p: double *toe-2; pig-1* mutants look like *pig-1* single mutants when scoring for extra A/PVMs. PIG-1 may act upstream of TOE-2 since it has a more penetrant extra neuron phenotype and, in addition to this, also affects positioning of the Q.p cleavage furrow (Cordes et al., 2006; Ou et al., 2010). However, *toe-2* mutants also have missing cells while *pig-1* mutants do not. In the double mutants, there are still missing cells at a frequency similar to what I see in *toe-2* mutants alone. These phenotypes suggest that PIG-1 and TOE-2 do function in the same pathway in Q.p, but that PIG-1 has no role in regulating the Q division.

Our future work will focus on determining the nature of the relationship between PIG-1 and TOE-2 in regulating the apoptotic fate in Q.p. In particular I am determining whether PIG-1 is required for TOE-2 localization by looking at GFP-tagged TOE-2 in Q.p in *pig-1* mutants. I will also investigate whether there is any connection between TOE-2 and the Fz receptors LIN-17 and MOM-5, which are also known to regulate the apoptotic fate in Q.p. In particular, I will investigate whether TOE-2 might regulate endocytosis of one or both receptors to either promote or prevent signaling.

In summary, I have demonstrated that TOE-2 functions autonomously in the Q lineage to promote the apoptotic fate. TOE-2 is also necessary for ACD of the Q neuroblast and may positively regulate posterior fates (or may repress anterior fates) in the posteriorly positioned cells of the lineage. TOE-2 regulates the apoptotic fate in Q.p independent of any effects on cell-size asymmetry, which is a role unique among the molecules known to affect this division. We are just beginning to understand how TOE-2 fits in with other molecules—PIG-1 in particular—known to regulate the apoptotic fate in the Q.p. I propose that TOE-2 is an interesting DEP domain-containing protein that may function to integrate signaling at the plasma membrane with the apoptosis pathway.

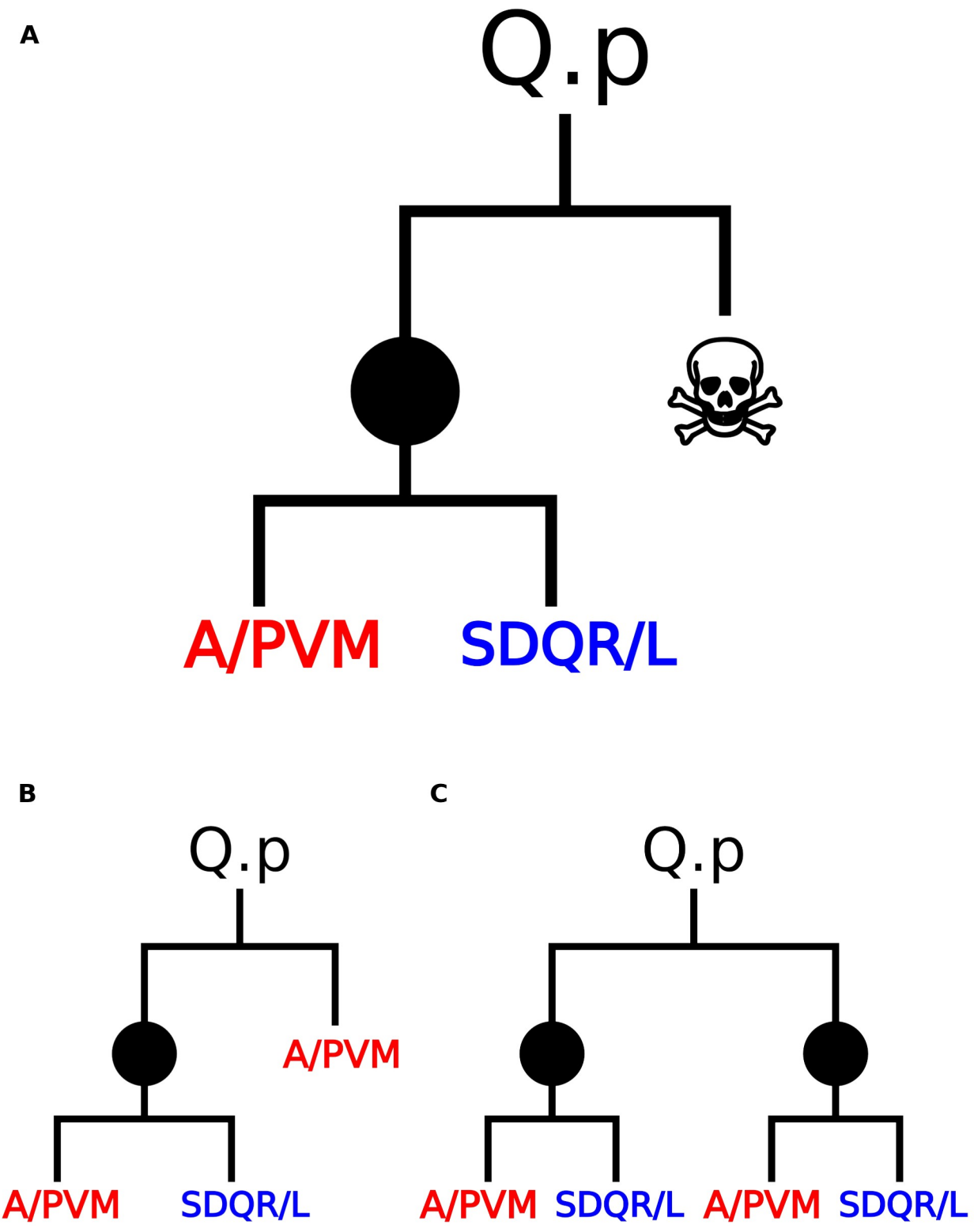
A
Q.p
A/PVM
SDQR/L
B
Q.p
A/PVM
A/PVM
SDQR/L
C
Q.p
A/PVM
SDQR/L
A/PVM
SDQR/L

Figure 1: Normal and abnormal divisions of the Q.p lineage. (A) The Q.p neuroblast divides into a posterior daughter that dies and an anterior daughter that divides again, giving rise to an A/PVM mechanosensory neuron and SDQ interneuron. (B) The posterior daughter of Q.p survives in cell death pathway mutants (e.g. *ced-3*) and sometimes expresses the markers of A/PVM or SDQ neurons (only an extra A/PVM is shown). (C) Mutations in *toe-2* allow the surviving posterior daughter of Q.p to adopt a mitotic fate and divide to form A/PVM and SDQ neurons. The same phenotype has been observed in *cnt-2* (Singhvi et al., 2011) and *pig-1* (Cordes et al., 2006) mutants.

Table 1: Extra and missing mechanosensory neurons (all scored in *zdIs5*)

genotype	AVM			PVM			Total		
	extra (%)	missing (%)	N	extra (%)	missing (%)	N	extra (%)	missing (%)	N
wild type	0.0	0.0	100	0.0	0.0	100	0.0	0.0	100
toe-2(ok2807)	7.7	0.0	39	0.0	0.0	46	3.5	0.0	85
toe-2(gm396)	26.1	3.9	153	23.4	14.6	137	24.8	9.0	290
toe-2(gm407)	31.8	4.5	132	24.8	8.8	113	28.6	6.5	245
toe-2(gm408ok2807)	40.6	1.0	101	21.8	19.8	101	31.2	10.4	202
rrf-3(pk1426); ced-3(n2436); (L4440 RNAi)	0.0	N.D.	26	5.6	N.D.	18	2.3	N.D.	44
rrf-3(pk1426); ced-3(n2436); toe-2(RNAi)	42.9	N.D.	42	29.8	N.D.	47	36.0	N.D.	89
toe-2(RNAi)	13.4	N.D.	112	7.8	N.D.	116	10.5	N.D.	228
toe-2(gm396); toe-2(RNAi)	27.3	N.D.	33	35.5	N.D.	31	31.3	N.D.	64
ced-3(n717)	0.9	0.0	112	17.8	0.0	101	8.9	0.0	213
toe-2(ok2807); ced-3(n717)	9.1	0.9	110	31.4	0.8	121	20.8	0.9	231
toe-2(gm396); ced-3(n717)	28.2	4.2	142	44.6	12.2	139	36.3	8.2	281
pig-1(gm301)[1]	26.2	0.0	126	54.0	0.0	124	40.0	0.0	250
toe-2(gm396 M+); pig-1(gm301)	34.4	2.2	90	63.4	11.9	101	49.7	7.3	191
toe-2(gm396); pig-1(gm301)	27.1	11.9	118	48.0	20.4	98	36.6	15.7	216
toe-2(gm396); gmEx678 -	29.1	3.5	86	23.2	10.1	69	26.5	6.5	155
toe-2(gm396); gmEx678 +	2.4	1.2	84	1.6	4.8	63	2.0	2.7	147
toe-2(gm396); gmEx681 -	26.1	3.2	188	33.0	15.4	182	29.5	9.2	370
toe-2(gm396); gmEx681 +	19.4	8.1	62	18.8	15.6	64	19.0	11.9	126
toe-2(gm396); gmEx674 -	36.8	5.9	68	31.6	22.8	57	34.4	13.6	125
toe-2(gm396); gmEx674 +	27.5	2.9	69	5.5	0.0	55	N.A.	N.A.	124
toe-2(gm396); gmEx675 -	29.0	4.3	69	25.0	14.3	56	27.2	8.8	125
toe-2(gm396); gmEx675 +	27.1	6.8	59	3.9	2.0	51	N.A.	N.A.	110
toe-2(gm396) 25°C	27.1	4.2	48	23.5	13.7	51	25.3	9.1	99
toe-2(gm396); mpk-1(ga111) 25°C	18.6	4.7	43	27.5	13.7	51	23.4	9.6	94

N.D., Not done. N.A., Not applicable: These transgenes only express TOE-2 on the left side. Combined A/PVM numbers are not meaningful in this context.

[1] Data from Jérôme Teulière

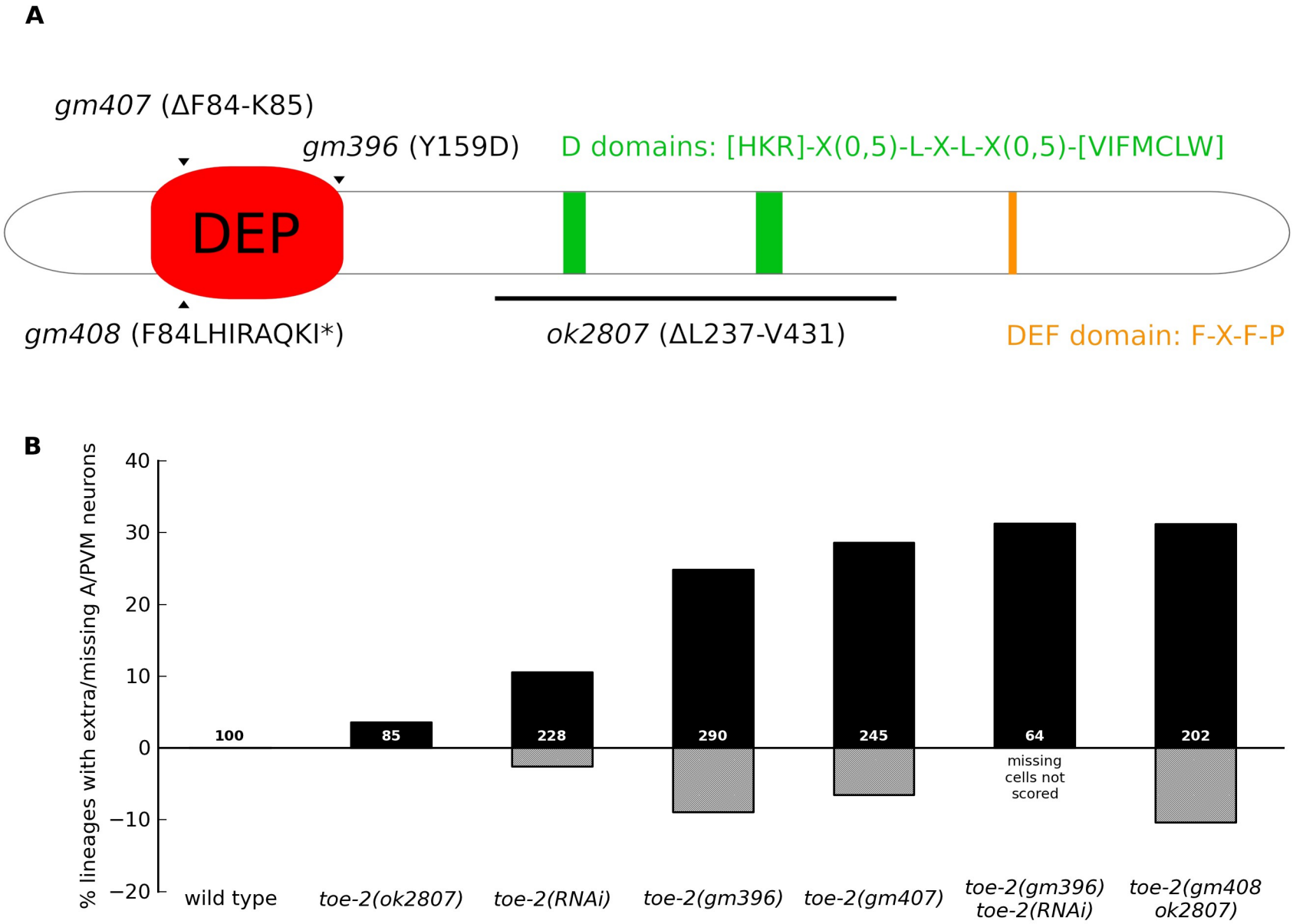
A
gm407 (ΔF84-K85)
gm396 (Y159D)
D domains: [HKR]-X(0,5)-L-X-L-X(0,5)-[VIFMCLW]
DEP
gm408 (F84LHIRAQKI*)
ok2807 (ΔL237-V431)
DEF domain: F-X-F-P
B
% lineages with extra/missing A/PVM neurons
40
30
20
10
0
−10
−20
100
85
228
290
245
64
202
missing cells not scored
wild type
toe-2(ok2807)
toe-2(RNAi)
toe-2(gm396)
toe-2(gm407)
toe-2(gm396) toe-2(RNAi)
toe-2(gm408 ok2807)

Figure 2: *toe-2* mutants and mutant phenotypes. (A) TOE-2 contains a DEP domain near its N-terminus, two D domains and a DEF domain. D and DEF domains are docking sites for MPK-1 (Arur et al., 2009). The sequences of the D and DEF domains are given in green and orange text, respectively. The location and the nature of the change of each allele are indicated. The *gm408* allele introduces a premature stop codon near the 5' end of the *toe-2* ORF. The *gm407* and *gm408* alleles carry a six base pair in-frame deletion and a missense mutation in the DEP domain, respectively. The *ok2807* allele contains a 633 base pair in-frame deletion that and encodes TOE-2 protein lacking the two D domains. (B) The percentages of lineages with extra and missing A/PVM neurons (y-axis) were scored in different genetic backgrounds and are shown with black and hatched bars, respectively. The number of lineages scored for each genotype appears along the x-axis. The number of missing neurons was not recorded for the *toe-2(gm396) toe-2(RNAi)* experiment. It should be noted that the *gm408* allele was generated using TALENs in a *toe-2(ok2807)* mutant background. The *ok2807* lesion is found downstream of the *gm408* lesion and does not affect the transcript. This was done to aid genotyping by PCR as the *ok2807* lesion is a deletion of 633 base pairs.

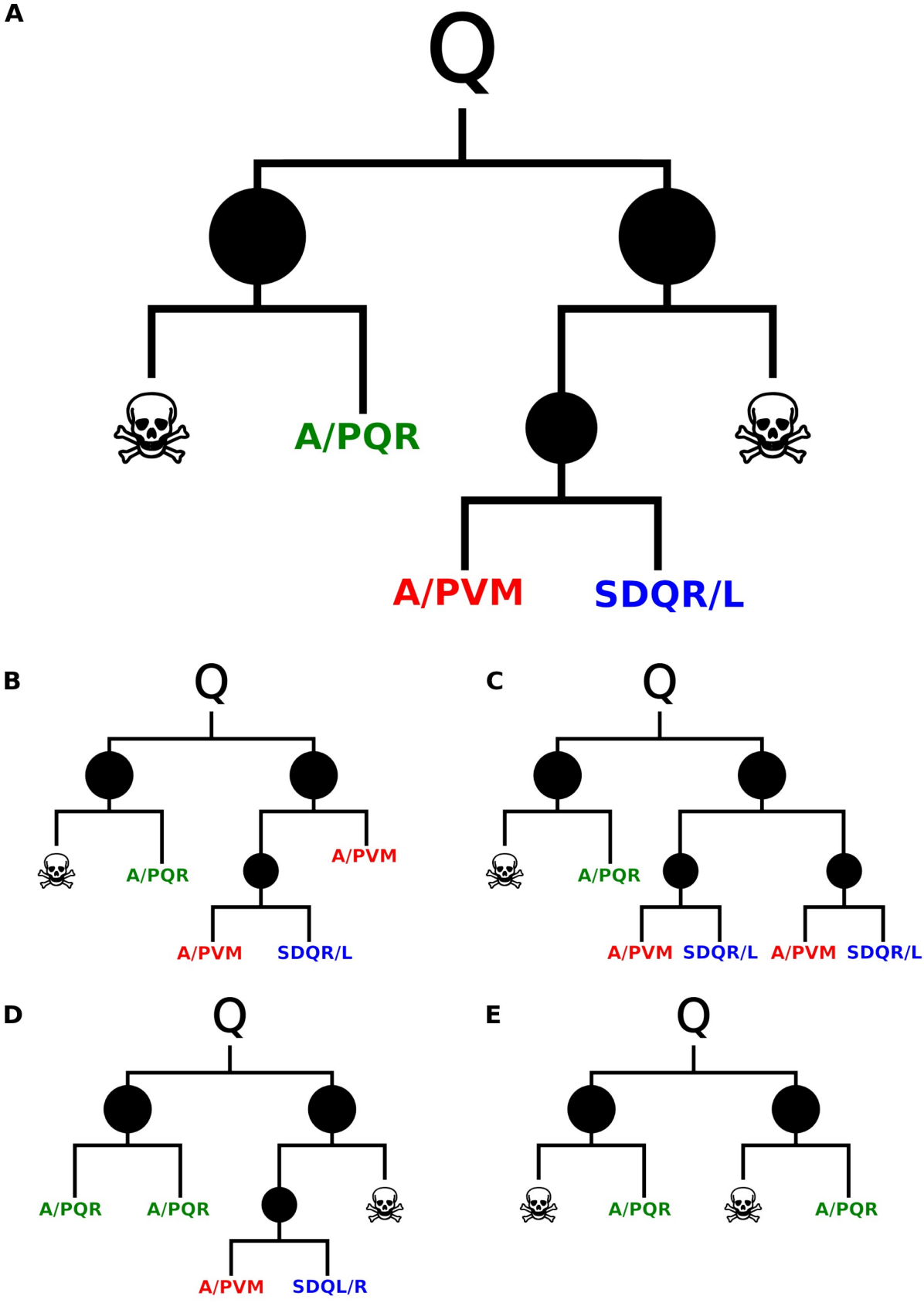
A
Q
A/PQR
A/PVM
SDQR/L
B
Q
A/PQR
A/PVM
A/PVM
SDQR/L
C
Q
A/PQR
A/PVM
SDQR/L
A/PVM
SDQR/L
D
Q
A/PQR
A/PQR
A/PVM
SDQL/R
E
Q
A/PQR
A/PQR

Figure 3: Normal and abnormal divisions of the Q lineage. (A) The Q neuroblast divides giving rise to daughters Q.a and Q.p. Q.a divides again to produce an anterior cell that dies and a posterior daughter that becomes the A/PQR oxygen sensing neuron. The Q.p neuroblast divides to produce a posterior daughter that dies and an anterior daughter that divides again, giving rise to an A/PVM mechanosensory neuron and SDQ interneuron. (B) The posterior daughter of Q.p survives in cell death pathway mutants (e.g. *ced-3*) and sometimes expresses the markers of A/PVM or SDQ neurons (only an extra A/PVM is shown). (C) Mutations in *toe-2* allow the surviving posterior daughter of Q.p to adopt a mitotic fate and divide to form A/PVM and SDQ neurons. (D) When the anterior daughter of Q.a survives in *toe-2* mutants it becomes an extra A/PQR. (E) In *toe-2* mutants Q.p will sometimes transform into Q.a. This produces two A/PQR neurons at the expense of A/PVM and SDQ neurons.

Table 2: Extra and missing Q-derived neurons (all scored in *gmIs86*)

A/PVM:SDQR/L:A/PQR	*toe-2(gm408ok2807)*	*toe-2(gm396)*	*toe-2(ok2807)*	*ced-3(n717)*[1]	*toe-2(gm396); ced-3(n717)*	*toe-2(ok2807); ced-3(n717)*
0:0:0	-	1.7	-	-	-	-
0:0:1	1.9	0.6	-	-	-	-
0:0:2	8.2	11.9	0.6	-	1.3	2.0
0:0:3	0.6	1.7	-	-	3.1	-
0:0:4	1.3	-	-	-	7.5	-
0:0:5	-	-	-	-	0.6	-
0:1:1	0.6	1.1	0.6	-	0.6	-
0:1:2	-	-	-	-	-	2.0
0:1:3	-	-	-	-	0.6	-
0:2:1	-	-	0.6	-	-	-
1:0:1	1.9	1.1	-	-	0.6	2.0
1:0:2	0.6	-	-	-	3.8	12.0
1:0:3	-	-	-	-	1.3	-
1:1:0	0.6	-	-	-	-	-
1:1:1	57.6	52.0	94.1	11.7	3.8	10.0
1:1:2	2.5	7.3	-	71.7	30.6	46.0
1:1:3	-	2.3	-	-	1.9	-
1:2:1	5.1	2.8	1.8	2.5	-	-
1:2:2	0.6	0.6	-	7.5	7.5	4.0
2:0:1	-	0.6	-	-	-	-
2:0:2	-	-	-	-	0.6	2.0
2:1:1	10.8	6.8	1.2	1.7	1.3	2.0
2:1:2	0.6	2.3	-	4.2	20.6	14.0
2:1:3	-	-	-	-	0.6	-
2:2:1	5.1	7.3	1.2	-	1.3	-
2:2:2	0.6	-	-	0.8	11.3	4.0
2:3:1	0.6	-	-	-	-	-
2:3:3	-	-	-	-	0.6	-
4:0:2	-	-	-	-	0.6	-
4:4:1	0.6	-	-	-	-	-
N	158	177	170	120	160	50

Percentages falling below 5.0% are marked in red. These fall within the misc. categories in figures 4-8.

[1] Data from Jérôme Teulière

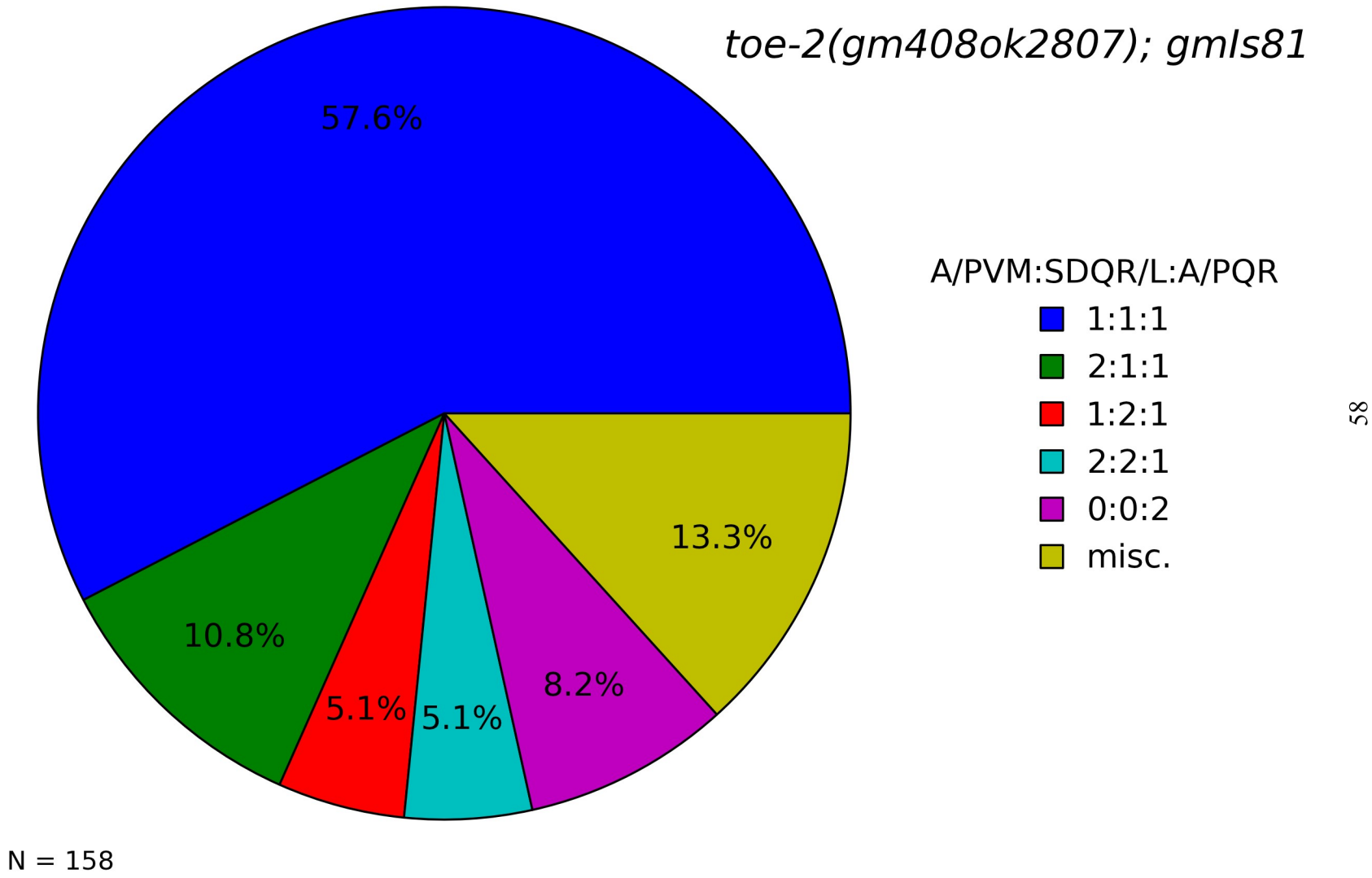
toe-2(gm408ok2807); gmIs81
57.6%
10.8%
5.1%
5.1%
8.2%
13.3%
A/PVM:SDQR/L:A/PQR
1:1:1
2:1:1
1:2:1
2:2:1
0:0:2
misc.
N = 158

Figure 4: Extra and missing neurons in *toe-2(gm408ok2807); gmIs81* worms. The *gmIs81* transgene allows for the counting of all the neurons present in a single Q lineage. The legend indicates categories of cell number ratios of A/PVM to SDQR/L to A/PQR neurons. "N" denotes the number of lineages scored in this experiment. The pie indicates the percentage of the total lineages (N) that fall into a particular cell number ratio category. The miscellaneous (misc.) category contains all of the cell number ratio categories that individually account for less than 5% of total lineages scored.

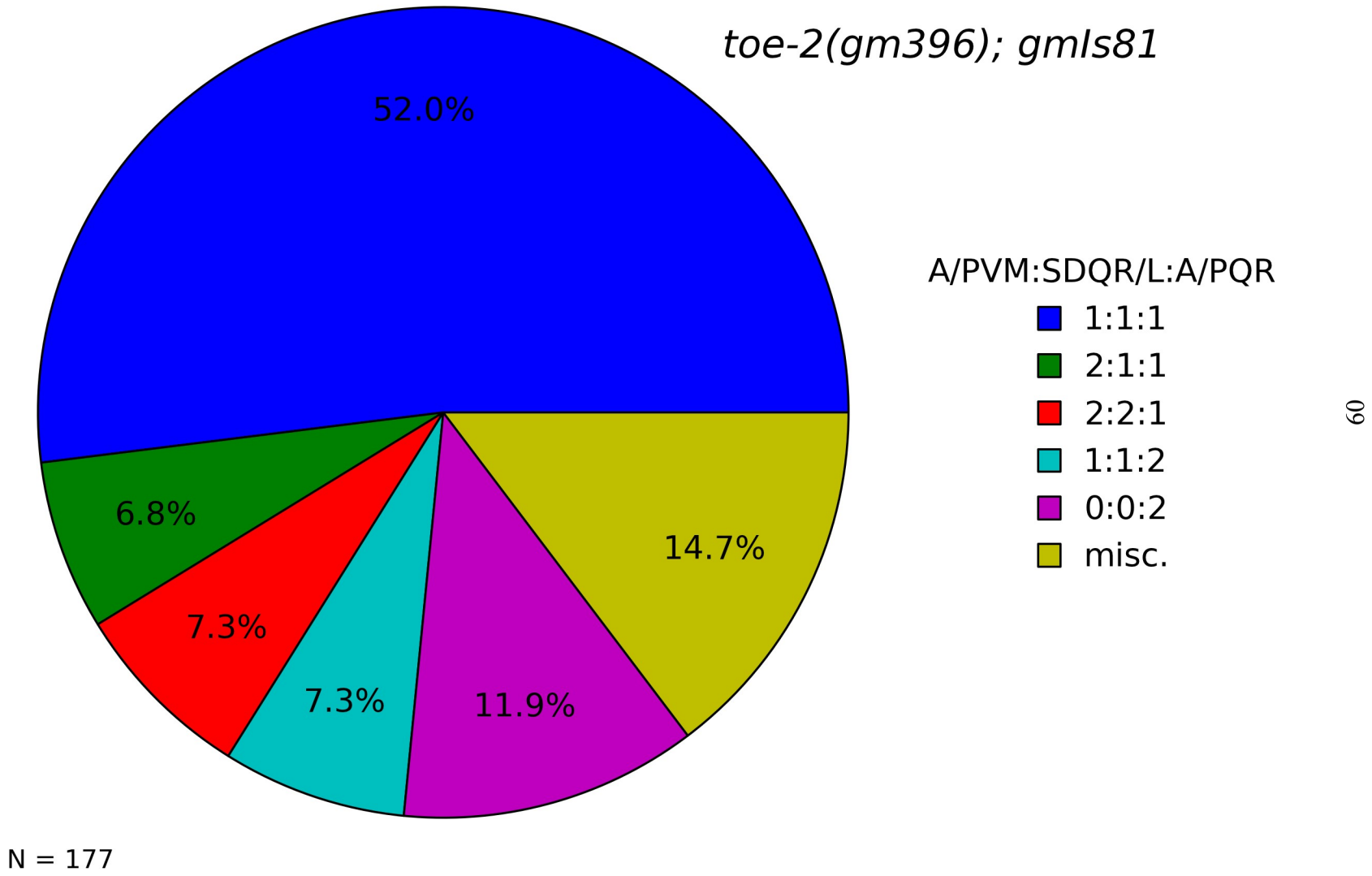
toe-2(gm396); gmIs81
52.0%
6.8%
7.3%
7.3%
11.9%
14.7%
A/PVM:SDQR/L:A/PQR
1:1:1
2:1:1
2:2:1
1:1:2
0:0:2
misc.
N = 177

Figure 5: Extra and missing neurons in *toe-2(gm396); gmIs81* worms. The *gmIs81* transgene allows for the counting of all the neurons present in a single Q lineage. The legend indicates categories of cell number ratios of A/PVM to SDQR/L to A/PQR neurons. "N" denotes the number of lineages scored in this experiment. The pie indicates the percentage of the total lineages (N) that fall into a particular cell number ratio category. The miscellaneous (misc.) category contains all of the cell number ratio categories that individually account for less than 5% of total lineages scored.

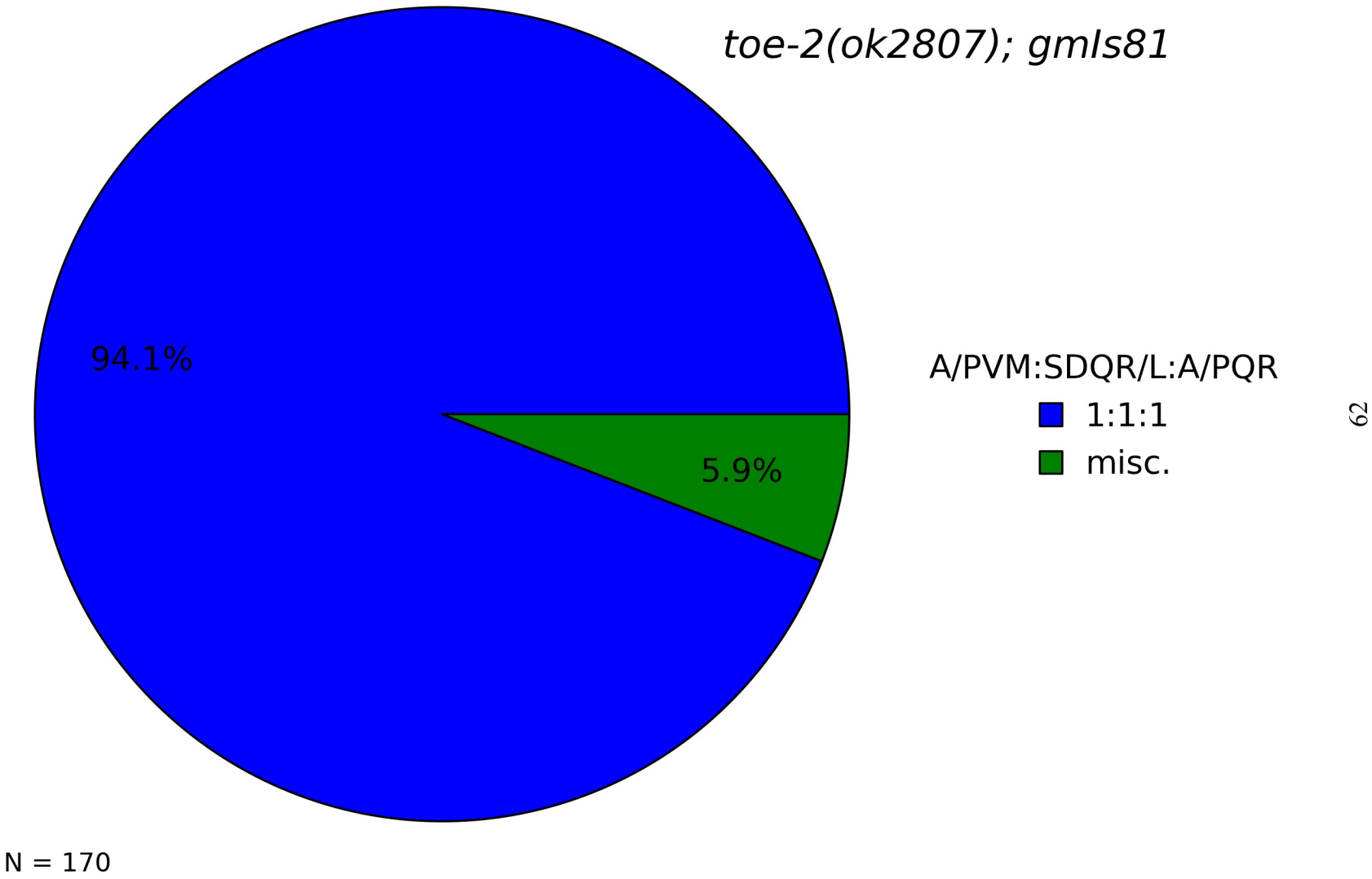
toe-2(ok2807); gmIs81
94.1%
5.9%
A/PVM:SDQR/L:A/PQR
1:1:1
misc.
N = 170

Figure 6: Extra and missing neurons in *toe-2(ok2807); gmIs81* worms. The *gmIs81* transgene allows for the counting of all the neurons present in a single Q lineage. The legend indicates categories of cell number ratios of A/PVM to SDQR/L to A/PQR neurons. "N" denotes the number of lineages scored in this experiment. The pie indicates the percentage of the total lineages (N) that fall into a particular cell number ratio category. The miscellaneous (misc.) category contains all of the cell number ratio categories that individually account for less than 5% of total lineages scored.

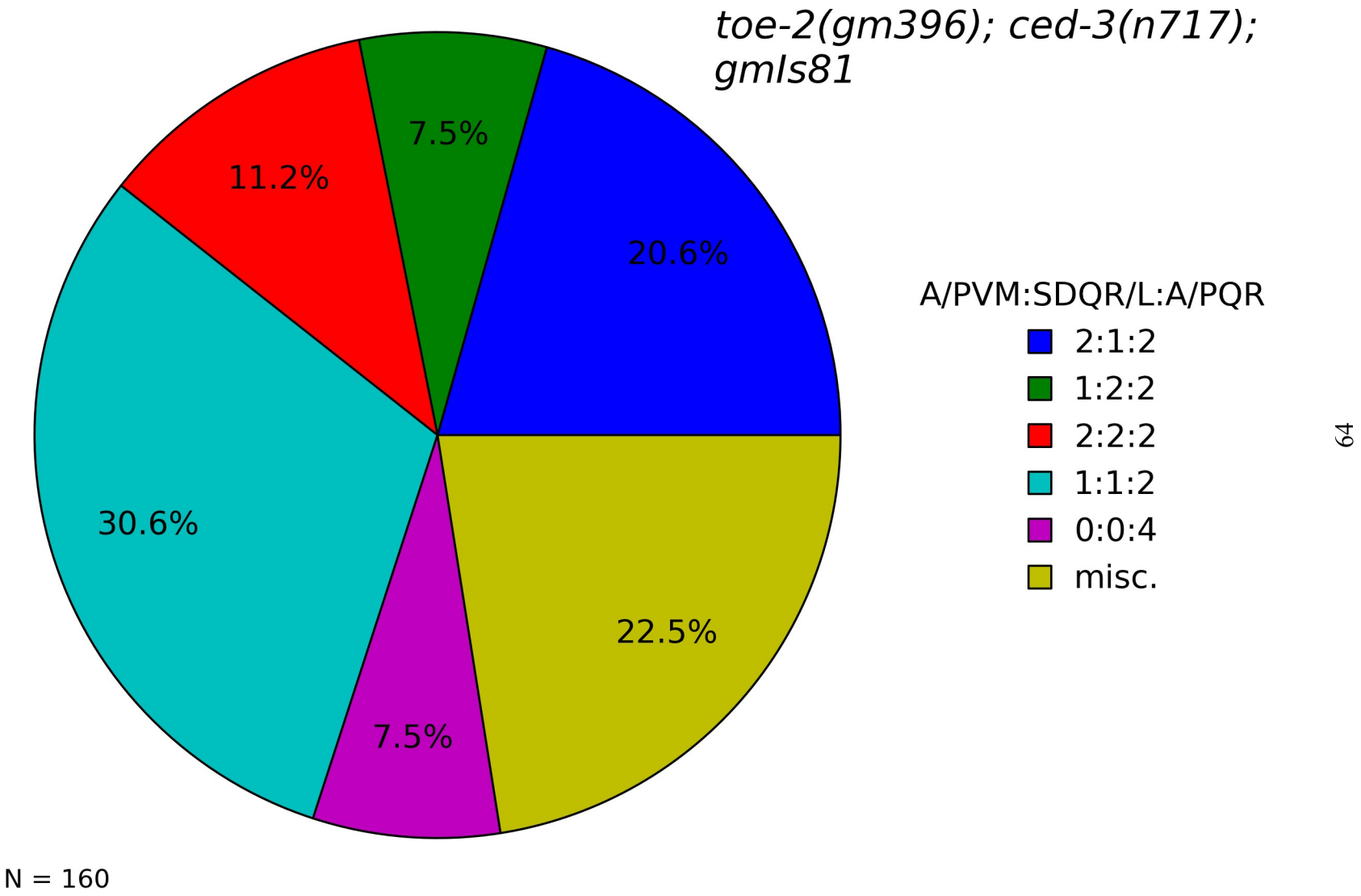
toe-2(gm396); ced-3(n717); gmIs81
7.5%
11.2%
20.6%
30.6%
22.5%
7.5%
A/PVM:SDQR/L:A/PQR
2:1:2
1:2:2
2:2:2
1:1:2
0:0:4
misc.
N = 160

Figure 7: Extra and missing neurons in *toe-2(gm396); ced-3(n717); gmIs81* worms. The *gmIs81* transgene allows for the counting of all the neurons present in a single Q lineage. The legend indicates categories of cell number ratios of A/PVM to SDQR/L to A/PQR neurons. "N" denotes the number of lineages scored in this experiment. The pie indicates the percentage of the total lineages (N) that fall into a particular cell number ratio category. The miscellaneous (misc.) category contains all of the cell number ratio categories that individually account for less than 5% of total lineages scored.

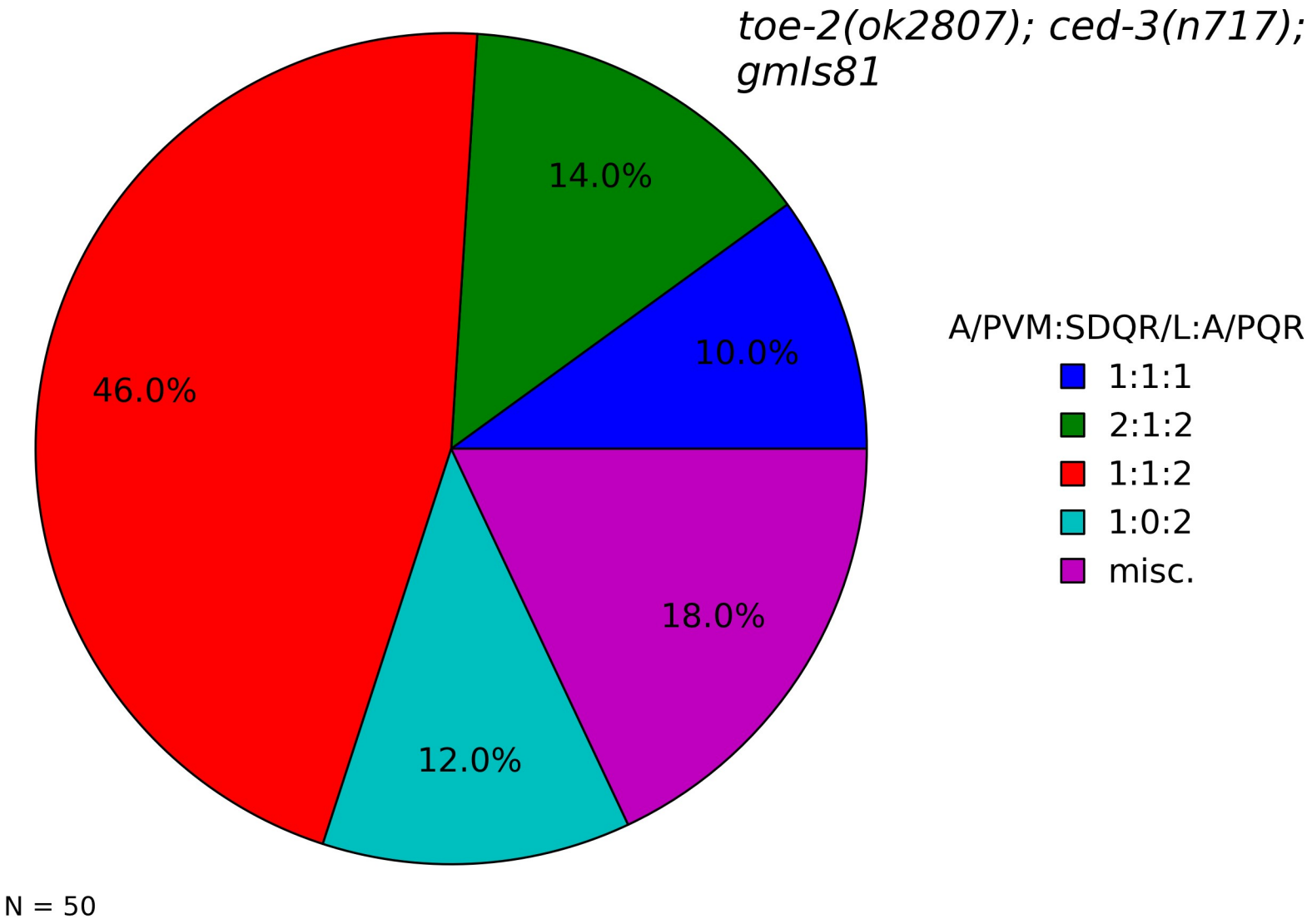
toe-2(ok2807); ced-3(n717); gmIs81
14.0%
10.0%
46.0%
18.0%
12.0%
A/PVM:SDQR/L:A/PQR
1:1:1
2:1:2
1:1:2
1:0:2
misc.
N = 50

Figure 8: Extra and missing neurons in *toe-2(ok2807); ced-3(n717); gmIs81* worms. The *gmIs81* transgene allows for the counting of all the neurons present in a single Q lineage. The legend indicates categories of cell number ratios of A/PVM to SDQR/L to A/PQR neurons. "N" denotes the number of lineages scored in this experiment. The pie indicates the percentage of the total lineages (N) that fall into a particular cell number ratio category. The miscellaneous (misc.) category contains all of the cell number ratio categories that individually account for less than 5% of total lineages scored.

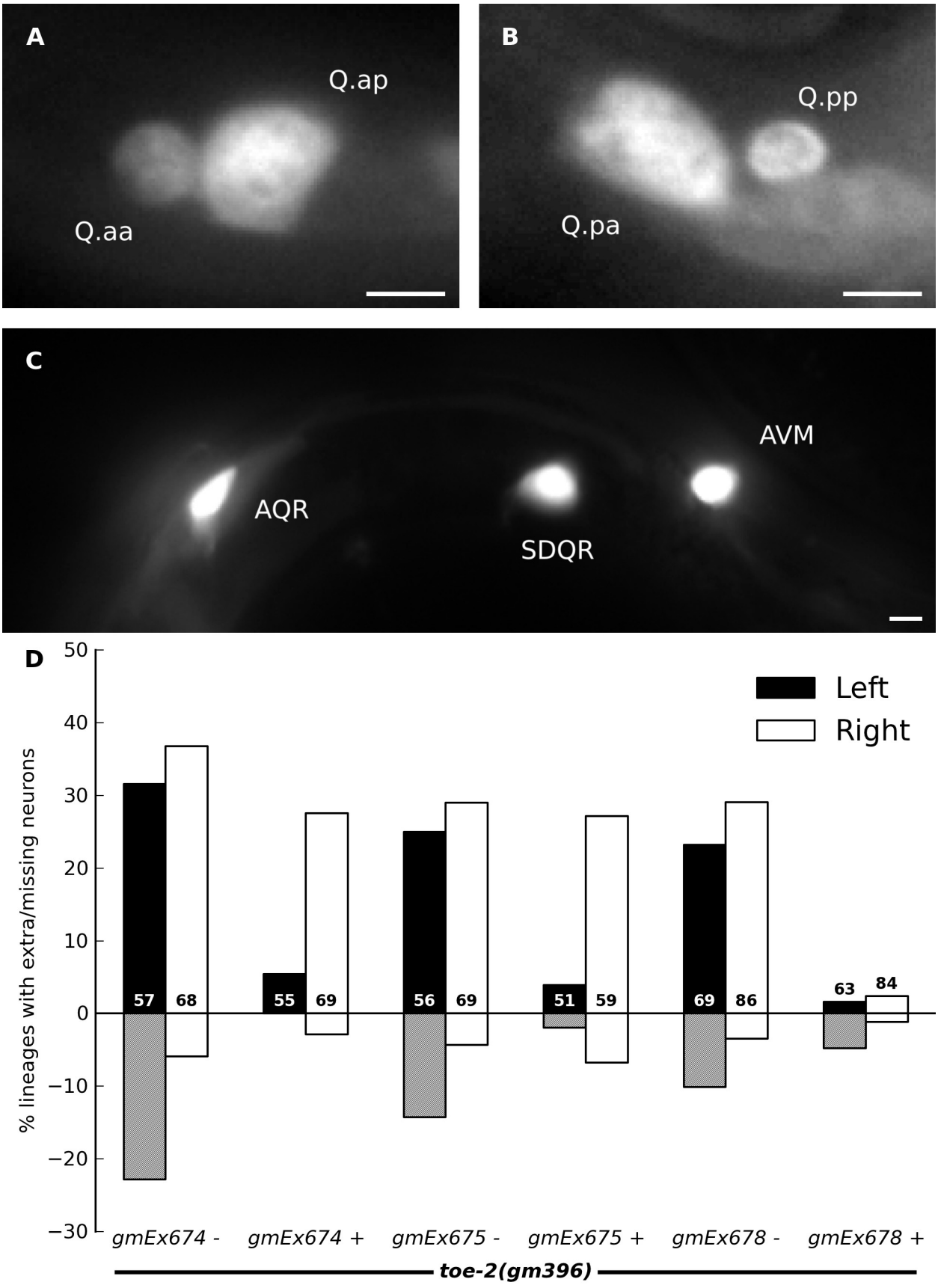
A
Q.ap
Q.aa
B
Q.pp
Q.pa
C
AVM
AQR
SDQR
D
Left
Right
% lineages with extra/missing neurons
50
40
30
20
10
0
−10
−20
−30
57
68
55
69
56
69
51
59
69
86
63
84
gmEx674 -
gmEx674 +
gmEx675 -
gmEx675 +
gmEx678 -
gmEx678 +
toe-2(gm396)

Figure 9: *Ptoe-2::gfp* expression and *toe-2* rescue. (A, B) *Ptoe-2::gfp* expression in Q.a (A) and Q.p daughters (B). (C) *Ptoe-2::gfp* expression in Q-derived neurons AQR, SDQR and AVM. These neurons are derived from the right Q neuroblast. *Ptoe-2::gfp* is also expressed throughout the left Q lineage. Scale bars represent 2.5 μm. (D) The percentage of lineages with extra and missing neurons (y-axis) was scored in *toe-2(gm396)* mutants that either carry or do not carry a transgene (x-axis). The percentage of extra A/PVM neurons was scored separately for the left (PVM) and right (AVM) Q lineages. The percentages of extra and missing PVMs are shown with black and hatched bars, respectively. The percentages of extra and missing AVMs are shown with white bars. The numbers of lineages scored for each group are shown along the x-axis. The *gmEx674* and *gmEx675* transgenes express TOE-2 from the promoter of *mab-5*, which is active only in the left Q lineage. In worms carrying either transgene, extra and missing neurons are observed on both sides when the transgene is not present (-); however, when the transgene is present (+) the defect is rescued on the left side. The *gmEx678* transgene expresses TOE-2 from the promoter of *egl-17*, which is active in both the left and right Q lineages. Rescue is observed on both sides when the transgene is present.

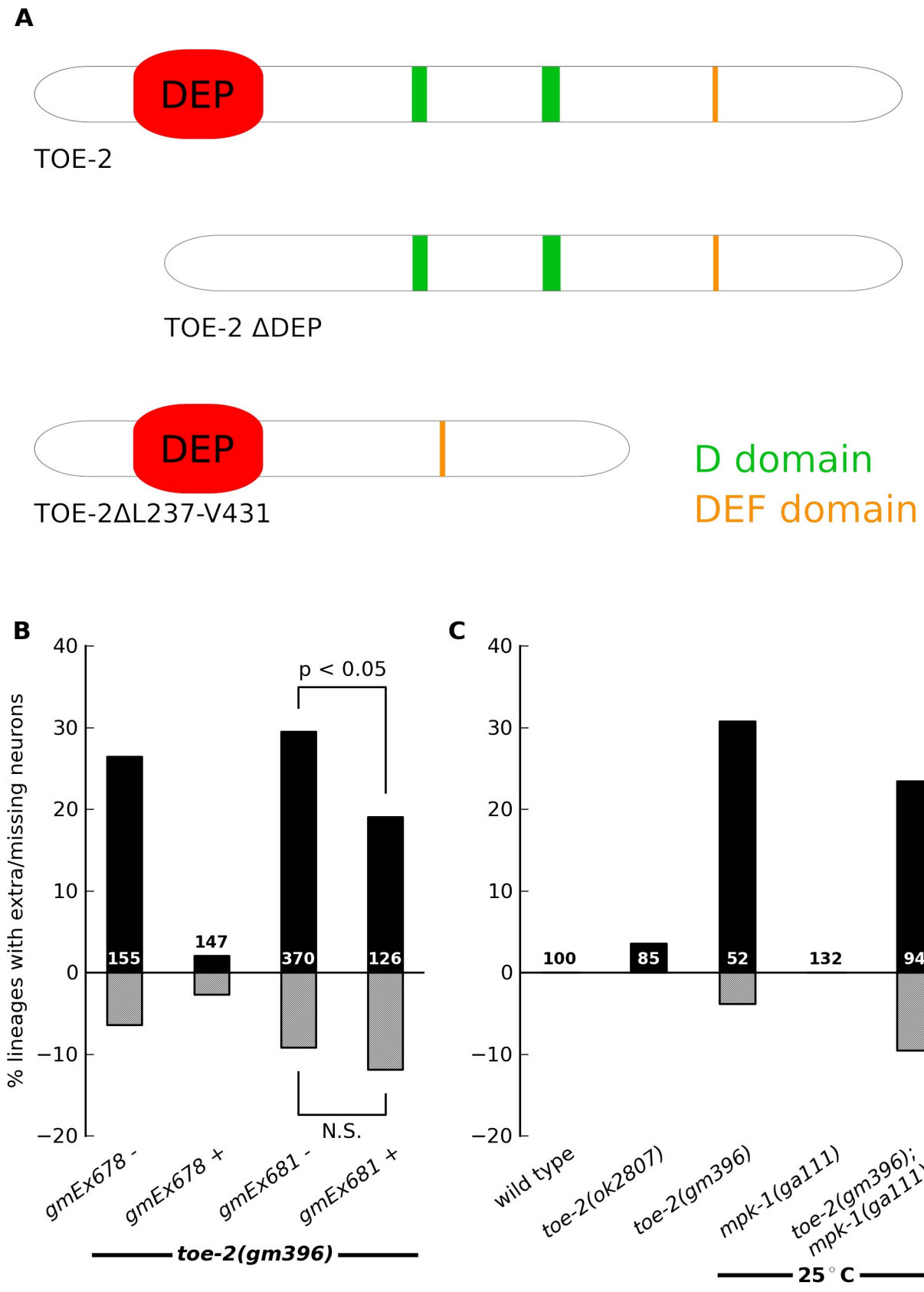
A
DEP
TOE-2
TOE-2 ΔDEP
DEP
TOE-2ΔL237-V431
D domain
DEF domain
B
% lineages with extra/missing neurons
40
30
20
10
0
−10
−20
p < 0.05
N.S.
155
147
370
126
gmEx678 -
gmEx678 +
gmEx681 -
gmEx681 +
toe-2(gm396)
C
100
85
52
132
94
wild type
toe-2(ok2807)
toe-2(gm396)
mpk-1(ga111)
toe-2(gm396); mpk-1(ga111)
25 ° C

Figure 10: TOE-2 structure-function analysis. (A) Wild-type TOE-2 protein, TOE-2 with the DEP domain removed and TOE-2 with the D domains and intervening amino acids removed (the hypothetical protein encoded by the *toe-2(ok2807)* allele). D domains and the DEF domain are shown in green and orange, respectively. (B) The percentages of lineages with extra and missing A/PVM neurons (y-axis) was scored in *toe-2(gm396)* mutants that either carry or do not carry a transgene (x-axis) and are shown with black and hatched bars, respectively. The numbers of lineages scored for each group are shown along the x-axis. The *gmEx678* transgene expresses full-length TOE-2 from the promoter of *egl-17*, which is active in the Q lineage. Rescue is not observed when the *gmEx678* transgene is absent (-), but rescue is observed when the transgene is present (+). The *gmEx681* transgene expresses TOE-2ΔDEP from the promoter of *egl-17*. Extra and missing cells are observed when the transgene is absent. The extra-cell phenotype is partially rescued when the transgene is present. (C) The percentages of lineages with extra and missing A/PVM neurons (y-axis) were scored in different genetic backgrounds and are shown with black and hatched bars, respectively. The number of lineages scored for each genotype appears along the x-axis. Wild-type and *toe-2(ok2807)* mutant worms were scored at 20° C while *toe-2(gm396)*, *mpk-1(ga111)* and *toe-2(gm396); mpk-1(ga111)* mutants were all scored at 25° C, the non-permissive temperature for the *mpk-1(ga111)* allele. The value $p < 0.05$ was acquired using the X^2 test. N. S., not significant.

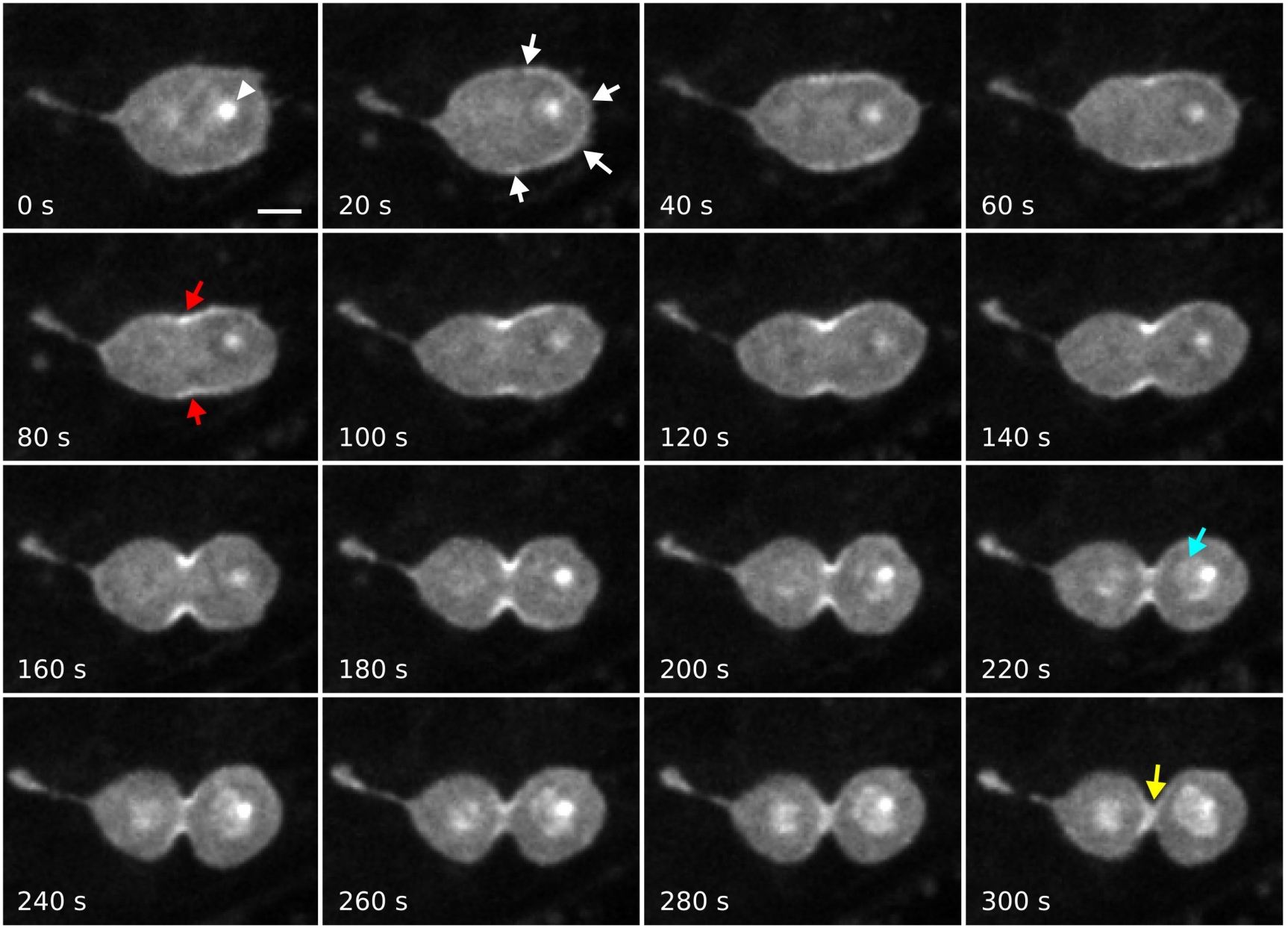
0 s
20 s
40 s
60 s
80 s
100 s
120 s
140 s
160 s
180 s
200 s
220 s
240 s
260 s
280 s
300 s

Figure 11: TOE-2::GFP localization in the Q neuroblast. An image was taken every 20 seconds during the division of a Q neuroblast (time of capture relative to the first image is indicated in the bottom left of each panel). TOE-2::GFP localizes at centrosomes (white arrowhead) from metaphase to the end of anaphase (present at both centrosomes, however, only the posterior centrosome is visible in these images). Prior to furrow ingression, TOE-2::GFP localizes to the posterior cortex (white arrows) and then becomes concentrated in the cleavage furrow (red arrows). Near the end of anaphase TOE-2::GFP accumulates on chromatin (cyan arrow). At the end of the division, TOE-2 is concentrated in the midbody (yellow arrow). The scale bar represents 2.5 μm. The data in this figure are representative of time-lapse micrographs taken of two Q neuroblasts. These time-lapse micrographs provide preliminary evidence suggesting an asymmetric localization of TOE-2 to the posterior cortex of the dividing Q neuroblast. Centrosomal, furrow and nuclear localization of TOE-2 were observed in these confocal time-lapses and in immuno-fluorescent (IF) micrographs of multiple Q neuroblasts using a compound microscope.

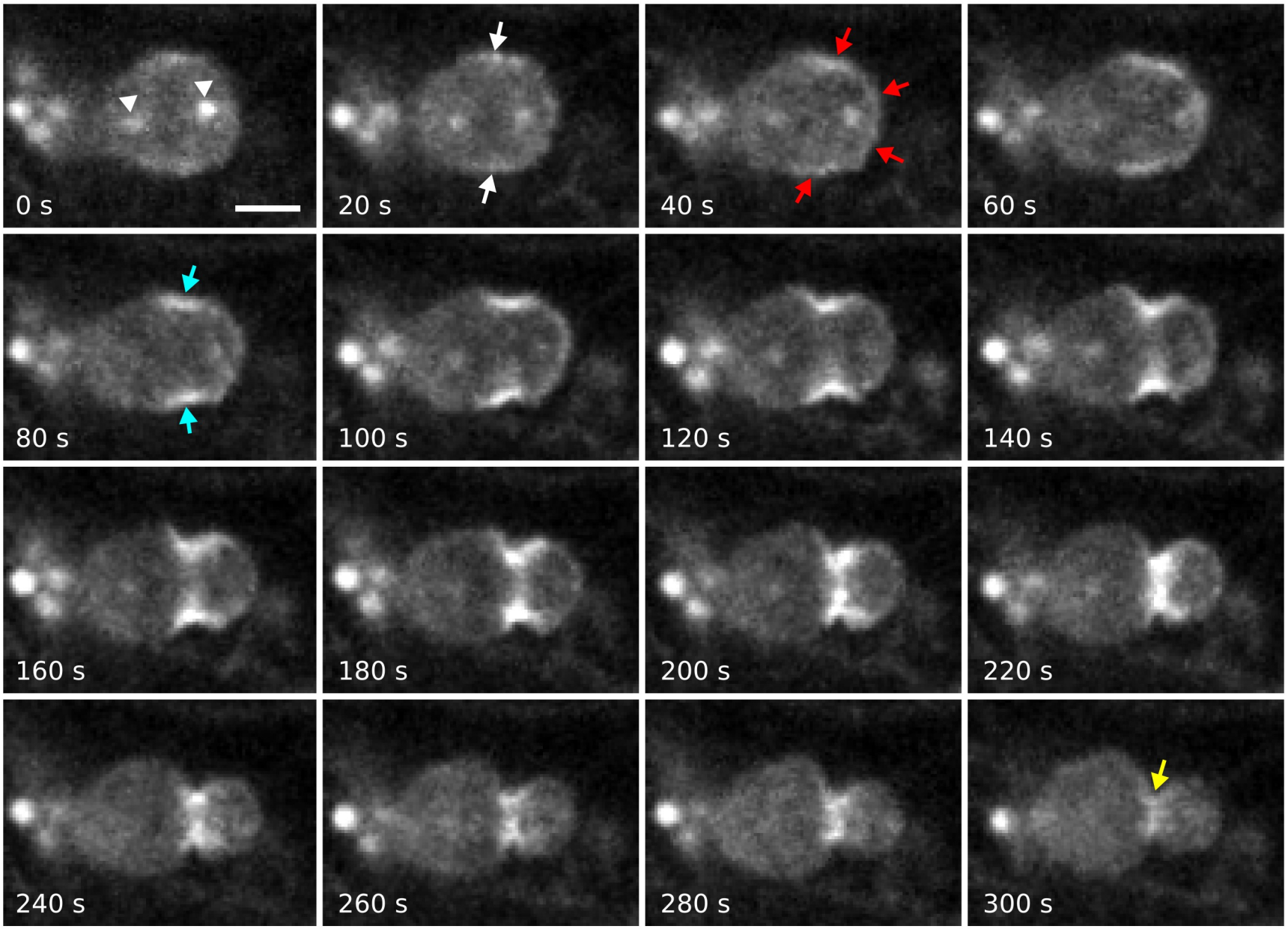
0 s
20 s
40 s
60 s
80 s
100 s
120 s
140 s
160 s
180 s
200 s
220 s
240 s
260 s
280 s
300 s

Figure 12: TOE-2::GFP localization in the Q.p neuroblast. An image was taken every 20 seconds during the division of a Q.p neuroblast (time of capture relative to the first image is indicated in the bottom left of each panel). TOE-2::GFP localizes at centrosomes (white arrowheads) from metaphase to the end of anaphase (not visible after 220s, though visible in other images at later time points). Prior to furrow ingression, TOE-2::GFP localizes to the region of the cortex where the furrow will ingress (white arrows) and then becomes concentrated at the posterior cortex (red arrows) and remains there through much of anaphase. TOE-2::GFP also begins to concentrate at the furrow when it begins to ingress (cyan arrows). At the end of the division TOE-2 is concentrated in the midbody (yellow arrow). The scale bar represents 2.5 μm. Only one time-lapse micrograph was taken of TOE-2 localization in a dividing Q.p neuroblast. This time-lapse micrograph provides preliminary evidence suggesting an asymmetric localization of TOE-2 to the posterior cortex of the dividing Q.p neuroblast. Centrosomal, furrow and nuclear localization of TOE-2 were observed in this confocal time-lapse and in IF micrographs of multiple Q.p neuroblasts using a compound microscope.

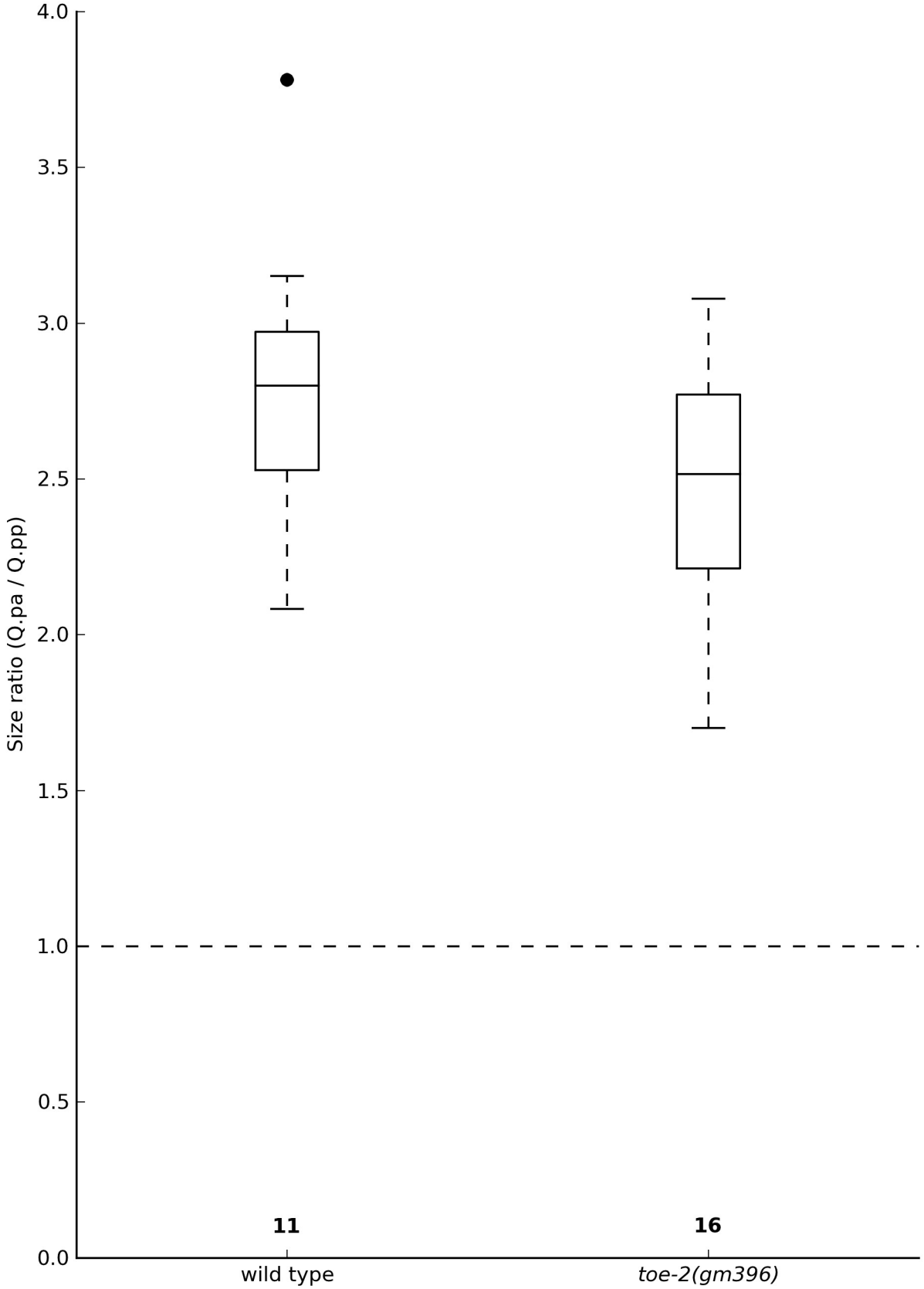
4.0
3.5
3.0
2.5
2.0
1.5
1.0
0.5
0.0
Size ratio (Q.pa / Q.pp)
11
16
wild type
toe-2(gm396)

Figure 13: Q.p daughter cell size asymmetry in *toe-2(gm396)*. Micrographs of Q.p daughters were captured and cell areas were measured as in Singhvi et al., 2011. The cell size ratios of Q.pa to Q.pp are plotted along the y-axis. Genotypes are listed along the x-axis. The numbers of micrographs measured for each genotype are listed along the x-axis. There is no statistical difference between the two distributions by the Mann-Whitney U test.

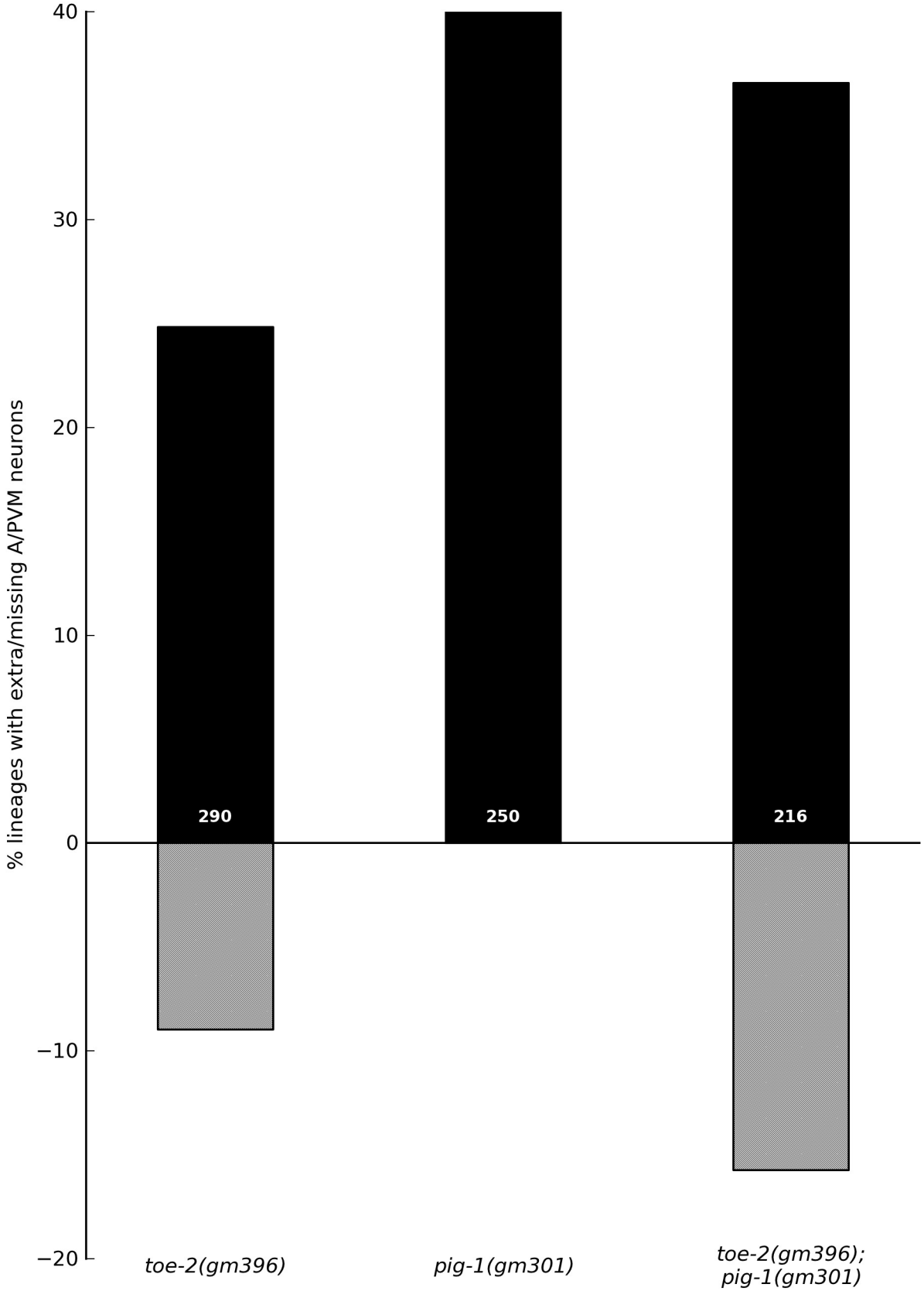
40
30
20
10
0
−10
−20
% lineages with extra/missing A/PVM neurons
290
250
216
toe-2(gm396)
pig-1(gm301)
toe-2(gm396);
pig-1(gm301)

Figure 14: Evidence for *toe-2* and *pig-1* being in the same pathway. The percentages of lineages with extra and missing A/PVM neurons (y-axis) were scored in different genetic backgrounds and are shown with black and hatched bars, respectively. The number of lineages scored for each genotype appears along the x-axis. Double mutants between *toe-2* and *pig-1* look like *pig-1* single mutants with respect to extra neurons; however, double mutants still have missing neurons while *pig-1* single mutants do not.

REFERENCES

Arur, S., Ohmachi, M., Nayak, S., Hayes, M., Miranda, A., Hay, A., Golden, A., and Schedl, T. (**2009**). Multiple ERK substrates execute single biological processes in Caenorhabditis elegans germ-line development. Proc. Natl. Acad. Sci. U.S.A. *106*, 4776–4781.

Ashkenazi, A., and Dixit, V.M. (**1998**). Death Receptors: Signaling and Modulation. Science *281*, 1305–1308.

Axelrod, J.D., Miller, J.R., Shulman, J.M., Moon, R.T., and Perrimon, N. (**1998**). Differential recruitment of Dishevelled provides signaling specificity in the planar cell polarity and Wingless signaling pathways. Genes Dev. *12*, 2610–2622.

Ballon, D.R., Flanary, P.L., Gladue, D.P., Konopka, J.B., Dohlman, H.G., and Thorner, J. (**2006**). DEP-domain-mediated regulation of GPCR signaling responses. Cell *126*, 1079–1093.

Barr, F.A., and Gruneberg, U. (**2007**). Cytokinesis: placing and making the final cut. Cell *131*, 847–860.

Bertrand, V., and Hobert, O. (**2009**). Linking asymmetric cell division to the terminal differentiation program of postmitotic neurons in C. elegans. Dev. Cell *16*, 563–575.

Bouillet, P., and Strasser, A. (**2002**). BH3-only proteins - evolutionarily conserved proapoptotic Bcl-2 family members essential for initiating programmed cell death. J. Cell. Sci. *115*, 1567–1574.

Boutros, M., Paricio, N., Strutt, D.I., and Mlodzik, M. (**1998**). Dishevelled activates JNK and discriminates between JNK pathways in planar polarity and wingless signaling. Cell *94*, 109–118.

Bratton, D.L., Fadok, V.A., Richter, D.A., Kailey, J.M., Guthrie, L.A., and Henson, P.M. (**1997**). Appearance of Phosphatidylserine on Apoptotic Cells Requires Calcium-mediated Nonspecific Flip-Flop and Is Enhanced by Loss of the Aminophospholipid Translocase. J. Biol. Chem. *272*, 26159–26165.

Brenner, S. (**1974**). The genetics of Caenorhabditis elegans. Genetics *77*, 71–94.

Cermak, T., Doyle, E.L., Christian, M., Wang, L., Zhang, Y., Schmidt, C., Baller, J.A., Somia, N.V., Bogdanove, A.J., and Voytas, D.F. (**2011**). Efficient design and assembly of custom TALEN and other TAL effector-based constructs for DNA targeting. Nucleic Acids Res. *39*, e82.

Chau, B.N., Cheng, E.H., Kerr, D.A., and Hardwick, J.M. (**2000**). Aven, a novel inhibitor of caspase activation, binds Bcl-xL and Apaf-1. Mol. Cell *6*, 31–40.

Chen, F., Hersh, B.M., Conradt, B., Zhou, Z., Riemer, D., Gruenbaum, Y., and Horvitz, H.R. (**2000**). Translocation of C. elegans CED-4 to nuclear membranes during programmed cell death. Science *287*, 1485–1489.

Chen, S., and Hamm, H.E. (**2006**). DEP Domains: More Than Just Membrane Anchors. Developmental Cell *11*, 436–438.

Chinnaiyan, A.M., O'Rourke, K., Lane, B.R., and Dixit, V.M. (**1997**). Interaction of CED-4 with CED-3 and CED-9: a molecular framework for cell death. Science *275*, 1122–1126.

Clark, S.G., and Chiu, C. (**2003**). C. elegans ZAG-1, a Zn-finger-homeodomain protein, regulates axonal development and neuronal differentiation. Development *130*, 3781–3794.

Conradt, B., and Horvitz, H.R. (**1998**). The C. elegans protein EGL-1 is required for programmed cell death and interacts with the Bcl-2-like protein CED-9. Cell *93*, 519–529.

Conradt, B., and Horvitz, H.R. (**1999**). The TRA-1A sex determination protein of C. elegans regulates sexually dimorphic cell deaths by repressing the egl-1 cell death activator gene. Cell *98*, 317–327.

Cordes, S., Frank, C.A., and Garriga, G. (**2006**). The C. elegans MELK ortholog PIG-1 regulates cell size asymmetry and daughter cell fate in asymmetric neuroblast divisions. Development *133*, 2747–2756.

Costa, M., Weir, M., Coulson, A., Sulston, J., and Kenyon, C. (**1988**). Posterior pattern formation in C. elegans involves position-specific expression of a gene containing a homeobox. Cell *55*, 747–756.

Cowing, D.W., and Kenyon, C. (**1992**). Expression of the homeotic gene mab-5 during Caenorhabditis elegans embryogenesis. Development *116*, 481–490.

Dubreuil, V., Marzesco, A.-M., Corbeil, D., Huttner, W.B., and Wilsch-Bräuninger, M. (**2007**). Midbody and primary cilium of neural progenitors release extracellular membrane particles enriched in the stem cell marker prominin-1. J. Cell Biol. *176*, 483–495.

Ellis, H.M., and Horvitz, H.R. (**1986**). Genetic control of programmed cell death in the nematode C. elegans. Cell *44*, 817–829.

Elmore, S. (**2007**). Apoptosis: a review of programmed cell death. Toxicol Pathol *35*, 495–516.

Fadok, V.A., Voelker, D.R., Campbell, P.A., Cohen, J.J., Bratton, D.L., and Henson, P.M. (**1992**). Exposure of phosphatidylserine on the surface of apoptotic lymphocytes triggers specific recognition and removal by macrophages. J Immunol *148*, 2207–2216.

Gerhold, A.R., Richter, D.J., Yu, A.S., and Hariharan, I.K. (**2011**). Identification and Characterization of Genes Required for Compensatory Growth in Drosophila. Genetics *189*, 1309–1326.

Goss, J.W., and Toomre, D.K. (**2008**). Both daughter cells traffic and exocytose membrane at the cleavage furrow during mammalian cytokinesis. J. Cell Biol. *181*, 1047–1054.

Gromley, A., Yeaman, C., Rosa, J., Redick, S., Chen, C.-T., Mirabelle, S., Guha, M., Sillibourne, J., and Doxsey, S.J. (**2005**). Centriolin anchoring of exocyst and SNARE complexes at the midbody is required for secretory-vesicle-mediated abscission. Cell *123*, 75–87.

Habas, R., Kato, Y., and He, X. (**2001**). Wnt/Frizzled activation of Rho regulates vertebrate gastrulation and requires a novel Formin homology protein Daam1. Cell *107*, 843–854.

Hengartner, M.O., Ellis, R.E., and Horvitz, H.R. (**1992**). Caenorhabditis elegans gene ced-9 protects cells from programmed cell death. Nature *356*, 494–499.

Hengartner, M.O., and Horvitz, H.R. (**1994**). C. elegans cell survival gene ced-9 encodes a functional homolog of the mammalian proto-oncogene bcl-2. Cell *76*, 665–676.

Hill, M.M., Adrain, C., Duriez, P.J., Creagh, E.M., and Martin, S.J. (**2004**). Analysis of the composition, assembly kinetics and activity of native Apaf-1 apoptosomes. EMBO J. *23*, 2134–2145.

Hodgkin, J. (**1987**). A genetic analysis of the sex-determining gene, tra-1, in the nematode Caenorhabditis elegans. Genes Dev. *1*, 731–745.

Hung, A.Y., and Sheng, M. (**2002**). PDZ domains: structural modules for protein complex assembly. J. Biol. Chem. *277*, 5699–5702.

Itoh, K., Antipova, A., Ratcliffe, M.J., and Sokol, S. (**2000**). Interaction of Dishevelled and XenopusAxin-Related Protein Is Required for Wnt Signal Transduction. Mol. Cell. Biol. *20*, 2228–2238.

Julius, M.A., Schelbert, B., Hsu, W., Fitzpatrick, E., Jho, E., Fagotto, F., Costantini, F., and Kitajewski, J. (**2000**). Domains of Axin and Disheveled Required for Interaction and Function in Wnt Signaling. Biochemical and Biophysical Research Communications *276*, 1162–1169.

Kishida, S., Yamamoto, H., Hino, S., Ikeda, S., Kishida, M., and Kikuchi, A. (**1999**). DIX domains of Dvl and axin are necessary for protein interactions and their ability to regulate beta-catenin stability. Mol. Cell. Biol. *19*, 4414–4422.

Krause, M., Park, M., Zhang, J.M., Yuan, J., Harfe, B., Xu, S.Q., Greenwald, I., Cole, M., Paterson, B., and Fire, A. (**1997**). A C. elegans E/Daughterless bHLH protein marks neuronal but not striated muscle development. Development *124*, 2179–2189.

Kuo, T.-C., Chen, C.-T., Baron, D., Onder, T.T., Loewer, S., Almeida, S., Weismann, C.M., Xu, P., Houghton, J.-M., Gao, F.-B., et al. (**2011**). Midbody accumulation through evasion of autophagy contributes to cellular reprogramming and tumorigenicity. Nature Cell Biology *13*, 1214–1223.

Lackner, M.R., and Kim, S.K. (**1998**). Genetic analysis of the Caenorhabditis elegans MAP kinase gene mpk-1. Genetics *150*, 103–117.

Lackner, M.R., Kornfeld, K., Miller, L.M., Horvitz, H.R., and Kim, S.K. (**1994**). A MAP kinase homolog, mpk-1, is involved in ras-mediated induction of vulval cell fates in Caenorhabditis elegans. Genes Dev. *8*, 160–173.

Leacock, S.W., and Reinke, V. (**2006**). Expression profiling of MAP kinase-mediated meiotic progression in Caenorhabditis elegans. PLoS Genet. *2*, e174.

Li, P., Nijhawan, D., Budihardjo, I., Srinivasula, S.M., Ahmad, M., Alnemri, E.S., and Wang, X. (**1997**). Cytochrome c and dATP-dependent formation of Apaf-1/caspase-9 complex initiates an apoptotic protease cascade. Cell *91*, 479–489.

Liu, X., Kim, C.N., Yang, J., Jemmerson, R., and Wang, X. (**1996**). Induction of apoptotic program in cell-free extracts: requirement for dATP and cytochrome c. Cell *86*, 147–157.

Locksley, R.M., Killeen, N., and Lenardo, M.J. (**2001**). The TNF and TNF receptor superfamilies: integrating mammalian biology. Cell *104*, 487–501.

Macdonald, B.T., Semenov, M.V., and He, X. (**2007**). SnapShot: Wnt/beta-catenin signaling. Cell *131*, 1204.

Marrari, Y., Crouthamel, M., Irannejad, R., and Wedegaertner, P.B. (**2007**). Assembly and trafficking of heterotrimeric G proteins. Biochemistry *46*, 7665–7677.

Marzesco, A.-M., Janich, P., Wilsch-Bräuninger, M., Dubreuil, V., Langenfeld, K., Corbeil, D., and Huttner, W.B. (**2005**). Release of extracellular membrane particles carrying the stem cell marker prominin-1 (CD133) from neural progenitors and other epithelial cells. J. Cell. Sci. *118*, 2849–2858.

Mello, C.C., Kramer, J.M., Stinchcomb, D., and Ambros, V. (**1991**). Efficient gene transfer in C.elegans: extrachromosomal maintenance and integration of transforming sequences. EMBO J. *10*, 3959–3970.

Metzstein, M.M., Hengartner, M.O., Tsung, N., Ellis, R.E., and Horvitz, H.R. (**1996**). Transcriptional regulator of programmed cell death encoded by Caenorhabditis elegans gene ces-2. Nature *382*, 545–547.

Metzstein, M.M., and Horvitz, H.R. (**1999**). The C. elegans cell death specification gene ces-1 encodes a snail family zinc finger protein. Mol. Cell *4*, 309–319.

Moreno, E., Yan, M., and Basler, K. (**2002**). Evolution of TNF signaling mechanisms: JNK-dependent apoptosis triggered by Eiger, the Drosophila homolog of the TNF superfamily. Curr. Biol. *12*, 1263–1268.

Mullins, J.M., and Biesele, J.J. (**1977**). Terminal phase of cytokinesis in D-98s cells. J. Cell Biol. *73*, 672–684.

Neves, S.R., Ram, P.T., and Iyengar, R. (**2002**). G protein pathways. Science *296*, 1636–1639.

Newmeyer, D.D., Bossy-Wetzel, E., Kluck, R.M., Wolf, B.B., Beere, H.M., and Green, D.R. (**2000**). Bcl-xL does not inhibit the function of Apaf-1. Cell Death Differ. *7*, 402–407.

Oldham, W.M., and Hamm, H.E. (**2006**). Structural basis of function in heterotrimeric G proteins. Q. Rev. Biophys. *39*, 117–166.

Ou, G., Stuurman, N., D'Ambrosio, M., and Vale, R.D. (**2010**). Polarized myosin produces unequal-size daughters during asymmetric cell division. Science *330*, 677–680.

Parrish, J., Metters, H., Chen, L., and Xue, D. (**2000**). Demonstration of the in vivo interaction of key cell death regulators by structure-based design of second-site suppressors. Proc. Natl. Acad. Sci. U.S.A. *97*, 11916–11921.

Pellegrino, M.W., Farooqui, S., Fröhli, E., Rehrauer, H., Kaeser-Pebernard, S., Müller, F., Gasser, R.B., and Hajnal, A. (**2011**). LIN-39 and the EGFR/RAS/MAPK pathway regulate C. elegans vulval morphogenesis via the VAB-23 zinc finger protein. Development *138*, 4649–4660.

del Peso, L., González, V.M., and Núñez, G. (**1998**). Caenorhabditis elegans EGL-1 disrupts the interaction of CED-9 with CED-4 and promotes CED-3 activation. J. Biol. Chem. *273*, 33495–33500.

Pohl, C., and Jentsch, S. (**2009**). Midbody ring disposal by autophagy is a post-abscission event of cytokinesis. Nat. Cell Biol. *11*, 65–70.

Rual, J.-F., Ceron, J., Koreth, J., Hao, T., Nicot, A.-S., Hirozane-Kishikawa, T., Vandenhaute, J., Orkin, S.H., Hill, D.E., van den Heuvel, S., et al. (**2004**). Toward improving Caenorhabditis elegans phenome mapping with an ORFeome-based RNAi library. Genome Res. *14*, 2162–2168.

Rutkowski, R., Dickinson, R., Stewart, G., Craig, A., Schimpl, M., Keyse, S.M., and Gartner, A. (**2011**). Regulation of Caenorhabditis elegans p53/CEP-1-dependent germ cell apoptosis by Ras/MAPK signaling. PLoS Genet. *7*, e1002238.

Salser, S.J., and Kenyon, C. (**1992**). Activation of a C. elegans Antennapedia homologue in migrating cells controls their direction of migration. Nature *355*, 255–258.

Semenov, M.V., Habas, R., Macdonald, B.T., and He, X. (**2007**). SnapShot: Noncanonical Wnt Signaling Pathways. Cell *131*, 1378.

Shaham, S. (**1998**). Identification of multiple Caenorhabditis elegans caspases and their potential roles in proteolytic cascades. J. Biol. Chem. *273*, 35109–35117.

Shaham, S., Reddien, P.W., Davies, B., and Horvitz, H.R. (**1999**). Mutational analysis of the Caenorhabditis elegans cell-death gene ced-3. Genetics *153*, 1655–1671.

Simmer, F., Tijsterman, M., Parrish, S., Koushika, S.P., Nonet, M.L., Fire, A., Ahringer, J., and Plasterk, R.H.A. (**2002**). Loss of the putative RNA-directed RNA polymerase RRF-3 makes C. elegans hypersensitive to RNAi. Curr. Biol. *12*, 1317–1319.

Simons, M., and Mlodzik, M. (**2008**). Planar cell polarity signaling: from fly development to human disease. Annu. Rev. Genet. *42*, 517–540.

Singh, J., Yanfeng, W.A., Grumolato, L., Aaronson, S.A., and Mlodzik, M. (**2010**). Abelson family kinases regulate Frizzled planar cell polarity signaling via Dsh phosphorylation. Genes Dev. *24*, 2157–2168.

Singhvi, A., Teuliere, J., Talavera, K., Cordes, S., Ou, G., Vale, R.D., Prasad, B.C., Clark, S.G., and Garriga, G. (**2011**). The Arf GAP CNT-2 regulates the apoptotic fate in C. elegans asymmetric neuroblast divisions. Curr. Biol. *21*, 948–954.

Spector, M.S., Desnoyers, S., Hoeppner, D.J., and Hengartner, M.O. (**1997**). Interaction between the C. elegans cell-death regulators CED-9 and CED-4. Nature *385*, 653–656.

Spilker, A.C., Rabilotta, A., Zbinden, C., Labbé, J.-C., and Gotta, M. (**2009**). MAP kinase signaling antagonizes PAR-1 function during polarization of the early Caenorhabditis elegans embryo. Genetics *183*, 965–977.

Steigemann, P., Wurzenberger, C., Schmitz, M.H.A., Held, M., Guizetti, J., Maar, S., and Gerlich, D.W. (**2009**). Aurora B-mediated abscission checkpoint protects against tetraploidization. Cell *136*, 473–484.

Thellmann, M., Hatzold, J., and Conradt, B. (**2003**). The Snail-like CES-1 protein of C. elegans can block the expression of the BH3-only cell-death activator gene egl-1 by antagonizing the function of bHLH proteins. Development *130*, 4057–4071.

Timmons, L., Court, D.L., and Fire, A. (**2001**). Ingestion of bacterially expressed dsRNAs can produce specific and potent genetic interference in Caenorhabditis elegans. Gene *263*, 103–112.

Verbrugge, I., Johnstone, R.W., and Smyth, M.J. (**2010**). SnapShot: Extrinsic apoptosis pathways. Cell *143*, 1192, 1192.e1–2.

Vogt, C.C. (**1842**). Untersuchungen über die Entwicklungsgeschichte der Geburtshelferkrœte (Alytes obstetricans). (Jent & Gassmann), pp. 82 – 86.

Wei, M.C., Zong, W.X., Cheng, E.H., Lindsten, T., Panoutsakopoulou, V., Ross, A.J., Roth, K.A., MacGregor, G.R., Thompson, C.B., and Korsmeyer, S.J. (**2001**). Proapoptotic BAX and BAK: a requisite gateway to mitochondrial dysfunction and death. Science *292*, 727–730.

Wicks, S.R., Yeh, R.T., Gish, W.R., Waterston, R.H., and Plasterk, R.H. (**2001**). Rapid gene mapping in Caenorhabditis elegans using a high density polymorphism map. Nat. Genet. *28*, 160–164.

Wong, H.C., Mao, J., Nguyen, J.T., Srinivas, S., Zhang, W., Liu, B., Li, L., Wu, D., and Zheng, J. (**2000**). Structural basis of the recognition of the dishevelled DEP domain in the Wnt signaling pathway. Nat. Struct. Biol. *7*, 1178–1184.

Wood, A.J., Lo, T.-W., Zeitler, B., Pickle, C.S., Ralston, E.J., Lee, A.H., Amora, R., Miller, J.C., Leung, E., Meng, X., et al. (**2011**). Targeted genome editing across species using ZFNs and TALENs. Science *333*, 307.

Wu, D., Wallen, H.D., and Nuñez, G. (**1997**). Interaction and regulation of subcellular localization of CED-4 by CED-9. Science *275*, 1126–1129.

Yan, N., Gu, L., Kokel, D., Chai, J., Li, W., Han, A., Chen, L., Xue, D., and Shi, Y. (**2004**). Structural, biochemical, and functional analyses of CED-9 recognition by the proapoptotic proteins EGL-1 and CED-4. Mol. Cell *15*, 999–1006.

Yuan, J., Shaham, S., Ledoux, S., Ellis, H.M., and Horvitz, H.R. (**1993**). The C. elegans cell death gene ced-3 encodes a protein similar to mammalian interleukin-1 beta-converting enzyme. Cell *75*, 641–652.

Yu, A., Xing, Y., Harrison, S.C., and Kirchhausen, T. (**2010**). Structural Analysis of the Interaction between Dishevelled2 and Clathrin AP-2 Adaptor, A Critical Step in Noncanonical Wnt Signaling. Structure *18*, 1311–1320.

Zarkower, D., and Hodgkin, J. (**1992**). Molecular analysis of the C. elegans sex-determining gene tra-1: a gene encoding two zinc finger proteins. Cell *70*, 237–249.

Zou, H., Henzel, W.J., Liu, X., Lutschg, A., and Wang, X. (**1997**). Apaf-1, a human protein homologous to C. elegans CED-4, participates in cytochrome c-dependent activation of caspase-3. Cell *90*, 405–413.

CHAPTER 2 APPENDIX

DATA RELEVANT TO THE CLONING OF THE *GM389* MUTATION INVOLVED IN ALM MECHANOSENSORY NEURON POLARITY

Contributions to this appendix:
Nathan Shih made the *gm389 zdIs5; cwn-1(ok546)* strain and first observed reversed polarity in ALM neurons. Maylee Wu generated the original SNP-mapping data for *gm389*.

SUMMARY

The mutant *gm389* was isolated in the same screen as *gm396*, and both were sequenced in parallel. This appendix is composed of all the information we have concerning *gm389* including mapping, sequencing and genetic interaction data. The *gm389* mutant exhibits Wnt phenotypes related to cell migration and neuronal polarity, raising the possibility of a role in Wnt signaling for the protein encoded at the locus carrying the mutation responsible for the phenotypes observed in *gm389* mutants.

INTRODUCTION

Wnts are secreted glycoproteins that signal through Frizzled (Fz) receptors to change gene transcription and direct various developmental processes (reviewed in Clevers and Nusse, 2012). In addition to their glycosylation, Wnts are also palmitoylated by the product of the segment polarity gene *porcupine* (Kadowaki et al., 1996; Tanaka et al., 2002; Willert et al., 2003; Takada et al., 2006). A recent crystal structure of the complex formed between Wnt8 from *Xenopus* and the cysteine-rich domain (CRD) of mouse Fz8 suggests that this lipid modification is important for binding between Wnt ligands and Fz receptors (Janda et al., 2012).

Fzs are seven-pass transmembrane cell-surface receptors that relay Wnt signals to cytoplasmic effectors (reviewed in Clevers and Nusse, 2012), but they can also act as receptors for another transmembrane protein, Van Gogh (Vang), in the planar cell polarity pathway (PCP; reviewed in Simons and Mlodzik, 2008). In canonical Wnt signaling, Fz interacts with the cytoplasmic signaling protein Dishevelled (Dsh) to modify the activity of a destruction complex that targets the transcriptional modifier and adhesion protein β-catenin. Dsh binds, via its PDZ domain, the c-terminal tail of Fz (Chen et al., 2003). Through their DIX domains, Dsh and Axin also interact (Schwarz-Romond et al., 2007; Fiedler et al., 2011). Axin is a component of the complex that normally phosphorylates β-catenin, leading to its ubiquitination and destruction at the proteosome (Aberle et al., 1997; Li et al., 2012).

Destruction of β-catenin occurs in the absence of a Wnt signal; however, upon the binding of Fz by Wnt ligand, the destruction complex is localized to the membrane and prohibited from targeting β-catenin for destruction (Li et al., 2012). The complex—which, in addition to Axin, includes Glycogen-synthase kinase 3 (Siegfried et al., 1992; Peifer et al., 1994), Casein kinase 1 (Bernatik et al., 2011) and Adenomatous polyposis coli, which binds β-catenin (Rubinfeld et al., 1993; Su et al., 1993)—localizes to phosphorylated LRP, which is a Wnt co-receptor (Pinson et al., 2000; Tamai et al., 2000; Wehrli et al., 2000; Mao et al., 2001). This is the case in *Drosophila* and vertebrates where homologs of LRP exist; however, in the nematode *C. elegans*, we know much less about the interaction between Fz and the destruction complex as there is no known LRP ortholog.

When β-catenin is no longer targeted for destruction, it accumulates in the cytoplasm and travels to the nucleus where it alters gene transcription through its interaction with the TCF/LEF transcription factor (Behrens et al., 1996; Molenaar et al., 1996). In the absence of β-catenin in the nucleus, TCF represses transcription of its targets by interacting with the transcriptional

repressor Groucho (Cavallo et al., 1998; Roose et al., 1998). However, when bound to β-catenin in the nucleus, TCF becomes a transcriptional activator (Lee et al., 2009; Hikasa et al., 2010).

Wnts can also cause changes in gene transcription, independent of β-catenin, through non-canonical pathways such as the Wnt-Calcium (Kohn and Moon, 2005) and Wnt-ROR pathways (Schambony and Wedlich, 2007). In addition to not requiring β-catenin, the Wnt-ROR pathway employs a non-Fz receptor, the ROR receptor tyrosine kinase, to alter transcription through the JNK signaling pathway and the transcription factor c-Jun (Schambony and Wedlich, 2007). In another non-canonical pathway, Wnt signals through the receptor tyrosine kinase Ryk to generate a chemorepulsive response in the migrating growth cones of neurons (Yoshikawa et al., 2003).

Components of the canonical pathway are also involved in Wnt-independent signaling. Fz and Dsh, in conjunction with the transmembrane protein Vang, are involved in signaling pathways that orient cells within a polarized epithelial sheet (Seifert and Mlodzik, 2007a; Wang and Nathans, 2007) and that guide the development of primary cilia (Park et al., 2006). Fz and Dsh also play a role in convergent extension movements during vertebrate development (reviewed in Seifert and Mlodzik, 2007b and Semenov et al., 2007).

In *C. elegans*, Wnt signaling has been shown to regulate various developmentally important processes including mitotic-spindle orientation (Goldstein, 1995), fate specification (Goldstein, 1992, 1993; Eisenmann et al., 1998), cell migration (Harris et al., 1996; Forrester et al., 1999, 2004; Maloof et al., 1999; Whangbo and Kenyon, 1999; Korswagen et al., 2002) and neuronal polarity (Hilliard and Bargmann, 2006; Pan et al., 2006; Prasad and Clark, 2006).

In the PLM mechanosensory neuron, the Wnt LIN-44 acts through the Fz LIN-17 to promote anterior polarization. In either *lin-44* or *lin-17* mutants, the polarity of the PLM is completely reversed. The Wnts CWN-1, CWN-2 and EGL-20 play a similar role in polarizing the ALM mechanosensory neuron toward the anterior of the worm (Hilliard and Bargmann, 2006; Pan et al., 2006; Prasad and Clark, 2006; Fleming et al., 2010), although, in the context of the ALM, we do not know which Fzs (if any at all) these Wnts are signaling through. In both the PLM and the ALM, it is also not known which molecules are acting downstream of Wnts to direct polarization.

The mutant *gm389* shares multiple phenotypes with Wnt signaling mutants and may be an interesting downstream effector of Wnt signaling. What follows are the data we have collected in order to identify, in *gm389,* the mutation that generates these phenotypes.

MATERIALS AND METHODS

Strains and Genetics
Worms were cultured as previously described (Brenner, 1974). All experiments were conducted using worms cultured at 20°C unless otherwise noted.

LG I: *gm389* (this study); *qDf6*, *qDf7*, *qDf8* and *qDf9* (Ellis and Kimble, 1995); *zdIs5[Pmec-4::GFP; lin-15(+)]* (Clark and Chiu, 2003), *hT2[bli-4(e937) let-?(q782) qIs48] (McKim and Rose, 1990)*

LG II: *cwn-1(ok546)* (Zinovyeva and Forrester, 2005)

LGIII: *hT2[bli-4(e937) let-?(q782) qIs48]* (McKim and Rose, 1990)

Zeiss imaging and scoring
Worms were anesthetized in 10 mM sodium azide. A Zeiss Axioskop 2 microscope was used to examine worms. Images were collected using an ORCA-ER CCD camera (Hammamatsu) and Open1ab imaging software (Improvision).

RESULTS AND DISCUSSION

The *gm389* mutant was isolated in the same extra-neuron screen as *gm396*. However, in addition to a low penetrance of extra neurons, *gm389* also had QL neuroblasts that migrated forward and HSNs that failed to migrate. These phenotypes are associated with mutations in Wnts and Fzs.

Nathan Shih, a rotation student in the lab, was interested in looking at an additional Wnt-related phenotype in the ALM mechanosensory neuron. The ALM normally has a long anterior process that extends into the head and branches into the nerve ring (Figure 1A); however, in certain Wnt and Fz double mutants, the polarity of ALM is reversed (Figure 1B). We have seen that mutations in *cwn-1* sensitize the ALM to the effects of other mutations such that double mutants with *cwn-1*, for example *cwn-1; egl-20*, have an ALM-reversal phenotype while neither single mutant alone has the phenotype. Nathan made a double mutant between *gm389* and *cwn-1* and noticed that the polarity of the ALM neuron is reversed or bipolar. I scored this phenotype and saw that the polarity of ALM is reversed approximately 9% of the time and ALMs are bipolar approximately 40% of the time.

I was interested in finding the mutation in the *gm389* mutant that is responsible for these phenotypes. I and a previous graduate student in the lab, Maylee, independently SNP mapped the mutation to regions of chromosome I containing 1313 and 185 genes, respectively. Maylee's region is nested within the larger region (Table 1). I also used deficiencies to map the mutation. The *gm389* mutant has a maternal-effect uncoordinated (Unc) phenotype. I crossed males that were heterozygous for a deficiency with *gm389* hermaphrodites and scored the Unc phenotype in male cross progeny. I observed Unc progeny in *qDf6 / gm389* and *qDf8 / gm389* worms. However, Unc males represented only a small percentage of the male progeny suggesting that

there was lethality in the worms heterozygous for the *gm389* and these deficiencies. Deficiencies *qDf7* and *qDf9* gave all nonUnc males when placed over *gm389*. This may be due to complementation or complete lethality of heterozygous males. If we assume that it is due to complementation, we would place the mutation somewhere right of the left break-point of *qDf8* and left of the left break-points of *qDf7* and *qDf9*. We do not know with much accuracy where these break-points are found. In fact, the left break-points of all three of these deficiencies fall somewhere between the genes *unc-29* and *mec-8*. This region contains 168 genes. There are two major concerns with taking these data too seriously. First, as mentioned above, the lack of an Unc phenotype may not be due to complementation between *gm389* and the deficiency but to lethality in embryos that would have been Unc had they survived. Second, deficiency break-points are not always clear. For example *qDf8* deletes *mec-8*, does not delete either *unc-29* or *unc-13* but does delete *cdc-25.1*. This leaves an island of sequence between *unc-29* and *unc-13*. Consequently, I cannot be sure that the non-complementation between *gm389* and *qDf6* or *qDf8* is due to lack of sequence within the assumed region of deficiency.

In addition to traditional mapping experiments, I used whole-genome sequencing (WGS) to find genes that were mutated in *gm389* mutants. A summary of mutations that change coding sequence and are found within the traditionally-mapped regions is found in Table 2. Prior to the completion of the WGS for *gm389*, I had performed RNAi in the *cwn-1(ok546)* background against many of the genes within the SNP-mapped regions. One of these genes, *madf-10*, was mutated in *gm389*. RNAi of *madf-10* did not cause an Unc phenotype or reversal of ALM polarity and is therefore unlikely to be the causative mutation. However, a mutation in *kin-3* was interesting for several reasons. First, *kin-3* resides within the small region to which Maylee first mapped *gm389*. Second, KIN-3 is the α subunit of Casein kinase II (CKII). The *gm389* mutant was originally isolated in a screen for extra neurons. A similar screen (using RNAi), performed by Aakanksha Singhvi, pulled out *kin-10*, the gene that codes for the β subunit of CKII. Third, the mutation in *gm389* at the *kin-3* locus changes glutamate 179 to a lysine (Table 2). This is a non-conservative change in a residue found within the activation loop required for activation of the protein kinase. Last, CKII has been shown to be upregulated by Wnt signaling (Gao and Wang, 2006) and has been shown to localize asymmetrically in neurons (Hu et al., 2006; Sanchez-Ponce et al., 2011).

I made a *kin-3(ok1516); cwn-1(ok546)* double mutant and scored for reversed ALM neurons and for the Unc phenotype (data not shown). I did not see a mutant phenotype in either case. The simplest explanation for this discrepancy is that the mutation in *kin-3* has nothing to do with the ALM-polarity or Unc phenotypes of *gm389* mutants. The fact that *kin-3(ok1516)* is a maternal-effect lethal mutant that must be balanced by *hT2* may also explain the lack of phenotype. We may not observe mutant phenotypes in this strain because maternal contribution rescues the defects in homozygous worms coming from balanced mothers. We can never observe homozygous worms without maternal contribution of KIN-3 because these worms are dead. It is also possible that the mutation in *gm389* at the *kin-3* locus is a gain-of-function mutation while *kin-3(ok1516)* is a loss-of-function allele.

I have still not mapped the causative mutation in *gm389*; it will be important to continue screening candidate genes by RNAi. The recent WGS data for this mutant will provide information useful for selecting candidates for this screen. The *kin-3* gene is an interesting

candidate; however, *kin-3* mutants do not have the ALM reversal phenotype. The mutation in *gm389* that is responsible for the reversal of ALMs in the *cwn-1* mutant background may prove to be an interesting component of the Wnt signaling pathway.

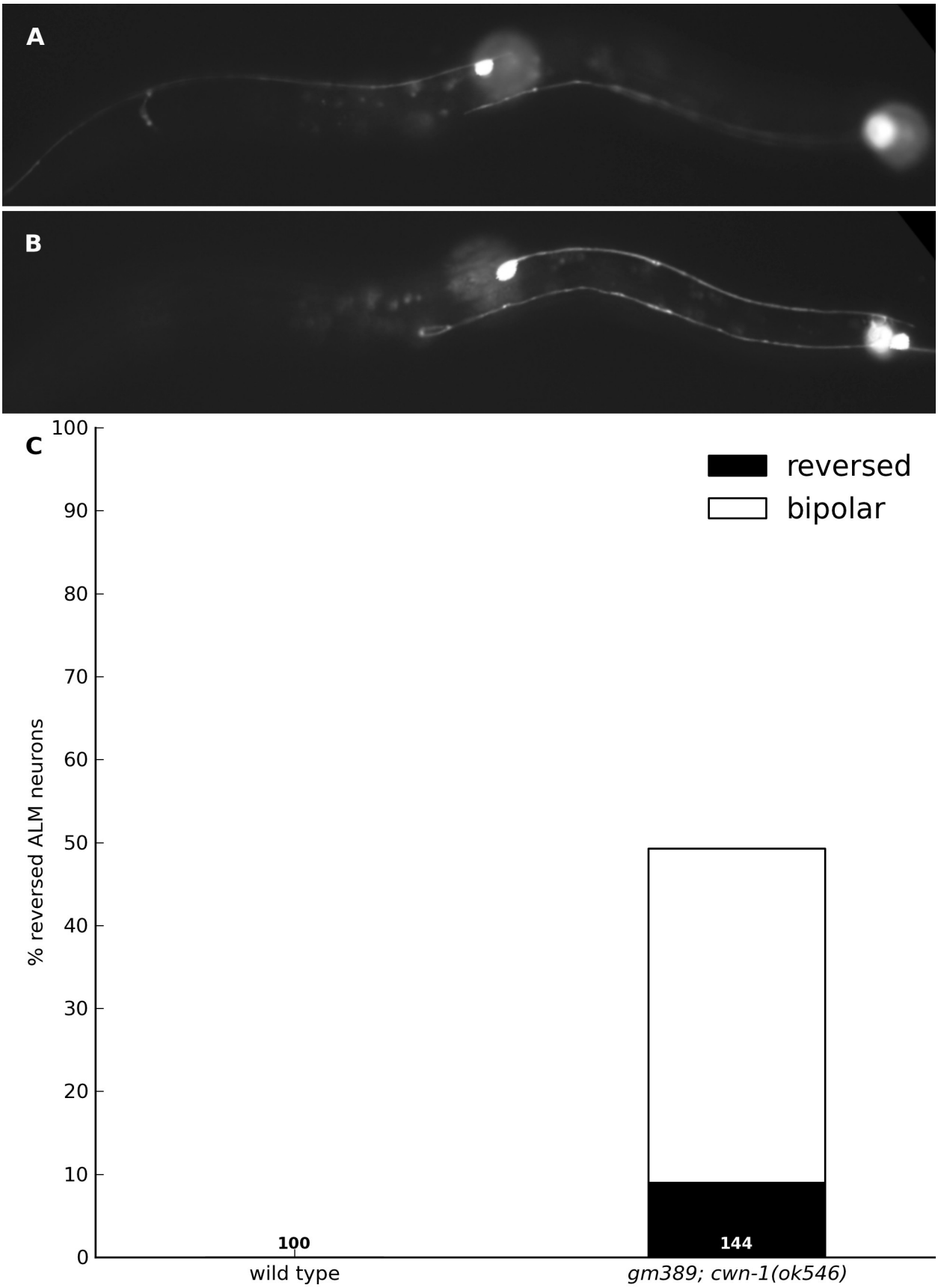
A
B
C
reversed
bipolar
% reversed ALM neurons
100
90
80
70
60
50
40
30
20
10
0
100
144
wild type
gm389; cwn-1(ok546)

Figure 1: The PLM polarity defect in *gm389; cwn-1(ok546)* mutants. (A, B) Anterior is to the left, posterior to the right. The ALM cell bodies are in the middle of the worm in each image. (A) The right ALM has a normal morphology. The long process extends anteriorly into the head of the worm. (B) The polarity of the left ALM is reversed. The long process extends posteriorly into the tail. (C) The percentage of ALMs with reversed (black) or bipolar (white) polarity is shown along the y-axis, genotypes along the x-axis. The number of ALMs scored is shown along the x-axis. An ALM was scored as bipolar if the posterior process was longer than 10 ALM cell diameters.

Table 1: SNP- and deficiency-mapping data for *gm389*

interval data		left[1]		right[2]	
		location[3]	sequence[4]	location	sequence
snp-mapping interval (Mark)		7581801	*mce-1*	11746916	*F35E2.5*
snp-mapping interval (Maylee)		10231172	*Y106G6E.7* (ncRNA)	10793081	*F55A3.7*
deficiency-mapping interval		8901428	*T08G11.8* (ncRNA)	9441007	*C17E4.14* (ncRNA)
		left		right	
deficiency	phen. over *gm389*	+	-	-	+
qDf6	Unc	*unc-13*	*unc-29*	*aph-2*	*srf-2*
qDf7	nonUnc	*unc-29*	*mec-8*	*stu-10*	*bah-1*
qDf8[5]	Unc	*unc-29*	*mec-8*	*fog-3*	*lin-11*
qDf9	nonUnc	*egl-32*	*mec-8*	*fog-3*	*lin-11*

[1] Left break-point
[2] Right break-point
[3] Physical map locations
[4] The closest sequence found just within each break-point
[5] In *qDf8*, *cdc-25.1* is not deleted but is found at position 6469387, far left of *unc-29*.
phen., phenotype; +, def. does not delete; -, def. deletes

Table 2: Mutations in *gm389* that fall within the largest snp-mapped region

		change		RNAi result[1]		
gene	location[2]	nucleotide	amino acid	Rev.	Bip.	Tot.
spr-4	8103975	CtoT	P111L	-	-	-
sod-2	8435506	GtoA	W184*	-	-	-
mef-2[3]	9098851	GtoA	A140T	-	-	-
F25H5.7[3]	9157229	GtoA	G448R	-	-	-
madf-10[4]	10437432	CtoT	A74T	0	1	41
kin-3[4]	10734972	GtoA	E179K	-	-	-

[1] The numbers of reversed (Rev.) and bipolar (Bip.) ALMs is shown; Tot., the total number of ALMs scored; -, not done

[2] Physical map locations

[3] Within the deficiency-mapped region

[4] Within Maylee's snp-mapped region

REFERENCES

Aberle, H., Bauer, A., Stappert, J., Kispert, A., and Kemler, R. (**1997**). β-catenin is a target for the ubiquitin–proteasome pathway. The EMBO Journal *16*, 3797–3804.

Behrens, J., von Kries, J.P., Kühl, M., Bruhn, L., Wedlich, D., Grosschedl, R., and Birchmeier, W. (**1996**). Functional interaction of beta-catenin with the transcription factor LEF-1. Nature *382*, 638–642.

Bernatik, O., Ganji, R.S., Dijksterhuis, J.P., Konik, P., Cervenka, I., Polonio, T., Krejci, P., Schulte, G., and Bryja, V. (**2011**). Sequential activation and inactivation of Dishevelled in the Wnt/beta-catenin pathway by casein kinases. J. Biol. Chem. *286*, 10396–10410.

Brenner, S. (**1974**). The genetics of Caenorhabditis elegans. Genetics *77*, 71–94.

Cavallo, R.A., Cox, R.T., Moline, M.M., Roose, J., Polevoy, G.A., Clevers, H., Peifer, M., and Bejsovec, A. (**1998**). Drosophila Tcf and Groucho interact to repress Wingless signalling activity. Nature *395*, 604–608.

Chen, W., Berge, D. ten, Brown, J., Ahn, S., Hu, L.A., Miller, W.E., Caron, M.G., Barak, L.S., Nusse, R., and Lefkowitz, R.J. (**2003**). Dishevelled 2 Recruits ß-Arrestin 2 to Mediate Wnt5A-Stimulated Endocytosis of Frizzled 4. Science *301*, 1391–1394.

Clark, S.G., and Chiu, C. (**2003**). C. elegans ZAG-1, a Zn-finger-homeodomain protein, regulates axonal development and neuronal differentiation. Development *130*, 3781–3794.

Clevers, H., and Nusse, R. (**2012**). Wnt/β-catenin signaling and disease. Cell *149*, 1192–1205.

Eisenmann, D.M., Maloof, J.N., Simske, J.S., Kenyon, C., and Kim, S.K. (**1998**). The beta-catenin homolog BAR-1 and LET-60 Ras coordinately regulate the Hox gene lin-39 during Caenorhabditis elegans vulval development. Development *125*, 3667–3680.

Ellis, R.E., and Kimble, J. (**1995**). The fog-3 gene and regulation of cell fate in the germ line of Caenorhabditis elegans. Genetics *139*, 561–577.

Fiedler, M., Mendoza-Topaz, C., Rutherford, T.J., Mieszczanek, J., and Bienz, M. (**2011**). Dishevelled interacts with the DIX domain polymerization interface of Axin to interfere with its function in down-regulating β-catenin. PNAS *108*, 1937–1942.

Fleming, T., Chien, S.-C., Vanderzalm, P.J., Dell, M., Gavin, M.K., Forrester, W.C., and Garriga, G. (**2010**). The role of C. elegans Ena/VASP homolog UNC-34 in neuronal polarity and motility. Dev. Biol. *344*, 94–106.

Forrester, W.C., Dell, M., Perens, E., and Garriga, G. (**1999**). A C. elegans Ror receptor tyrosine kinase regulates cell motility and asymmetric cell division. Nature *400*, 881–885.

Forrester, W.C., Kim, C., and Garriga, G. (**2004**). The Caenorhabditis elegans Ror RTK CAM-1 Inhibits EGL-20/Wnt Signaling in Cell Migration. Genetics *168*, 1951–1962.

Gao, Y., and Wang, H. (**2006**). Casein Kinase 2 Is Activated and Essential for Wnt/β-Catenin Signaling. J. Biol. Chem. *281*, 18394–18400.

Goldstein, B. (**1992**). Induction of gut in Caenorhabditis elegans embryos. Nature *357*, 255–257.

Goldstein, B. (**1993**). Establishment of gut fate in the E lineage of C. elegans: the roles of lineage-dependent mechanisms and cell interactions. Development *118*, 1267–1277.

Goldstein, B. (**1995**). Cell contacts orient some cell division axes in the Caenorhabditis elegans embryo. J Cell Biol *129*, 1071–1080.

Harris, J., Honigberg, L., Robinson, N., and Kenyon, C. (**1996**). Neuronal cell migration in C. elegans: regulation of Hox gene expression and cell position. Development *122*, 3117–3131.

Hikasa, H., Ezan, J., Itoh, K., Li, X., Klymkowsky, M.W., and Sokol, S.Y. (**2010**). Regulation of TCF3 by Wnt-dependent phosphorylation during vertebrate axis specification. Dev. Cell *19*, 521–532.

Hilliard, M.A., and Bargmann, C.I. (**2006**). Wnt Signals and Frizzled Activity Orient Anterior-Posterior Axon Outgrowth in C. elegans. Developmental Cell *10*, 379–390.

Hu, J., Bae, Y.-K., Knobel, K.M., and Barr, M.M. (**2006**). Casein kinase II and calcineurin modulate TRPP function and ciliary localization. Mol. Biol. Cell *17*, 2200–2211.

Janda, C.Y., Waghray, D., Levin, A.M., Thomas, C., and Garcia, K.C. (**2012**). Structural basis of Wnt recognition by Frizzled. Science *337*, 59–64.

Kadowaki, T., Wilder, E., Klingensmith, J., Zachary, K., and Perrimon, N. (**1996**). The segment polarity gene porcupine encodes a putative multitransmembrane protein involved in Wingless processing. Genes Dev. *10*, 3116–3128.

Kohn, A.D., and Moon, R.T. (**2005**). Wnt and calcium signaling: beta-catenin-independent pathways. Cell Calcium *38*, 439–446.

Korswagen, H.C., Coudreuse, D.Y.M., Betist, M.C., Water, S. van de, Zivkovic, D., and Clevers, H.C. (**2002**). The Axin-like protein PRY-1 is a negative regulator of a canonical Wnt pathway in C. elegans. Genes Dev. *16*, 1291–1302.

Lee, W., Swarup, S., Chen, J., Ishitani, T., and Verheyen, E.M. (**2009**). Homeodomain-interacting protein kinases (Hipks) promote Wnt/Wg signaling through stabilization of β-catenin/Arm and stimulation of target gene expression. Development *136*, 241–251.

Li, V.S.W., Ng, S.S., Boersema, P.J., Low, T.Y., Karthaus, W.R., Gerlach, J.P., Mohammed, S., Heck, A.J.R., Maurice, M.M., Mahmoudi, T., et al. (**2012**). Wnt signaling through inhibition of β-catenin degradation in an intact Axin1 complex. Cell *149*, 1245–1256.

Maloof, J.N., Whangbo, J., Harris, J.M., Jongeward, G.D., and Kenyon, C. (**1999**). A Wnt signaling pathway controls hox gene expression and neuroblast migration in C. elegans. Development *126*, 37–49.

Mao, J., Wang, J., Liu, B., Pan, W., Farr, G.H., 3rd, Flynn, C., Yuan, H., Takada, S., Kimelman, D., Li, L., et al. (**2001**). Low-density lipoprotein receptor-related protein-5 binds to Axin and regulates the canonical Wnt signaling pathway. Mol. Cell *7*, 801–809.

McKim, K.S., and Rose, A.M. (**1990**). Chromosome I Duplications in Caenorhabditis Elegans. Genetics *124*, 115–132.

Molenaar, M., van de Wetering, M., Oosterwegel, M., Peterson-Maduro, J., Godsave, S., Korinek, V., Roose, J., Destrée, O., and Clevers, H. (**1996**). XTcf-3 transcription factor mediates beta-catenin-induced axis formation in Xenopus embryos. Cell *86*, 391–399.

Pan, C.-L., Howell, J.E., Clark, S.G., Hilliard, M., Cordes, S., Bargmann, C.I., and Garriga, G. (**2006**). Multiple Wnts and Frizzled Receptors Regulate Anteriorly Directed Cell and Growth Cone Migrations in Caenorhabditis elegans. Developmental Cell *10*, 367–377.

Park, T.J., Haigo, S.L., and Wallingford, J.B. (**2006**). Ciliogenesis defects in embryos lacking inturned or fuzzy function are associated with failure of planar cell polarity and Hedgehog signaling. Nat. Genet. *38*, 303–311.

Peifer, M., Sweeton, D., Casey, M., and Wieschaus, E. (**1994**). wingless signal and Zeste-white 3 kinase trigger opposing changes in the intracellular distribution of Armadillo. Development *120*, 369–380.

Pinson, K.I., Brennan, J., Monkley, S., Avery, B.J., and Skarnes, W.C. (**2000**). An LDL-receptor-related protein mediates Wnt signalling in mice. Nature *407*, 535–538.

Prasad, B.C., and Clark, S.G. (**2006**). Wnt signaling establishes anteroposterior neuronal polarity and requires retromer in C. elegans. Development *133*, 1757–1766.

Roose, J., Molenaar, M., Peterson, J., Hurenkamp, J., Brantjes, H., Moerer, P., van de Wetering, M., Destrée, O., and Clevers, H. (**1998**). The Xenopus Wnt effector XTcf-3 interacts with Groucho-related transcriptional repressors. Nature *395*, 608–612.

Rubinfeld, B., Souza, B., Albert, I., Müller, O., Chamberlain, S.H., Masiarz, F.R., Munemitsu, S., and Polakis, P. (**1993**). Association of the APC gene product with beta-catenin. Science *262*, 1731–1734.

Sanchez-Ponce, D., Muñoz, A., and Garrido, J.J. (**2011**). Casein kinase 2 and microtubules control axon initial segment formation. Molecular and Cellular Neuroscience *46*, 222–234.

Schambony, A., and Wedlich, D. (**2007**). Wnt-5A/Ror2 regulate expression of XPAPC through an alternative noncanonical signaling pathway. Dev. Cell *12*, 779–792.

Schwarz-Romond, T., Fiedler, M., Shibata, N., Butler, P.J.G., Kikuchi, A., Higuchi, Y., and Bienz, M. (**2007**). The DIX domain of Dishevelled confers Wnt signaling by dynamic polymerization. Nature Structural & Molecular Biology *14*, 484–492.

Seifert, J.R.K., and Mlodzik, M. (**2007a**). Frizzled/PCP signalling: a conserved mechanism regulating cell polarity and directed motility. Nat. Rev. Genet. *8*, 126–138.

Seifert, J.R.K., and Mlodzik, M. (**2007b**). Frizzled/PCP signalling: a conserved mechanism regulating cell polarity and directed motility. Nat. Rev. Genet. *8*, 126–138.

Semenov, M.V., Habas, R., Macdonald, B.T., and He, X. (**2007**). SnapShot: Noncanonical Wnt Signaling Pathways. Cell *131*, 1378.

Siegfried, E., Chou, T.B., and Perrimon, N. (**1992**). wingless signaling acts through zeste-white 3, the Drosophila homolog of glycogen synthase kinase-3, to regulate engrailed and establish cell fate. Cell *71*, 1167–1179.

Simons, M., and Mlodzik, M. (**2008**). Planar cell polarity signaling: from fly development to human disease. Annu. Rev. Genet. *42*, 517–540.

Su, L.K., Vogelstein, B., and Kinzler, K.W. (**1993**). Association of the APC tumor suppressor protein with catenins. Science *262*, 1734–1737.

Takada, R., Satomi, Y., Kurata, T., Ueno, N., Norioka, S., Kondoh, H., Takao, T., and Takada, S. (**2006**). Monounsaturated fatty acid modification of Wnt protein: its role in Wnt secretion. Dev. Cell *11*, 791–801.

Tamai, K., Semenov, M., Kato, Y., Spokony, R., Liu, C., Katsuyama, Y., Hess, F., Saint-Jeannet, J.P., and He, X. (**2000**). LDL-receptor-related proteins in Wnt signal transduction. Nature *407*, 530–535.

Tanaka, K., Kitagawa, Y., and Kadowaki, T. (**2002**). Drosophila Segment Polarity Gene Product Porcupine Stimulates the Posttranslational N-Glycosylation of Wingless in the Endoplasmic Reticulum. J. Biol. Chem. *277*, 12816–12823.

Wang, Y., and Nathans, J. (**2007**). Tissue/planar cell polarity in vertebrates: new insights and new questions. Development *134*, 647–658.

Wehrli, M., Dougan, S.T., Caldwell, K., O'Keefe, L., Schwartz, S., Vaizel-Ohayon, D., Schejter, E., Tomlinson, A., and DiNardo, S. (**2000**). arrow encodes an LDL-receptor-related protein essential for Wingless signalling. Nature *407*, 527–530.

Whangbo, J., and Kenyon, C. (**1999**). A Wnt Signaling System that Specifies Two Patterns of Cell Migration in C. elegans. Molecular Cell *4*, 851–858.

Willert, K., Brown, J.D., Danenberg, E., Duncan, A.W., Weissman, I.L., Reya, T., Yates, J.R., and Nusse, R. (**2003**). Wnt proteins are lipid-modified and can act as stem cell growth factors. Nature *423*, 448–452.

Yoshikawa, S., McKinnon, R.D., Kokel, M., and Thomas, J.B. (**2003**). Wnt-mediated axon guidance via the Drosophila Derailed receptor. Nature *422*, 583–588.

Zinovyeva, A.Y., and Forrester, W.C. (**2005**). The C. elegans Frizzled CFZ-2 is required for cell migration and interacts with multiple Wnt signaling pathways. Developmental Biology *285*, 447–461.

CHAPTER 3

THE ANTAGONISTIC FUNCTIONS OF FRIZZLEDS LIN-17 AND MIG-1 IN REGULATING PLM MECHANOSENSORY NEURON POLARITY

Contributions to this chapter:
Chun-Liang Pan generated the *gmEx414[Pmec-7::mig-1::gfp]* transgene and first characterized the effects of MIG-1 over expression on PLM polarity.

SUMMARY

The function of a neuron is facilitated by its distinct morphology. Electrical signals are propagated along neuronal processes that extend from the cell body to form connections with muscle cells, sensory structures or other neurons. *In vitro* studies of developing neurons have shown that a neuronal process forms at random from one of many smaller processes protruding from the developing cell. Many intracellular molecules necessary for this process have been identified. However, many neurons display invariant polarity in vivo, suggesting specific regulation of the polarization process by external signals. Wnts and Frizzled receptors have been shown to direct polarization of mechanosensory neurons along the *C. elegans* anterior/posterior (AP) axis. This chapter describes our attempts to address how Wnts and Frizzleds interact to direct the AP polarization of the PLM mechanosensory neurons.

INTRODUCTION

The polarized morphology of a neuron defines how it receives and sends information. The typical neuron has a single long process called an axon, along which electrical signals are propagated to other cells. Dendrites, shorter processes that receive signals from other neurons, are usually more numerous. Initial studies of how neuronal polarity is established were conducted in *ex vivo* cell cultures. Dotti *et al*. (1988) used the embryonic rat hippocampal neuron in cell culture to observe the development of early cells into polarized neurons.

These investigators divided this developmental process into five stages: 1) lamellipodia originate from the membrane of the cell, then 2) regions of the lamellipodia condense to form small filopodial spines—Banker termed these 'minor processes.' The minor processes cyclically extend and retract, but all maintain the same approximate length until 3) one minor process begins to grow much more rapidly than the others. This rapidly growing process will become the axon and the remaining processes the dendrites. After the initial polarity is established 4) dendrites grow at a steady rate, yet still slower than the axon. Finally, 5) the neuron is completely polarized and dendrites and axon are distinguishable by use of axon- and dendrite-specific markers (Dotti et al., 1988).

In this system, polarity is established randomly from one of the many minor processes in the absence of any external cues. Further studies showed that axon specification is dependent on the relative lengths of minor processes. In hippocampal cell culture, Goslin and Banker (1989) amputated newly formed axons at various distances from the cell body. They observed that if the remaining axonal stump was longer than the longest minor process by ≥10μm, the stump would retain axonal specification and continue to grow at the same pre-amputation rate. However, when the new axon was severed forming a stump that was shorter than the longest minor process by 10μm or more, axonal specification was delayed and any one of the minor processes (including the axonal stump) could emerge as the new axon (Goslin and Banker, 1989).

From these and other studies emerged a model in which minor processes experience cycling positive and negative elongation signals. When positive feedback is established in one of these processes, continuous elongation will occur, and the process is specified as the axon (reviewed in Arimura and Kaibuchi, 2007).

Many of the intracellular components involved in this signaling are now known but their exact functional relationships are not completely clear. PI3K has been shown to be important in axonal specification and is important for asymmetric localization of the PAR-3/PAR-6/aPKC complex (Shi et al., 2003). This asymmetry is probably achieved indirectly by generating PIP3 in the tips of axons to recruit PH domain containing proteins. The activity of a Ras superfamily GTPase, RAP1B has been shown to be important for axon formation (Schwamborn and Püschel, 2004), and excess RAP1B can rescue deficient axon formation caused by loss of PI3K. Cdc42 has been shown to act downstream of RAP1B and to interact directly with the PAR complex (Schwamborn and Püschel, 2004). Through this complex and Rac GEFs STEF and Tiam1, Cdc42 indirectly activates Rac1 (Nishimura et al., 2005). Effectors of Rac1 and Cdc42 are known to regulate actin and microtubule dynamics (Daniels et al., 1998; Nikolic et al., 1998; Chen et al., 1999; Banzai et al., 2000; Wang et al., 2007), suggesting a possible role for these Rho GTPases in neural process elongation. In addition, aPKC is known to regulate microtubule production through inhibition of MARK2 (Chen et al., 2006). Finally, Rac1 can activate PI3K (Chan et al., 2002), closing a possible positive-feedback loop that would support the model described above (reviewed in Arimura and Kaibuchi, 2007). This loop could be regulated at multiple steps such as PIP3 regulation by phosphatases like PTEN or by direct inactivation of Cdc42 and Rac1 by Rho GAPs, etc. (Arimura and Kaibuchi, 2007).

It is obvious from experiments in cell culture that neurons have intrinsic polarity machinery capable of specifying a single axon and many dendrites; however, the determination of neuronal polarity *in vivo* is directed by external signals. For example, Semaphorin 3A is an extracellular signal that usually repulses axons; however, it has been shown that in early rat cortical neurons, Semaphorin 3A acts as a dendritic chemoattractant. Polleux *et al.* cultured cortical neurons on top of postnatal cortical slices and showed that these neurons form dendrites that polarize toward the pial (distal) side of the slice. When cultured on slices harvested from *sema3a* null mice, cortical neurons formed randomly oriented dendrites. Though the semaphorin signal was not important for dendritic growth, this experiment showed that Semaphorin 3A can polarize cortical neurons (Polleux et al., 2000).

Netrins are highly conserved siganling molecules involved in axon guidance. Studies in *C. elegans* have shown that *unc-6* (Netrin) and one of its receptors, *unc-40* (DCC) are necessary for ventral polarization of the hermaphrodite specific neuron (HSN). In *unc-6* and *unc-40* single mutants, HSNs do not polarize ventrally, rather they form many small processes reminiscent of the minor processes seen in rat hippocampal neuron cell culture. It was also shown that, in *unc-6* mutants, transient ectopic over expression of UNC-6 protein caused random polarization of the

HSN. This finding suggested that, apart from acting as an instructional cue for polarization, UNC-6 can act to enhance random intrinsic asymmetric polarization. Furthermore, MIG-10—a PH domain-containing protein—localizes to the ventral side of HSN in an UNC-6 dependent manner. MIG-10 localization is disrupted in *age-1* (PI3K) and *daf-18* (PTEN), suggesting a link between an external *unc-6* signal and putative intracellular polarization machinery (Adler et al., 2006).

Wnts have also been shown to regulate neuronal polarity along the AP axis of *C. elegans*. The worm genome contains five known Wnt proteins (EGL-20, LIN-44, CWN-1, CWN-2, MOM-2). Although single Wnt mutants do not display defects in the polarity of the ALM mechanosensory neuron, double or triple mutant combinations of *cwn-1, cwn-2* and *egl-20* have been shown to reverse the polarity of a mechanosensory neuron ALM (Hilliard and Bargmann, 2006; Pan et al., 2006; Prasad and Clark, 2006; Fleming et al., 2010). Loss of LIN-44 has also been shown to affect the polarity of another mechanosensory neuron: PLM (Hilliard and Bargmann, 2006; Prasad and Clark, 2006). It is known that LIN-44 acts through the Frizzled receptor LIN-17; however, the role of Frizzleds in neuronal polarity is also unclear, and likely to be complex. There are four known Frizzled receptors in the worm genome (LIN-17, CFZ-2, MIG-1, MOM-5) that bind Wnt ligand. We know that LIN-44 acts through LIN-17 to regulate PLM polarity; however, outside of this context we do not know much about how Wnts and Frizzleds control polarity. And whether or not Wnts and Fzs act through known intracellular polarity components, is not yet completely understood.

MATERIALS AND METHODS

Strains and Genetics
Worms were cultured as previously described (Brenner, 1974). All experiments were conducted using worms cultured at 20°C unless otherwise noted.

LG I: *zdIs5[Pmec-4::GFP; lin-15(+)]* (Clark and Chiu, 2003), *mig-1(e1787)* (Desai et al., 1988), *lin-17(n671)* (Ferguson and Horvitz, 1985), *mom-5(ne12)* (Rocheleau et al., 1997), *hT2[bli-4(e937) let-?(q782) qIs48] (McKim and Rose, 1990)*

LG II: *cwn-1(ok546)* (Zinovyeva and Forrester, 2005), *dsh-1(ok1445)* (*C. elegans* Gene Knockout Project at OMRF), *mig-5(rh147)* (Walston et al., 2006), *cam-1(gm122)* (Forrester et al., 1999)

LGIII: *hT2[bli-4(e937) let-?(q782) qIs48]* (McKim and Rose, 1990)

LGIV: *egl-20(n585)* (Maloof et al., 1999), *cwn-2(ok895)* (Zinovyeva and Forrester, 2005)

LGV: *cfz-2(ok1201)* (Zinovyeva and Forrester, 2005), *mom-2(or309)*

LGX: *lin-18(e620)* (Inoue et al., 2004)*, bar-1(ga80)* (Eisenmann et al., 1998)

Extra-chromosomal arrays: *gmEx414[Pmec-7::mig-1::gfp]* (Pan et al., 2006), *gmEx581[Pmec07::mig-1δc::gfp]* (this study), *gmEx606[Pmec-7::mig-1W382L::gfp]* (this study)

Molecular biology and transgene construction
The *gmEx581* transgenic construct was generated using the *Pmec-7::mig-1::gfp* construct described previously (Pan et al., 2006). The forward primer TGGCCAATGGGACCATTTCGTGGTTACC and the reverse primer ACCGGTCCGAACTGATCTTTAAACGAAATGCTCAC were used to amplify a portion of the *mig-1* cDNA extending from the start codon to just beyond the end of the region that codes for the second transmembrane region. The truncated cDNA was subcloned into the pCR2.1 TOPO vector. The primers incorporated MscI and AgeI sites at the five-prime and three-prime ends of the cDNA, respectively. This truncated cDNA was then ligated back into the backbone of the original *Pmec-7::mig-1::gfp* construct.

The *gmEx606* transgenic construct was also generated using the previously described *Pmec-7::mig-1::gfp* construct. The forward primer CCCGGGCACCGACTTGA and the reverse primer GTTTAAACTTACCCATGGAACAGGT were used to make a fragment of the *mig-1* cDNA with a five-prime XmaI site and a three-prime NcoI site. The forward primer contains a mismatch in the third nucleotide back from the three-prime end that changes the tryptophan codon (TGG) in the *mig-1* cDNA to a leucine codon (TTG). This fragment was subcloned into the TOPO vector pCR2.1. The fragment was then ligated into the original *Pmec-7::mig-1::gfp* plasmid using the restriction enzymes XmaI and NcoI.

Transgenes were generated by injecting construct and co-injection marker DNA into the gonad of young adult worms (Mello et al., 1991).

Zeiss imaging and scoring
Worms were anesthetized in 10 mM sodium azide. A Zeiss Axioskop 2 microscope was used to examine worms. Images were collected using an ORCA-ER CCD camera (Hammamatsu) and Open1ab imaging software (Improvision).

RESULTS

Frizzleds LIN-17 and MIG-1 have antagonistic functions in regulating PLM polarity
Wild type PLMs have a short process that extends into the tail of the animal and a long process that extends anteriorly (Figure 1A). In worms mutant for *lin-44* or the Frizzled (Fz) receptor gene *lin-17*, PLM polarity is reversed (Figure 1B): defective neurons have a short anterior process and a long posterior process that extends to the tip of the tail and then turns around and extends anteriorly (Hilliard and Bargmann, 2006; Prasad and Clark, 2006; Table 1; Figure 1C). Previous work in the lab suggested that a mutant in *mig-1*, which encodes another Fz, suppressed the PLM polarity-reversal phenotype of *lin-17* mutants. This interaction suggested antagonistic roles for these receptors in regulating PLM polarity. Consistent with these results, Chun-Liang Pan showed that over expression of MIG-1 (*gmEx414*) in PLM led to a polarity reversal around

50% of the time (Chun-Liang Pan, unpublished data; Table 1; Figure 1C). When MIG-1 was overexpressed in *lin-17* mutants the phenotype was indistinguishable from *lin-17* mutants alone.

Two models to explain the antagonism between MIG-1 and LIN-17

There are two possible explanations for how excess MIG-1 causes a reversal of PLM polarity. In one model, excess MIG-1 protein sequesters ligand, thereby reducing signaling through LIN-17. Because previous data suggested that loss of MIG-1 in a *lin-17* mutant suppresses the polarity defect, other Wnts and Frizzled receptors would be necessary to promote polarity in this model. In wild type, Wnt would signal through LIN-17 to promote anterior polarization of PLM (Figure 2A). In the absence of LIN-17, MIG-1 would sequester Wnt from interacting with another Wnt-binding receptor (Figure 2B). In the absence of both MIG-1 and LIN-17, Wnt is free to signal through a third receptor (Figure 2C).

In a second model, excess MIG-1 receptor on the membrane of PLM binds more of its Wnt ligand than normal, resulting in increased signaling that antagonizes LIN-17 function. In wild type, signaling through LIN-17 would promote anterior polarization, while MIG-1 would promote posterior polarization. When present, LIN-17 signaling wins out over MIG-1; however, when LIN-17 is absent MIG-1 signaling reverses the polarity. If both receptors are absent, the polarity of PLM is still reversed though less frequently.

MIG-1 does not seem to be antagonizing LIN-17 function by sequestering Wnt

I reasoned that if the first model were correct I might find additional receptors by screening triple mutants with *mig-1* and *lin-17* and looking for combinations that enhanced the frequency of PLM reversals back to the level observed in *lin-17* single mutants. I looked at triple mutants between *mig-1*, *lin-17* and receptors known to bind Wnt: Fzs *cfz-2* and *mom-5*; the Ryk receptor *lin-18*; and the worm ROR-1/2 ortholog *cam-1*. Contrary to previous data for *mig-1 lin-17* double mutants, I saw that *mig-1(e1787) lin-17(n671)* (Figure 3; Table 1) had the same penetrance of reversed PLMs as *lin-17(n671)* single mutants (Figure 1C; Table 1); in other words *mig*-1 did not suppress *lin-17*. In light of this result it is not surprising that I saw no change in the phenotype in any of the triple mutants observed (Figure 3; Table 1). None of the other Wnt-binding receptors seem to have a role in regulating PLM polarity.

Although I did not observe a genetic interaction between *mig-1* and *lin-17*, I still had not determined the mechanism by which MIG-1 was reversing the polarity of PLM when over expressed. If the first model were correct—if over expression of MIG-1 sequestered Wnt away from LIN-17 reducing its ability to signal for anterior polarization of PLM—we would expect the cysteine rich domain (CRD) of MIG-1 to be sufficient to produce the over expression phenotype. The CRD is a domain of 10 conserved cysteines that binds Wnts (Saldanha et al., 1998; Dann et al., 2001). Using the promoter of *mec-7* I expressed MIG-1ΔC::GFP in PLMs (*gmEx581*). This truncation contains the CRD and the first two transmembrane regions of the protein followed by a C-terminal GFP tag. 1.4% of the PLMs scored were reversed in *gmEx581* worms (Figure 4A; Table 1). This is significantly lower than the 50.0% penetrance I see with over expression of the full length protein (Figure 4A; Table 1). Despite the low penetrance phenotype, MIG-1ΔC::GFP localized near the plasma membrane of PLMs suggesting that the protein was expressed at high levels and localized properly (Figure 4B).

EGL-20 is the ligand for MIG-1

These results were inconsistent with the sequestration model of MIG-1 function in regulating PLM polarity. I wanted to directly test the other model in which signaling downstream of MIG-1 was important for antagonism of LIN-17 signaling. I made double mutants between *lin-17* and downstream components of Wnt canonical and non-canonical signaling pathways. If any of these components were functioning downstream of MIG-1 to antagonize LIN-17 signaling we might expect mutations in these components to suppress the PLM polarity defect of *lin-17* mutants. I tested Dishevelleds (Dsh) *dsh-1* and *mig-5* as well as the β-catenin *bar-1*. I did not observe suppression in any of these double mutants (Figure 5; Table 1). This finding was not surprising, as I had already seen that loss of *mig-1* did not suppress *lin-17* (Figure 3; Table 1). I also tested whether these downstream effectors of Wnt signaling could suppress the MIG-1 over expression phenotype. None of the *C. elegans* Dshs suppressed *gmEx414* (Figure 5; Table 1).

I continued to test the signaling model by screening Wnt mutants in the background of MIG-1 over expression. I reasoned that, if MIG-1 were signaling to antagonize LIN-17, removing its ligand would relieve the antagonism. I screened through all of the Wnts except *lin-44*, which is already known to act through *lin-17* in this process (Hilliard and Bargmann, 2006; Prasad and Clark, 2006). I found that the *egl-20(n585)* mutant completely suppressed PLM reversals caused by over expression of MIG-1, suggesting that EGL-20 is the MIG-1 ligand regulating PLM polarity (Figure 6; Table 1). I also tested whether loss of *egl-20* can suppress PLM reversals caused by loss of *lin-17* and saw that it did not (Figure 6; Table 1).

An alignment between MIG-1 and Smoothened suggested that an important tryptophan residue (W539 in mouse Smoothened; Figure 6), which when changed to a leucine makes Smoothened constitutively active, was conserved. I changed the corresponding residue in MIG-1 (W382) to a leucine to see if I could create a constitutively active version of the receptor (*gmEx606*). To the contrary, MIG-1W382L appears to have reduced activity compared to the full-length protein (Figure 6; Table 1). Furthermore, this activity is completely abrogated in an *egl-20* mutant (Figure 6; Table 1).

DISCUSSION

Previous results generated in the lab suggested that loss-of-function mutations in *mig-1* suppressed the PLM reversal phenotype of *lin-17* mutants. Here I have shown conflicting results suggesting that no such genetic interaction exists. The difference between previous and present data for *mig-1 lin-17* double mutants is likely due to a differences in genetic background between the strains scored. It is difficult to say what the nature of this genetic difference at this time, but despite these contradictory results, it is still clear that MIG-1 and LIN-17 function antagonistically, with respect to PLM polarity: excess MIG-1 and loss of LIN-17 each result in reversed PLM polarity (Figure 1C). Unfortunately, the genetic interaction between the two genes was the only evidence that suggested a genuine role for MIG-1 in PLM. It is still possible that the function of MIG-1 in PLM is biologically relevant, but for now it seems that the effects of ectopic expression of MIG-1 on PLM polarity are the result of an artificial signaling pathway.

Strains that are mutant for *lin-17* and ectopically express MIG-1 have reversed PLMs at the same frequency as *lin-17* mutants alone (Figure 1C). This observation suggests that MIG-1 activity directly antagonizes the function of LIN-17 rather than promoting posterior polarization in parallel to LIN-17. Prior to this work, it was still unclear whether ectopically expressed MIG-1 sequesters Wnt away from LIN-17 or signals to antagonize LIN-17 signaling. Failure of MIG-1ΔC to reverse PLM polarity argues against the sequestering model. However, I only know that MIG-1ΔC localizes near the plasma membrane of PLMs. It is possible that the CRD of MIG-1ΔC does not make it to the extra-cellular surface, that the topology of the truncated protein with respect to the membrane is reversed, or that the CRD of MIG-1ΔC is not functional.

Fortunately, I have positive evidence supporting the idea that MIG-1 signaling is important for antagonism of LIN-17. I have shown that EGL-20 is the ligand that activates MIG-1 in PLMs (Figure 6). In light of this evidence, the Wnt-sequestering model seems unlikely, however, it is possible that activated MIG-1 sequesters intracellular signaling components, such as Dshs, away from LIN-17. Though I have not seen PLM reversals in any of the single Dsh mutants, they may play redundant roles downstream of LIN-17. Ectopically expressed MIG-1 that is activated by EGL-20 may sequester multiple relevant Dshs away from LIN-17.

In an attempt to generate a constitutively active version of MIG-1 I have also shown that the tryptophan 382 residue is not likely to be analagous to tryptophan 539 in mouse Smoothened. Furthermore, changing tryptophan 382 in MIG-1 to a leucine may reduce its function—though the difference in the abilities of MIG-1 and MIG-1W382L to reverse PLM polarity could simply be due to differences in expression between the transgene arrays.

In summary, it has yet to be shown that MIG-1 normally regulates PLM polarity, but I have described a requirement of the Wnt ligand EGL-20 in order for MIG-1 to polarize PLMs posteriorly. Unfortunately, this is likely to be an artificial function of MIG-1; however, biologically relevant antagonism between MIG-1 and LIN-17 is not unprecedented. For example LIN-17 and MIG-1 play antagonistic roles in regulating the migration of the HSN (Pan et al., 2006). Though not likely to be biologically relevant in PLM, the antagonism between MIG-1 and LIN-17 in the PLM may still inform relevant interactions occurring in other contexts.

Table 1: PLM polarity-reversal defects (all scored in *zdIs5*)

genotype	PLM reversed (%)	PLM N
wild type	0.0	100
lin-17(n671)	66.3	267
lin-17(n671); dsh-1(ok1445)	70.2	188
lin-17(n671); mig-5(rh147)	64.8	230
lin-17(n671); bar-1(ga80)	63.4	295
lin-17(n671); egl-20(n585)	62.0	79
mig-1(e1787) lin-17(n671)	66.3	160
mig-1(e1787) lin-17(n671); cfz-2(ok1201)	63.7	146
mig-1(e1787) lin-17(n671) mom-5(ne12) (M+)[1]	62.8	43
mig-1(e1787) lin-17(n671); lin-18(e620)	66.8	283
mig-1(e1787) lin-17(n671); cam-1(gm122)	64.4	216
gmEx414[Pmec-7::mig-1::gfp]	50.0	58
lin-17(n671); gmEx414	66.4	280
dsh-1(ok1445); gmEx414	53.4	73
dsh-2(ez25); gmEx414	44.7	38
mig-5(rh147); gmEx414	52.6	38
cwn-1(ok546); gmEx414	52.6	78
cwn-2(ok895); gmEx414	50.7	67
mom-2(or309); gmEx414	61.5	26
egl-20(n585); gmEx414	1.3	76
egl-20(+)[2]*; gmEx414*	50.0	30
gmEx606[Pmec-7::mig-1W382L::gfp]	38.9	18
egl-20(n585); gmEx606	0.0	19
gmEx581[Pmec-7::mig-1δc::gfp]	1.4	208

[1] All three alleles were balanced by *hT2* in the mothers of these worms.
[2] The *egl-20(n585)* mutation was crossed out of this strain.

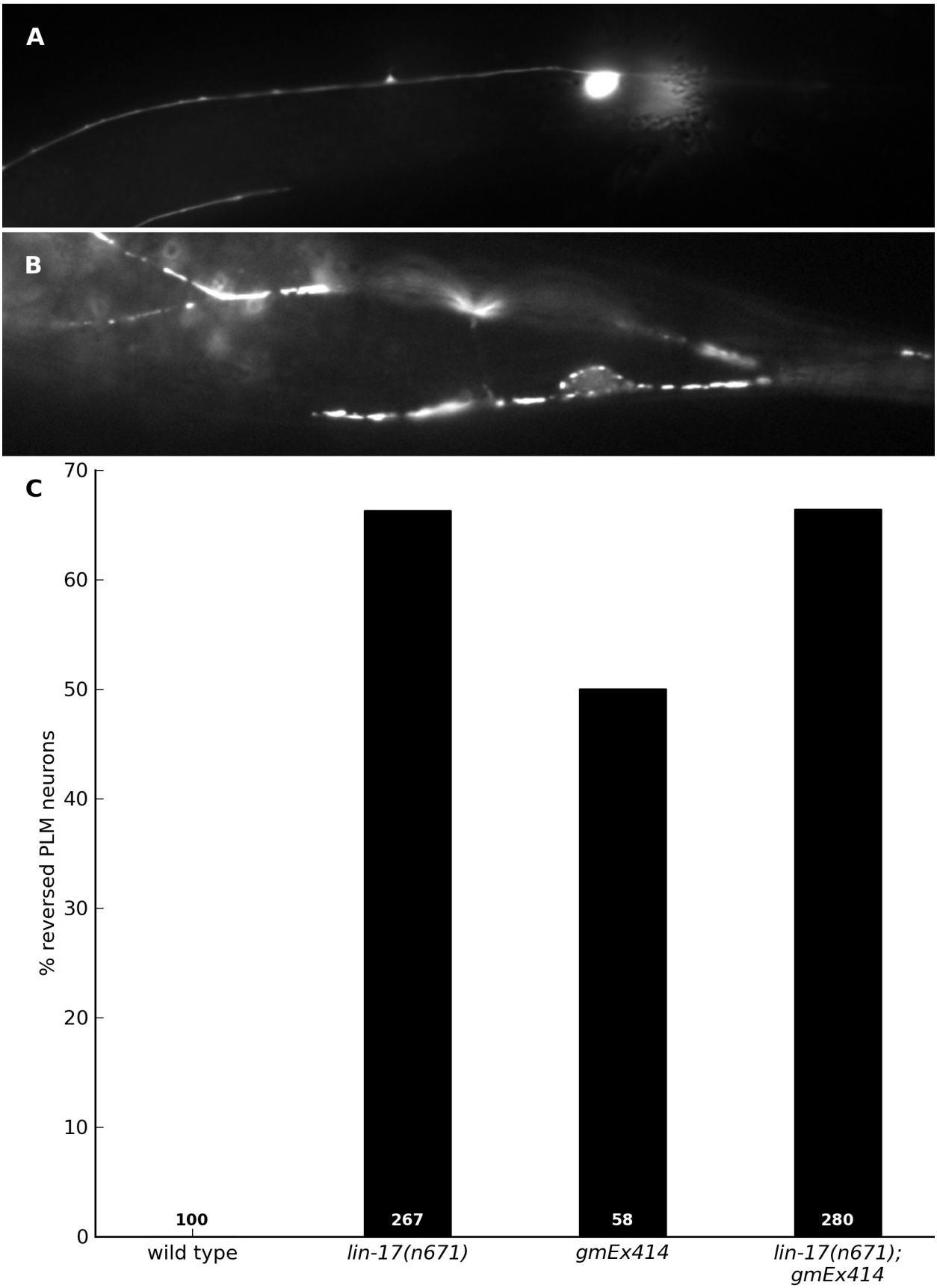
A
B
C
% reversed PLM neurons
70
60
50
40
30
20
10
0
100
267
58
280
wild type
lin-17(n671)
gmEx414
lin-17(n671);
gmEx414

Figure 1: Loss of *lin-17* and ectopic expression of *mig-1* lead to reversal of PLM polarity. (A) Wild-type PLM polarity. The PLM has a long anterior process (left) and a shorter posterior process (right). (B) A PLM with reversed polarity. The PLM has a short anterior process (left) and a long posterior process (right) that enters the tail, turns and runs anteriorly (C) The percentage of reversed PLMs out of the total number scored is shown along the y-axis. The total number of neurons scored for each genotype is shown along the x-axis. In wild-type animals, PLM polarity is never reversed; however, in *lin-17* loss-of-function mutants—and when MIG-1 is ectopically expressed (*gmEx414[Pmec-7::mig-1::gfp]*)—the polarity of PLMs is often reversed. When MIG-1 is ectopically expressed in the *lin-17* mutant, the phenotype is identical to the *lin-17* mutant alone.

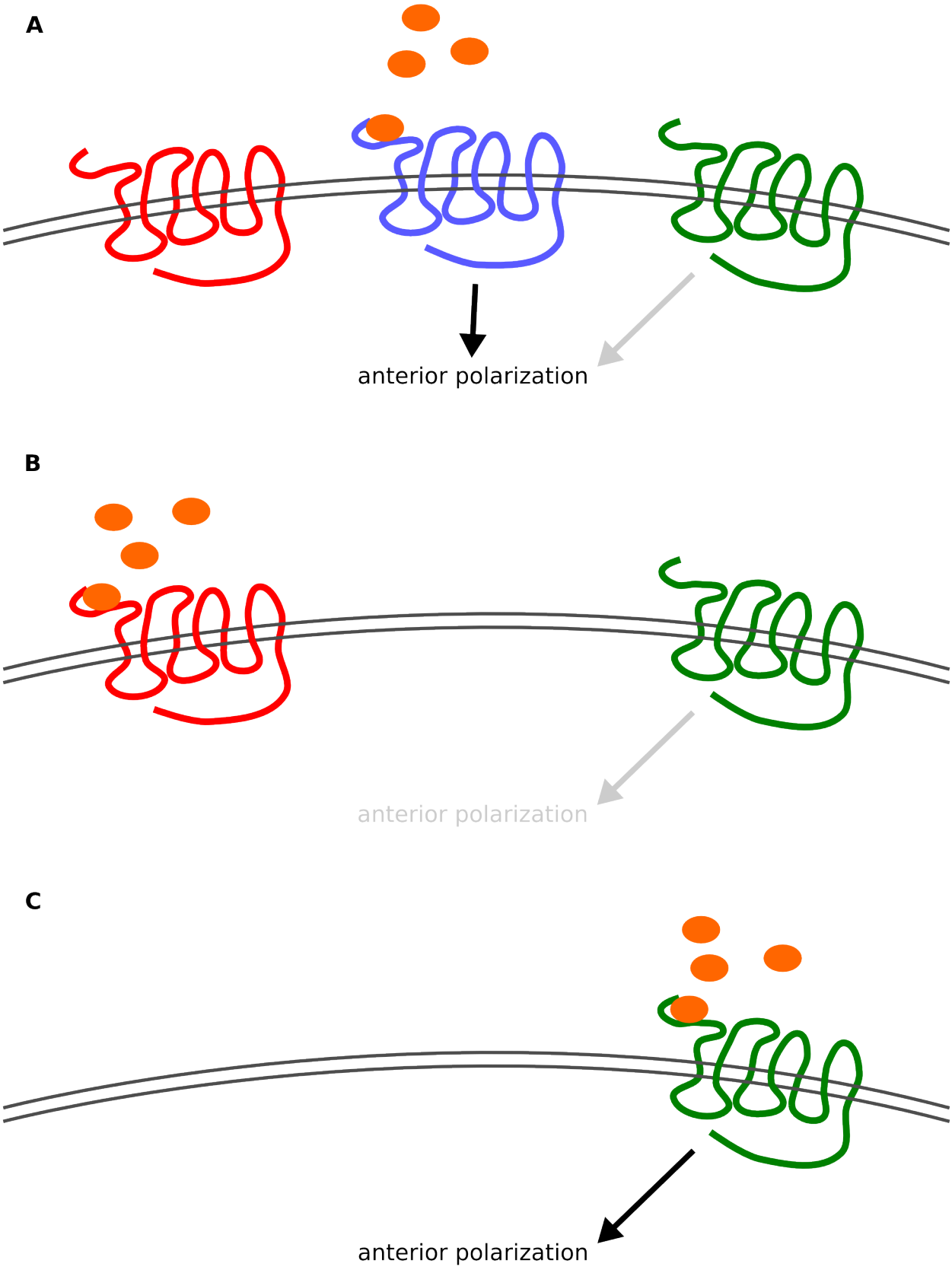
A
anterior polarization
B
anterior polarization
C
anterior polarization

Figure 2: The sequestration model to explain *mig-1* suppression of the PLM polarity defect in *lin-17* mutant worms. (A) In wild-type worms, Wnts (orange) signal through LIN-17 (blue) to promote anterior polarization of the PLM. Signaling through other Wnt-binding receptors (green) may play a minor role in promoting anterior polarization. (B) In *lin-17* mutants, LIN-17 can no longer promote anterior polarization. Other Wnt-binding receptors, which might have bound Wnt and promoted anterior polarization, are unable to do so because in the absence of LIN-17, MIG-1 (red) has a higher affinity for Wnt than other receptors. (C) In *mig-1 lin-17* double mutants, Wnt is free to bind other receptors that signal to promote anterior polarization of PLM.

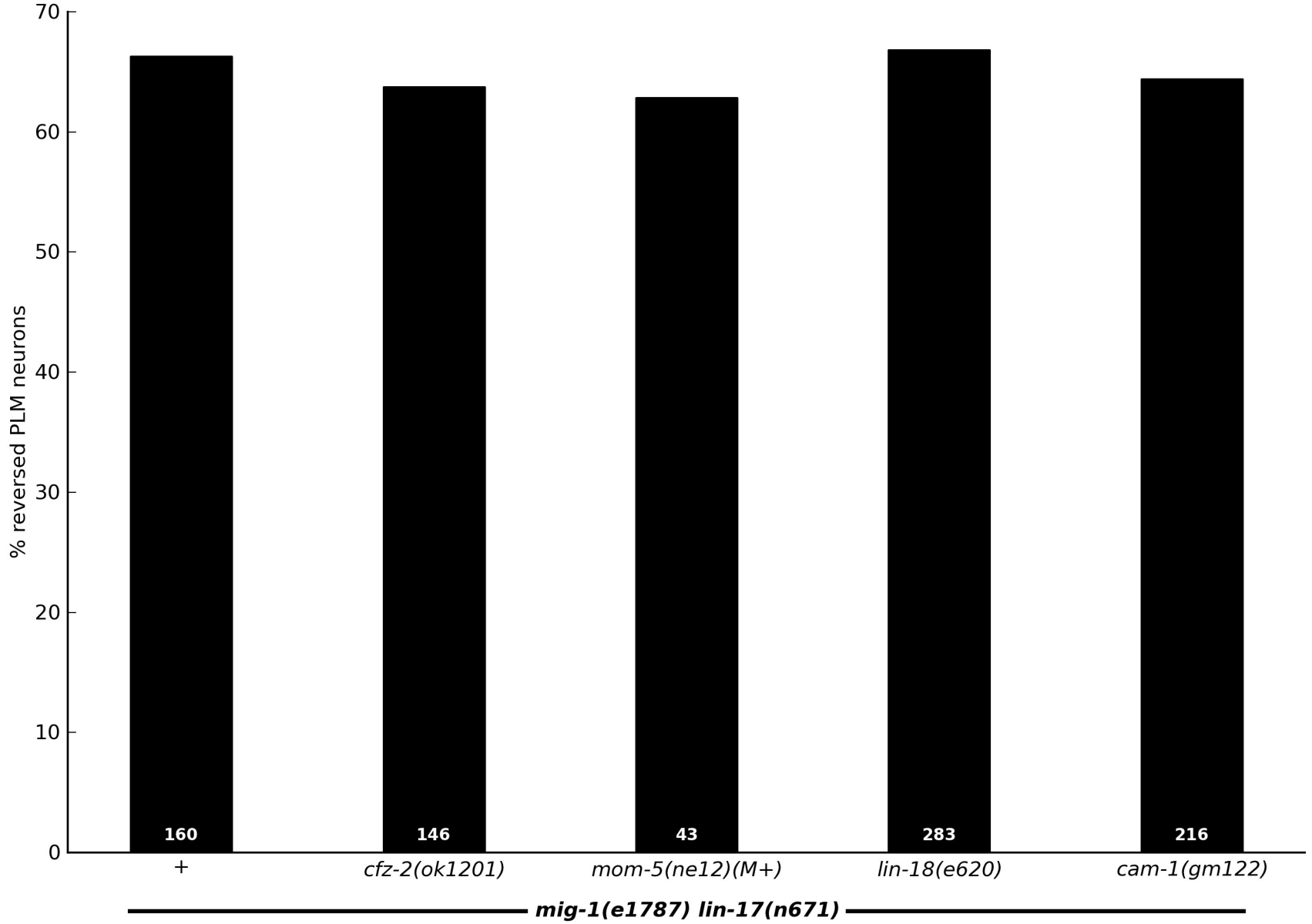
70
60
50
40
30
20
10
0
% reversed PLM neurons
160
146
43
283
216
+
cfz-2(ok1201)
mom-5(ne12)(M+)
lin-18(e620)
cam-1(gm122)
mig-1(e1787) lin-17(n671)

Figure 3: Triple mutants among *mig-1*, *lin-17* and other receptors known to bind Wnt. The percentage of reversed PLMs out of the total number scored is shown along the y-axis. The total number of neurons scored for each genotype is shown along the x-axis. All strains are mutant for *mig-1* and *lin-17*. For each triple mutant the third mutant locus is shown under the x-axis. A '+' indicates a *mig-1 lin-17* double mutant. Contrary to a previous report, *mig-1* did not suppress the PLM-reversal phenotype of *lin-17* mutants. No phenotypic change was observed in any of the triple mutants I scored. Because *mom-5* is a maternal-effect embryonic lethal gene, the *mig-1 lin-17 mom-5* triple mutant has to be balanced. All three mutant loci were balanced in the mothers of the animals scored.

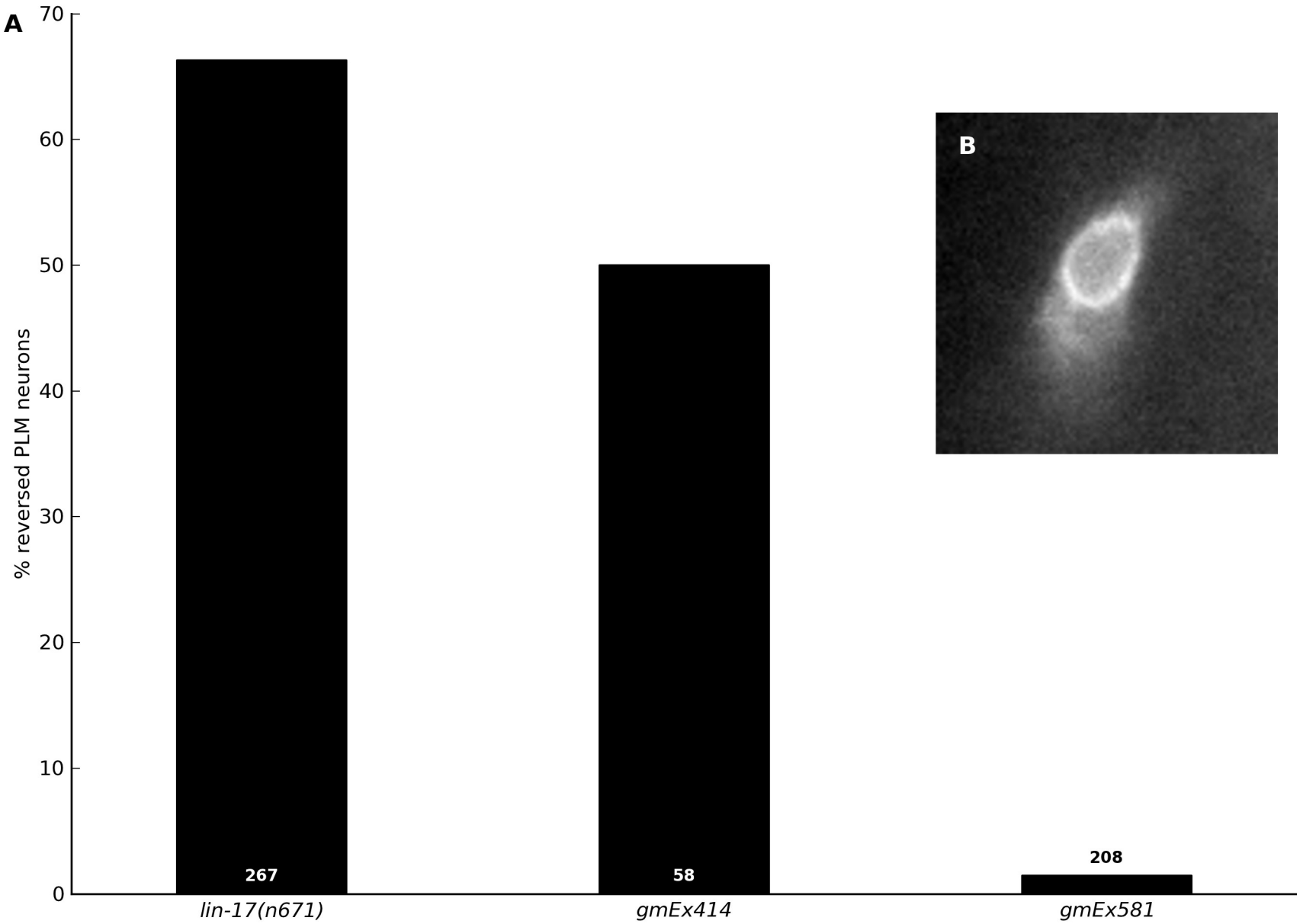
A
B
% reversed PLM neurons
70
60
50
40
30
20
10
0
267
58
208
lin-17(n671)
gmEx414
gmEx581

Figure 4: The CRD of MIG-1 is not sufficient to reverse PLM polarity. (A) The percentage of reversed PLMs out of the total number scored is shown along the y-axis. The total number of neurons scored for each genotype is shown along the x-axis. In *lin-17* loss-of-function mutants—and when MIG-1 is ectopically expressed (*gmEx414[Pmec-7::mig-1::gfp]*)—the polarity of PLMs is often reversed. Ectopic expression of MIG-1ΔC (*gmEx581[Pmec-7::mig-1δc::gfp]*) does not reverse the polarity of PLM neurons at the frequencies that I see when wild-type MIG-1 is expressed. (B) Expression of MIG-1ΔC::GFP at or near the membrane of the PLM cell body.

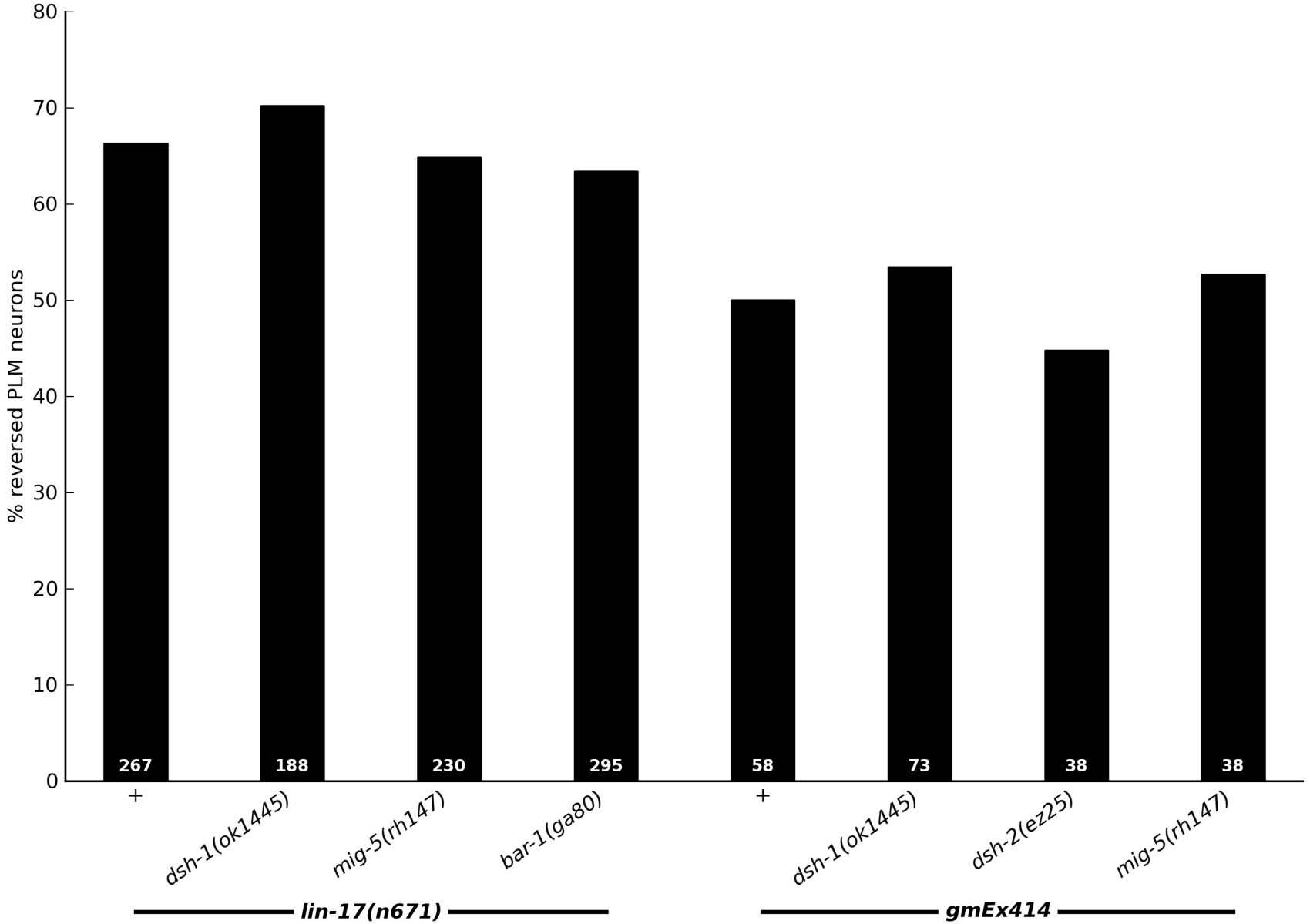
80
70
60
50
40
30
20
10
0
% reversed PLM neurons
267
188
230
295
58
73
38
38
+
dsh-1(ok1445)
mig-5(rh147)
bar-1(ga80)
+
dsh-1(ok1445)
dsh-2(ez25)
mig-5(rh147)
lin-17(n671)
gmEx414

Figure 5: Screening for effectors downstream of MIG-1. The percentage of reversed PLMs out of the total number scored is shown along the y-axis. The total number of neurons scored for each genotype is shown along the x-axis. All strains are either mutant for *lin-17* or ectopically express MIG-1 (*gmEx414*) as indicated. For each strain additional mutant loci are indicated under the x-axis. A '+' indicates either a mutant for *lin-17* or ectopic expression of MIG-1 without additional mutations at other loci. No phenotypic change was observed in any of the strains I scored.

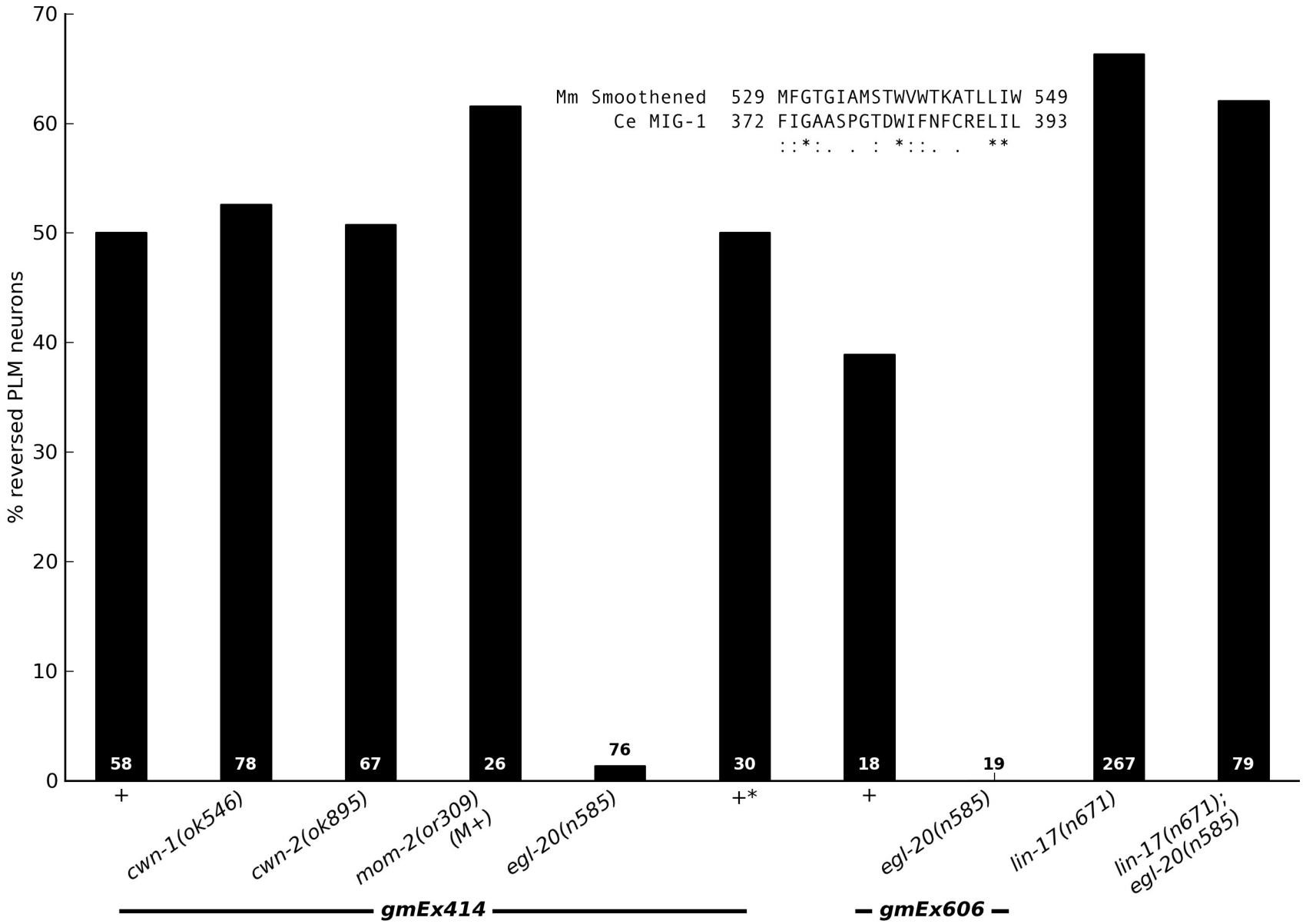
Mm Smoothened 529 MFGTGIAMSTWVWTKATLLIW 549
Ce MIG-1 372 FIGAASPGTDWIFNFCRELIL 393
::*:. . : *::. . **
% reversed PLM neurons
70
60
50
40
30
20
10
0
58
78
67
26
76
30
18
19
267
79
+
cwn-1(ok546)
cwn-2(ok895)
mom-2(or309) (M+)
egl-20(n585)
+*
+
egl-20(n585)
lin-17(n671)
lin-17(n671); egl-20(n585)
gmEx414
gmEx606

Figure 6: Testing Wnt ligands for interaction with MIG-1; Testing a mutant version of MIG-1 for constitutive activity; and the *lin-17; egl-20* double mutant. The percentage of reversed PLMs out of the total number scored is shown along the y-axis. The total number of neurons scored for each genotype is shown along the x-axis. All strains ectopically express either MIG-1 (*gmEx414*) or MIG-1W382L (*gmEx606[Pmec-7::mig-1W382L::gfp]*) as indicated. For each strain additional mutant loci are indicated under the x-axis. A '+' indicates a transgenic strain without additional mutations at other loci. I see that the PLM reversal phenotype is suppressed significantly when EGL-20 is removed. PLM polarity reversal was observed again when the *egl-20* mutation was crossed away from the *gmEx414* transgene (+*). A sequence alignment between mouse (Mm) Smoothened and worm (Ce) MIG-1 is shown. It was suggested that MIG-1 shared a conserved tryptophan with the mouse protein Smoothened. Changing W539 in the mouse protein to leucine leads to constitutive signaling activity (Xie et al., 1998; Hynes et al., 2000). I changed the corresponding tryptophan (W382) in *C. elegans* MIG-1 to a leucine (*gmEx606*) and observed a PLM polarity defect. However, I did not see constitutive activity as the PLM polarity defect in worms carrying the transgene was completely suppressed when the EGL-20 Wnt ligand was removed. EGL-20 is clearly the ligand for MIG-1 in the context of PLM polarity. Consistent with our observation that *lin-17* mutants are not suppressed by loss of *mig-1*, loss of *egl-20* does not suppress *lin-17*. In the alignment, '*', ':' and '.' indicate identical, conserved and semi-conserved residues between the sequences, respectively.

REFERENCES

Adler, C.E., Fetter, R.D., and Bargmann, C.I. (**2006**). UNC-6/Netrin induces neuronal asymmetry and defines the site of axon formation. Nat. Neurosci. *9*, 511–518.

Arimura, N., and Kaibuchi, K. (**2007**). Neuronal polarity: from extracellular signals to intracellular mechanisms. Nature Reviews Neuroscience *8*, 194–205.

Banzai, Y., Miki, H., Yamaguchi, H., and Takenawa, T. (**2000**). Essential role of neural Wiskott-Aldrich syndrome protein in neurite extension in PC12 cells and rat hippocampal primary culture cells. J. Biol. Chem. *275*, 11987–11992.

Chan, T.O., Rodeck, U., Chan, A.M., Kimmelman, A.C., Rittenhouse, S.E., Panayotou, G., and Tsichlis, P.N. (**2002**). Small GTPases and tyrosine kinases coregulate a molecular switch in the phosphoinositide 3-kinase regulatory subunit. Cancer Cell *1*, 181–191.

Chen, X.Q., Tan, I., Leung, T., and Lim, L. (**1999**). The myotonic dystrophy kinase-related Cdc42-binding kinase is involved in the regulation of neurite outgrowth in PC12 cells. J. Biol. Chem. *274*, 19901–19905.

Chen, Y.M., Wang, Q.J., Hu, H.S., Yu, P.C., Zhu, J., Drewes, G., Piwnica-Worms, H., and Luo, Z.G. (**2006**). Microtubule affinity-regulating kinase 2 functions downstream of the PAR-3/PAR-6/atypical PKC complex in regulating hippocampal neuronal polarity. Proc. Natl. Acad. Sci. U.S.A. *103*, 8534–8539.

Daniels, R.H., Hall, P.S., and Bokoch, G.M. (**1998**). Membrane targeting of p21-activated kinase 1 (PAK1) induces neurite outgrowth from PC12 cells. EMBO J. *17*, 754–764.

Dann, C.E., Hsieh, J.C., Rattner, A., Sharma, D., Nathans, J., and Leahy, D.J. (**2001**). Insights into Wnt binding and signalling from the structures of two Frizzled cysteine-rich domains. Nature *412*, 86–90.

Dotti, C.G., Sullivan, C.A., and Banker, G.A. (**1988**). The establishment of polarity by hippocampal neurons in culture. J. Neurosci. *8*, 1454–1468.

Fleming, T., Chien, S.-C., Vanderzalm, P.J., Dell, M., Gavin, M.K., Forrester, W.C., and Garriga, G. (**2010**). The role of C. elegans Ena/VASP homolog UNC-34 in neuronal polarity and motility. Dev. Biol. *344*, 94–106.

Goslin, K., and Banker, G. (**1989**). Experimental observations on the development of polarity by hippocampal neurons in culture. J. Cell Biol. *108*, 1507–1516.

Hilliard, M.A., and Bargmann, C.I. (**2006**). Wnt Signals and Frizzled Activity Orient Anterior-Posterior Axon Outgrowth in C. elegans. Developmental Cell *10*, 379–390.

Hynes, M., Ye, W., Wang, K., Stone, D., Murone, M., Sauvage, F. de, and Rosenthal, A. (**2000**). The seven-transmembrane receptor Smoothened cell-autonomously induces multiple ventral cell types. Nature Neuroscience *3*, 41–46.

Nikolic, M., Chou, M.M., Lu, W., Mayer, B.J., and Tsai, L.H. (**1998**). The p35/Cdk5 kinase is a neuron-specific Rac effector that inhibits Pak1 activity. Nature *395*, 194–198.

Nishimura, T., Yamaguchi, T., Kato, K., Yoshizawa, M., Nabeshima, Y., Ohno, S., Hoshino, M., and Kaibuchi, K. (**2005**). PAR-6-PAR-3 mediates Cdc42-induced Rac activation through the Rac GEFs STEF/Tiam1. Nat. Cell Biol. *7*, 270–277.

Pan, C.-L., Howell, J.E., Clark, S.G., Hilliard, M., Cordes, S., Bargmann, C.I., and Garriga, G. (**2006**). Multiple Wnts and Frizzled Receptors Regulate Anteriorly Directed Cell and Growth Cone Migrations in Caenorhabditis elegans. Developmental Cell *10*, 367–377.

Polleux, F., Morrow, T., and Ghosh, A. (**2000**). Semaphorin 3A is a chemoattractant for cortical apical dendrites. Nature *404*, 567–573.

Prasad, B.C., and Clark, S.G. (**2006**). Wnt signaling establishes anteroposterior neuronal polarity and requires retromer in C. elegans. Development *133*, 1757–1766.

Saldanha, J., Singh, J., and Mahadevan, D. (**1998**). Identification of a Frizzled-like cysteine rich domain in the extracellular region of developmental receptor tyrosine kinases. Protein Sci *7*, 1632–1635.

Schwamborn, J.C., and Püschel, A.W. (**2004**). The sequential activity of the GTPases Rap1B and Cdc42 determines neuronal polarity. Nat. Neurosci. *7*, 923–929.

Shi, S.-H., Jan, L.Y., and Jan, Y.-N. (**2003**). Hippocampal neuronal polarity specified by spatially localized mPar3/mPar6 and PI 3-kinase activity. Cell *112*, 63–75.

Wang, S., Watanabe, T., Noritake, J., Fukata, M., Yoshimura, T., Itoh, N., Harada, T., Nakagawa, M., Matsuura, Y., Arimura, N., et al. (**2007**). IQGAP3, a novel effector of Rac1 and Cdc42, regulates neurite outgrowth. J Cell Sci *120*, 567–577.

Xie, J., Murone, M., Luoh, S.-M., Ryan, A., Gu, Q., Zhang, C., Bonifas, J.M., Lam, C.-W., Hynes, M., Goddard, A., et al. (**1998**). Activating Smoothened mutations in sporadic basal-cell carcinoma. Nature *391*, 90–92.